BMC Medicine

https://doi.org/10.1186/s12916-026-04866-0

Article in Press

Epigenetic aging markers in the association between frailty and mortality among U.S. adults

Received: 01 Sep 2025

Accepted: 08 Apr 2026

Published online: 15 April 2026

Cite this article as: Beydoun, M., Hooten, N., Beydoun, H. *et al.* Epigenetic aging markers in the association between frailty and mortality among U.S. adults. *BMC Med* (2026). https://doi.org/10.1186/s12916-026-04866-0

May Beydoun, Nicole Hooten, Hind Beydoun, Michael Georgescu, Jack Tsai, Michele Evans & Alan Zonderman

Epigenetic Aging Markers in the Association Between Frailty and Mortality Among U.S. Adults

May A. Beydoun[1,†]; Nicole Noren Hooten[1]; Hind A. Beydoun[2,3]; Michael F. Georgescu[1]; Jack Tsai[2,3]; Michele K. Evans[1,#]; Alan B. Zonderman[1,#]

[#]*Co-senior authors*

[1] *Laboratory of Epidemiology and Population Sciences, National Institute on Aging, NIA/NIH/IRP, Baltimore, MD, 21224,USA*

[2] *VA National Center on Homelessness Among Veterans, U.S. Department of Veterans Affairs, Washington, DC, 20420,USA*

[3] *Department of Management, Policy, and Community Health, School of Public Health, University of Texas Health Science Center at Houston, Houston, TX, 77030,USA*

[†] Performed statistical analyses.

*** Address of correspondence:** May A. Beydoun, PhD, MPH, NIH Biomedical Research Center, National Institute on Aging Intramural Research Program, 251 Bayview Blvd, Suite 100, Baltimore, MD 21224, E-mail: baydounm@mail.nih.gov, Fax: 410-558-8236

Funding sources of the study. This work received partial support from the Intramural Research Program of the NIH, specifically the National Institute on Aging, under NIH Project AG000513.

Financial Disclosure: Dr. M.A. Beydoun reports no disclosures; Dr. N. Noren Hooten reports no disclosures; Dr. H. A. Beydoun reports no disclosures; Dr. J. Tsai reports no disclosures; Dr. M. K. Evans reports no disclosures; Dr. A. B. Zonderman reports no disclosures

Word count (Abstract): 230; **Word count (Text):** 7,127; **Character count (Title):** 91.

Number of references: 80; Number of tables: 3; Number of figures: 4; Number of appendices: 4 Figures, 8 supplementary Appendices, 6 supplementary datasheets.

ABBREVIATIONS

ABN = Additive Bayesian Networks
ACM = All-cause mortality
BMI = Body mass index
CDE = Controlled direct effect
CES-D = Center for Epidemiologic Studies Depression Scale
CI = Confidence interval
CpG = Cytosine–phosphate–guanine site
DAG = Directed acyclic graphs
DIED = Death event (binary outcome)
DNAm = DNA methylation
DNAm age = DNA methylation age
DPQ = Depression Questionnaire
DunedinPACE = Dunedin Pace of Aging Calculated from the Epigenome
DunedinPoAm = Dunedin Pace of Aging DNA methylation
EAA = Epigenetic age acceleration
EFTF = Enhanced Face-to-Face Interview
EWAS = Epigenome-wide association study
FFS = Fried frailty score / Fried frailty phenotype
FI = Frailty index
FRAIL = Fatigue, Resistance, Ambulation, Illness, Loss of weight scale
GrimAgeEAA = Grim DNA methylation age epigenetic age acceleration
GSEM = Generalized structural equation modeling
GWAS = Genome-wide association studies
HANDLS = Healthy Aging in Neighborhoods of Diversity across the Life Span
HannumAgeEAA = Hannum DNA methylation age epigenetic age acceleration
HISP = Hispanic
HorvathAgeEAA = Horvath DNA methylation age epigenetic age acceleration
HR = Hazard ratio
HRS = Health and Retirement Study
INTmed = Mediated interaction
INTref = Reference interaction
IQR = Interquartile range
IRB = Institutional Review Board
Kaplan–Meier = Non-parametric survival estimator
LASSO = Least Absolute Shrinkage and Selection Operator
LE8 = Life's Essential 8
Ln = Natural logarithm
MRV = Medical Research Vehicles
NCHS = National Center for Health Statistics
NDI = National Death Index
NDE = Natural direct effect
NHB = Non-Hispanic Black
NHANES = National Health and Nutrition Examination Survey
NHW = Non-Hispanic White
NIA = National Institute on Aging
NIE = Natural indirect effect
NIH = National Institutes of Health
op_e = Proportion eliminated
op_m = Overall proportion mediated

OTHER = Other race/ethnicities
PCA = Principal components analysis
P_CDE = Percentage controlled direct effect
PhenoAgeEAA = Pheno/Levine DNA methylation age epigenetic age acceleration
PIE = Pure indirect effect
PIR = Poverty income ratio
Person-years = Time-at-risk metric in survival analysis
PSU = Primary sampling units
qPCR = Quantitative polymerase chain reaction
RAND = Research and Development (RAND HRS dataset)
SD = Standard deviation
SE = Standard error
SES = Socioeconomic status
TE = Total effect
Tracker file = HRS mortality linkage dataset
U.S. = United States
VA = Department of Veterans Affairs
WBC = White blood cell
Weibull model = Parametric survival model
Z-score = Standardized score

ABSTRACT

Background: Frailty reflects diminished physiological reserve and increased vulnerability to adverse health outcomes. It has been linked to biological aging, including epigenetic age acceleration (EAA), a DNA methylation–based marker of aging, but the extent to which EAA accounts for the frailty–mortality association remains unclear.

Methods: We analyzed three U.S. cohorts—NHANES (1999–2002), HRS (2016), and HANDLS (2004–2009)—with mortality follow-up through 2019–2022. Frailty was defined using harmonized adaptations of the Fried phenotype and FRAIL scale. EAA was derived from five epigenetic clocks (Horvath, Hannum, PhenoAge, GrimAge, DunedinPoAm). Additive Bayesian networks, Cox proportional hazards models, and counterfactual four-way decomposition were used to assess potential mediation and moderation of the frailty–mortality association by EAA, adjusting for age, sex, race/ethnicity, and socioeconomic status.

Results: Frailty was strongly associated with higher all-cause mortality in NHANES and HRS. GrimAge and DunedinPoAm showed the strongest mediation. In NHANES, GrimAge accounted for 33% ($p<0.001$) and DunedinPoAm 17% ($p=0.006$) of the association. In HRS, DunedinPoAm mediated 9% ($p=0.040$) and GrimAge 16% ($p=0.020$). Other clocks showed limited mediation. HANDLS findings were consistent. Higher socioeconomic status was associated with slower aging and lower frailty risk. Female sex was inversely associated with multiple epigenetic clocks but positively associated with frailty.

Conclusions: Epigenetic aging, particularly GrimAge and DunedinPoAm, explains part of the frailty–mortality association, supporting a role for biological aging pathways linking frailty to mortality.

KEYWORDS: Frailty, epigenetic clocks, biological aging, mortality, Additive Bayesian Networks

BACKGROUND

Frailty is a multidimensional clinical syndrome marked by decreased physiological reserve and increased vulnerability to adverse health outcomes(1). Strongly associated with aging, frailty predicts a wide range of age-related conditions, including disability, hospitalization, and all-cause mortality (2). Frailty is most commonly operationalized using physical and functional criteria—such as the Fried frailty phenotype (FFS), deficit accumulation frailty indices (FI), or related survey- and hospital-based adaptations, each capturing complementary aspects of vulnerability across aging populations(3). Although frailty is traditionally measured using physical and functional indicators, accumulating evidence suggests that it also reflects underlying biological aging processes, including epigenetic regulation captured through DNA methylation patterns across the genome (4).

Over the past 7–8 years, several studies have directly linked frailty to DNA methylation–based markers of biological aging. Early epigenome-wide association studies (EWAS) demonstrated that frailty status is associated with differential methylation at CpG sites involved in inflammatory, metabolic, and stress-response pathways, providing molecular evidence that frailty reflects biological aging rather than functional decline alone (5). Subsequent work has shown that frailty, whether measured using phenotype-based or index-based approaches—is associated with DNA methylation–derived epigenetic age acceleration (EAA), particularly for second- and third-generation clocks that capture multisystem physiological dysregulation (6, 7).

EAA quantifies the gap between an individual's epigenetic age and their chronological age, with higher values indicating accelerated epigenetic aging (8, 9). Elevated EAA has been associated with a broad spectrum of adverse outcomes, including cardiovascular disease, neurodegeneration, cognitive decline, and increased mortality risk (10, 11, 12, 13, 14, 15, 16, 17). Despite evidence that frailty and EAA may reflect overlapping aging pathways, only a handful of studies have directly examined whether EAA mediates the link between frailty and mortality (18).

To capture the complexity of these relationships, traditional regression models may be insufficient, as they often assume linearity and independence among predictors. Additive Bayesian networks (ABN), a

probabilistic graphical modeling approach, offers a flexible, data-driven framework to uncover direct and indirect associations among variables without imposing strict parametric assumptions (19, 20, 21, 22). ABNs allow for the exploration of complex dependency structures, which is especially useful when investigating multifaceted pathways involving biological aging (19, 20, 21, 22). Furthermore, to test mediation and moderation simultaneously, four-way decomposition can determine the proportion of the total effect of an exposure such as frailty on the mortality risk outcome that is explained by pure mediation, pure interaction, both, or none (i.e controlled direct effect) through or with EAA measures(23, 24, 25).

In this study, we use three large datasets─ two nationally representative samples of U.S. adults and a probability sample of urban adults residing in Baltimore city, MD─ all linked with death data to examine the interconnections among frailty, epigenetic age acceleration, and all-cause mortality. Specifically, we aim to: (1) investigate the association between frailty status and epigenetic aging markers; (2) assess whether EAA mediates or moderates the relationship between frailty and mortality; and (3) identify plausible biological pathways linking frailty, EAA, and mortality using additive Bayesian network modeling. By integrating causal discovery and epidemiological methods, this study advances our understanding of how physical frailty may exert long-term effects on mortality risk via epigenetic mechanisms, offering new mechanistic insights that can be used for future aging trajectory interventions.

METHODS

Databases

National Health and Nutrition Surveys

The National Health and Nutrition Examination Survey (NHANES) is a series of cross-sectional, nationally representative surveys administered by the National Center for Health Statistics (NCHS), initiated in the early 1970s (https://wwwn.cdc.gov/nchs/nhanes/default.aspx). In 1999, NHANES transitioned to a continuous, biennial data collection model (26). Key anthropometric and physiological measurements were gathered through standardized physical examinations conducted within several

mobile examination centers. This study utilized data collected between 1999 and 2002, with mortality follow-up obtained by linkage to the National Death Index through 2019. All NHANES data collection procedures during this period were conducted in accordance with rigorous ethical protocols, including informed consent, assurance of participant confidentiality, risk minimization, and approval by the NCHS Research Ethics Review Board.

Health and Retirement Study

The Health and Retirement Study (HRS) is a nationally representative, longitudinal panel study that investigates a wide range of factors influencing health, aging, and retirement among U.S. adults aged 50 and older (https://hrs.isr.umich.edu/about)(27). Sponsored by the National Institute on Aging (NIA) and conducted by the University of Michigan, the HRS collects data biennially through structured interviews, with supplemental waves focusing on physical, biological, and psychosocial domains. The core dataset includes comprehensive self-reported and objectively measured variables obtained through the Enhanced Face-to-Face Interview (EFTF), as well as off-cycle components that capture biological markers of aging. For harmonized longitudinal analysis, the RAND HRS dataset provides a user-friendly, cleaned version of key variables across waves. In this study, we utilized data from the 2014 and 2016 waves, incorporating physical measures, psychosocial factors, and biomarkers, and linked them to mortality data from the National Death Index through 2019. All study protocols were approved by the University of Michigan Institutional Review Board and were conducted in accordance with strict ethical guidelines, including informed consent, confidentiality protections, and risk minimization procedures.

Healthy Aging in Neighborhoods of Diversity across the Life Span

The Healthy Aging in Neighborhoods of Diversity across the Life Span (HANDLS) study is a population-based, prospective cohort study designed to examine the influences of race and socioeconomic status (SES) on health disparities and aging trajectories in urban-dwelling adults. Initiated in 2004 by the National Institute on Aging Intramural Research Program (NIA/IRP), HANDLS recruited African American and White participants aged 30–64 years from neighborhoods in Baltimore, Maryland, using an area probability sampling design (https://handls.nih.gov/) (28). The study collects longitudinal data

including sociodemographic characteristics, clinical and cognitive assessments, psychosocial measures, dietary intake, and a broad range of biological markers. Physical measures and biospecimens (e.g., blood, saliva, and DNA) are obtained during structured clinical visits. For this analysis, we utilized data from baseline (Wave 1, 2004–2009) and follow-up waves through 2019, linked to mortality outcomes via the National Death Index (NDI). HANDLS study protocols received approval from the Institutional Review Board of the National Institutes of Health and were conducted in accordance with ethical standards, including informed consent, confidentiality protections, and risk minimization procedures. **Appendix I** in **Additional File 1** provides more details on all three cohorts and **Table 1** summarizes survey characteristics and measures used in each. In summary, NHANES and HRS are publicly available, de-identified datasets with prior IRB approval and participant consent; the present secondary analyses did not require additional IRB review. HANDLS was approved by the NIH Intramural Research Program IRB, and participants provided written informed consent.

Mortality linkage

All three cohorts—NHANES, HRS, and HANDLS—provide linkage to mortality outcomes via the NDI, enabling longitudinal analysis of vital status and time of death. In NHANES, mortality data are linked to participant records through NDI and provided in a mortality file that can be merged with demographic, health, and examination data for each survey wave. The HRS links mortality data using NDI through 2022, in addition to information from follow-up interviews and public records, with key death variables integrated into the Tracker file—this includes month and year of death, which can be merged with the Core survey and RAND longitudinal files. Similarly, the HANDLS study is linked to the NDI to ascertain mortality status and timing for participants through 2022. Therefore, death outcomes were derived from linkage to the National Death Index (NDI) for NHANES and HANDLS and from the National Death Index and HRS exit interviews for HRS, with follow-up through the specified censoring dates.

Frailty Score and status

Frailty was assessed across three U.S. cohort studies—HRS, NHANES, and HANDLS—using harmonized adaptations of established frailty phenotype frameworks. In the HRS, frailty was measured using the Fried phenotype model, which includes five criteria: unintentional weight loss, weakness, slowness, exhaustion, and low physical activity (1). For the 2016 wave, unintentional weight loss ("shrinking") was operationalized using a calculated annualized change in body mass index (BMI) between 2014 and 2016, equivalent to a weight loss >1.48 kg/m^{-2}/year indicating the criterion. Weakness was assessed by average handgrip strength across four trials, with sex-specific cutoffs set at the 20th percentile (≤27.1 kg for men, ≤16.6 kg for women). Due to limited performance testing, slowness was approximated via self-reported difficulty walking several blocks. Exhaustion was based on a shorter version of the Center for Epidemiologic Studies-Depression (CES-D) questionnaire items, with endorsement of “everything was an effort” or “could not get going” indicating presence. Low physical activity was defined by self-reported frequency of vigorous and moderate exercise, with infrequent engagement (≤1–3 times/month or never) considered low. Each component was scored as present or absent (1/0), summed to a frailty score (0–5), and classified as robust (0), pre-frail (1–2), or frail (≥3).

In NHANES 1999–2002, which overlaps with epigenetic biomarker data, frailty was also defined using the Fried framework (1). Because NHANES lacks longitudinal weight data, shrinking was proxied by BMI <18.5 kg/m^2. Exhaustion was identified using responses to DPQ items on fatigue and disinterest. Weakness was assessed via self-reported difficulty lifting 10 pounds, while slowness was defined by difficulty walking a quarter-mile. Low physical activity was based on responses indicating no or minimal walking/bicycling. As in HRS, a frailty score (0–5) and status (robust, pre-frail, frail) were calculated.

In HANDLS, frailty was defined using the five-item FRAIL scale: fatigue, resistance, ambulation, illness, and weight loss (29, 30, 31). Fatigue and weight loss were derived from CES-D items (frequent fatigue and poor appetite, respectively). Resistance and ambulation were measured via self-reported

difficulty climbing stairs and walking a quarter-mile respectfully. Illness was defined as the presence of five or more physician-diagnosed chronic conditions from a list of 11. One point was assigned per criterion present, yielding a score of 0–5. Participants were classified as robust (0), pre-frail (1–2), or frail (3–5). Those with ≥3 valid components were included in analyses. The ordinal version of the FRAIL score was used in part of the analysis. **Appendix II** of **Additional File 1** details harmonized frailty algorithms as applied to NHANES, HRS and HANDLS studies. In most analyses, frail vs. pre-frail/robust was used as the main exposure of interest with part of the analyses including the frailty sum score ranging from 0 to 5.

Epigenetic clocks and age acceleration measures

HRS, NHANES, and HANDLS have incorporated DNA methylation based epigenetic clocks. employing the Illumina MethylationEPIC v1.0 BeadChip array for DNAm profiling. In HRS, five epigenetic clocks were computed: Horvath, Hannum, Levine (PhenoAge), GrimAge, and Dunedin Pace of Aging DNA methylation (DunedinPoAm). EAA was derived for the first four clocks by regressing DNAm age on chronological age and using the residuals, while DunedinPoAm, which inherently reflects aging pace, required no transformation. NHANES applied similar residual-based methods to calculate EAA for the same four clocks. HANDLS derived the same clocks mirroring those available in HRS and NHANES, with the exception of Dunedin Pace of Aging Calculated from the Epigenome (DunedinPACE). The computation of EAA via residuals was standardized across studies for consistency (see **Appendix III** of **Additional File 1** for detailed methodology and potential adjustments for leukocyte cell counts as a sensitivity analysis). In NHANES and HANDLS, DNAm and frailty were measured contemporaneously, while in HRS, frailty (2016) was measured up to 4 years prior to DNAm collection (2016). A similar approach was adopted in an earlier study(32), and other studies used a similar set of clocks (14, 28, 33, 34, 35).

Socio-economic status (SES) index

In both the HRS and NHANES datasets, educational attainment and household income were integrated into a composite socioeconomic status (SES) index using principal components analysis (PCA). The first

principal component was extracted and standardized into a z-score for use in analyses. In the HRS, educational attainment was classified into five categories: "No degree," "GED," "High school graduate," "Some college," and "College degree or higher." Household income and wealth were categorized into the following brackets: "< $25,000," "$25,000–$125,999," "$125,000–$299,999," "$300,000–$649,999," and "≥ $650,000." Total household wealth was derived from the RAND HRS dataset, which aggregates financial and non-financial assets (e.g., checking and savings accounts, bonds, IRAs, and property) and subtracts total debt to estimate net wealth. For the present study, household wealth values were taken from the 2016 HRS wave and measured at the household level.

In NHANES, educational attainment (assessed among adults aged 20 years and older) was grouped into: "Less than 9th grade," "9th–11th grade," "High school graduate or GED," "Some college or Associate's degree," and "College graduate or above." Household income was assessed using the poverty income ratio (PIR), a continuous variable representing the ratio of household income to the federal poverty threshold. PIR values below 1.0 indicate income below the poverty line, whereas values above 1.0 indicate income above poverty level. This continuous PIR measure was used as the household income indicator in our analysis.

In the HANDLS study, SES was summarized using two primary indicators: educational attainment and poverty status. Educational attainment was self-reported and categorized into: "Less than high school," "High school or GED," "Some college or vocational training," and "College degree or higher." Poverty status was determined at enrollment based on the 2004 U.S. federal poverty guideline (36) and operationalized as a binary variable indicating whether a participant's household income fell below or at/above 125% of the federal poverty level. For the purposes of this study, educational attainment and poverty status were combined using principal components analysis (PCA) to derive a standardized composite SES index (z-score), consistent with approaches applied to HRS and NHANES data.

Covariates

In this study, key demographic variables were treated as exogenous factors and included baseline self-reported age, sex (coded as 0 = Male, 1 = Female), and race/ethnicity. To enable cross-cohort

comparability, race and ethnicity were harmonized across NHANES, HRS, and HANDLS wherever possible. Standardized categories included Non-Hispanic White (NHW), Non-Hispanic Black (NHB), and Hispanic, with an additional category for "Other" racial/ethnic groups. These categories were operationalized using three mutually exclusive dummy variables. In the HANDLS study specifically, race was self-identified and limited to NHW and NHB participants by design, enabling a focused investigation of various risk factors of health outcomes in an urban population. A sensitivity analysis adjusted for White Blood Cell (WBC) composition for NHANES and HRS four-way decomposition models, discussed later, focusing on largest available sub-classes of WBCs as percentage of total WBC. Due to heterogeneity in data available, in NHANES, this amounted to adjusting for percentages in lymphocytes, monocytes and neutrophils. In contrast, for HRS, adjustment was made for percentages in B cells, T cells, NK cells, monocytes and dendritic cells. Further details are provided in **Appendix VII** of **Additional File 1**, with **Appendices IV** through **VI** of **Additional File 1** detailing statistical methodologies applied in this study.

Study samples

Figure S1 (Additional File 2) presents participant flowcharts for the NHANES 1999–2002, HRS 2016, and HANDLS analytic samples. All three studies include epigenetic clock data for adults aged 50 and older. In HRS, the flowchart traces the progression from the initial RAND longitudinal dataset—comprising data from HRS and earlier cohorts dating back to 1992—to individuals aged 50+ in the 2016 wave, then to those with frailty data, and finally to participants with available epigenetic clock measures in the 2016 wave. In NHANES, participants aged 50 and older from the 1999–2002 cycles were selected, then narrowed to those with complete frailty and epigenetic data. In HANDLS, the sample selection began with the initial cohort recruited between 2004 and 2009, comprising urban-dwelling African American and White adults aged 30–64 at baseline. From this cohort, we selected participants who were aged 30-64y at Visit 1 (2004–2009) assessment, had completed frailty status measurements, and had available DNA methylation data for epigenetic clock calculation. Mortality follow-up in HANDLS extended up to 17 years. The final analytic samples included 1,537 participants in NHANES, 1,466 in

HRS and 455 in HANDLS, all aged 50+ at baseline with complete data on frailty, epigenetic clocks, and relevant covariates, except for HANDLS for which baseline age ranged between 30-64y.

Statistical methods

All statistical analyses were performed using Stata version 18.0 (37), with supplementary visualizations and advanced analytical methods conducted with R version 4.4.1 (38). Data from three nationally representative or community-based cohorts—NHANES, HRS, and HANDLS—were harmonized to enable a stratified analyses focused on the role of frailty in all-cause mortality and its potential mediation (along with moderation) through DNA methylation (DNAm)-based epigenetic age acceleration (EAA) measures.

Initial analyses characterized the distribution of key variables, including frailty status [based on Fried criteria (NHANES and HRS) or FRAIL scale in HANDLS], DNAm-based EAA metrics (Horvath, Hannum, PhenoAge, GrimAge, DunedinPACE), mortality status, and covariates (age, sex, race/ethnicity, SES). Means, medians, standard deviations, interquartile ranges, and frequency distributions were computed. Histograms were examined to detect outliers, and standardized procedures were applied to remove them from continuous variables. Descriptive comparisons across cohorts used weighted linear regression for continuous variables and multinomial logistic regression for categorical variables, accounting for survey design features in HRS, NHANES, and HANDLS that are in common to all three cohorts, namely sampling weights. Pearson correlation coefficients were used to assess descriptive (non-inferential) relationships between EAA measures and the frailty sum score (0–5) across the three cohorts, with results visualized using correlation heatmaps. Analyses were unweighted due to methodological limitations in estimating weighted correlations.

Kaplan-Meier survival curves were generated for each cohort to estimate time to all-cause mortality, stratified by EAA measures and frailty status (0=pre-frail/robust vs. 1=frail). Sampling weights were applied to adjust for design complexities, and survival differences across strata were tested using Cox-regression based tests. These non-parametric methods allowed visual and statistical assessment of survival patterns across biological aging and frailty categories.

In our main analyses, we first fitted survey-weighted Cox regression models to evaluate the association between frailty status, EAA metrics, and SES z-score with all-cause mortality, adjusting for age, sex and race/ethnicity. Each of these listed predictors were entered separately. Proportional hazards assumptions were evaluated using Schoenfeld residuals. Models were stratified by study cohort and used attained age as the time scale. As a sensitivity analysis, Age-squared was entered into these models in addition to the main effect of age.

Second, to model the probabilistic interdependencies among frailty, EAA measures, and mortality risk, ABNs were constructed using a discrete-time survival framework. Data were transformed into person-period format with binary indicators for 2-year follow-up intervals. Variables were treated as Gaussian or binomial; continuous predictors were discretized using percentile-based binning, with median values representing each bin. The optimal network structure was determined by comparing model fit across configurations allowing one to three parent nodes per variable; the two-parent configuration was selected when improvement plateaued. This analysis was conducted on the HRS and NHANES cohorts and was not adjusted for sampling weights due to current ABN software limitations (**Appendices IV** and **V** of **Additional File 1**).

Third, we subsequently employed generalized structural equation modeling (GSEM) to replicate the ABN-derived networks and estimate standard errors for the identified paths. Additionally, parametric survival models using a Weibull distribution were fitted to assess the direct and indirect relationships among frailty, EAA measures, sociodemographic covariates, and mortality. These models adjusted for the complex sampling design (sampling weights, strata, and PSUs) and were compared to simpler models assuming a simple random sampling design (**Appendix VI** in **Additional File 1**).

Finally, to quantify the mediating role of each EAA measure in the frailty–mortality relationship, we implemented a four-way decomposition approach based on counterfactual mediation methods (23, 39). This technique partitioned the total effect of frailty on mortality into: (1) the controlled direct effect, or CDE (2) the reference interaction, (3) the mediated interaction, and (4) the pure indirect effect through EAA. Identification of CDEs depends on assumptions of no unmeasured exposure–outcome, mediator–

outcome, or exposure–mediator confounding, correct model specification, and consistency/positivity. Substantively, the CDE represents the effect of the exposure on the outcome when the mediator is fixed at a specified level for all individuals, namely at the mean of each EAA, isolating pathways not operating through the mediator (23, 39). Analyses were adjusted for age, sex, race/ethnicity, and SES, and were carried out in for each cohort sample, using a Cox proportional hazards regression model as the final outcome equation (**Appendix VII** in **Additional File 1**). A Type I error rate of 0.05 was considered for statistical significance. Similar to ABN and GSEM, four-way decomposition was applied only to the NHANES and HRS cohort data.

Two main sensitivity analyses were carried out on four-way decomposition models. The first one considered binary frailty as the potential mediator or moderator in the epigenetic aging → mortality risk relationship, thus addressing bi-directionality of the relationships among frailty, epigenetic aging and mortality. The second sensitivity analysis was carried out on both frailty → epigenetic aging → mortality and epigenetic aging → frailty → mortality four-way decomposition models by including leukocyte cell count as an exogenous set of covariates. This approach distinguishes immune-inclusive from immune-independent epigenetic aging signals without removing biologically meaningful variation from the primary mediation models. Detailed methods and results are provided in **Appendices VII** and **VIII** within **Additional File 1**.

RESULTS

Table 2 summarizes baseline characteristics and mortality outcomes across NHANES (1999–2002; *n* = 1,537), HRS (2016; *n* = 1,415), and HANDLS (2004–2009; *n* = 455). NHANES and HRS participants were comparable with respect to mean age, sex distribution, racial/ethnic composition, and EAA metrics, expressed as residual-based measures ± SE. Frailty prevalence was modestly higher in NHANES (24.6%) than in HRS (22.7%), and mortality rates were correspondingly greater in NHANES (43.3 per 1,000 person-years; 95% CI: 39.8–47.0) than in HRS (24.7; 95% CI: 21.4–28.6). In contrast, HANDLS participants were substantially younger at baseline (mean age = 46.9 years), included a racially diverse

urban population with a majority of non-Hispanic Black participants, and exhibited more favorable survival profiles. Consistent with this younger age structure, HANDLS showed a markedly lower frailty prevalence (7.3%) and a substantially lower mortality rate (10.2 per 1,000 person-years; 95% CI: 7.6–13.8), reflecting earlier life-course stages and reduced competing mortality risk relative to NHANES and HRS. SES z-scores and Dunedin pace of aging measures differed between cohorts and thus were not readily comparable.

Figure S2 (Additional file 3) and **Supplementary Datasheet 1 (Additional file 4)** show Pearson correlation matrices of standardized SES, frailty, and five epigenetic aging measures in NHANES and HRS. Frailty was positively correlated with PhenoAgeEAA, GrimAgeEAA, and DunedinPoAm in both cohorts, while SES was inversely associated with frailty and most aging metrics, especially in NHANES. GrimAgeEAA and DunedinPoAm showed the strongest inter-correlations and links to frailty, whereas HorvathEAA and HannumEAA were weakly related, particularly in HRS. Similar patterns were observed in HANDLS, where frailty was associated with DunedinPACE and lower SES, with minimal associations for HorvathEAA and HannumEAA.

Figure 1 displays Kaplan-Meier survival curves stratified by tertiles of socioeconomic status (SES), frailty status (binary), and epigenetic aging markers in NHANES (1999–2002; follow-up to 2019) and HRS (2016; follow-up to 2022). In NHANES, survival curves differed significantly by frailty status and all epigenetic clocks (HorvathAgeEAA, HannumAgeEAA, PhenoAgeEAA, GrimAgeEAA, and DunedinPoAm). SES showed an inverse relationship with all-cause mortality risk ($p<0.001$). In HRS, similar patterns were observed: frailty and all five epigenetic markers were significantly associated with mortality ($p<0.001$), while SES showed a strong inverse association with all-cause mortality ($p<0.001$). These results suggest that higher frailty and accelerated biological aging—specifically as measured by DNA methylation clocks—are consistently associated with reduced survival across both cohorts, despite a longer follow-up observed in the NHANES (up to 20 years) compared to ~8 years in HRS. In HANDLS, SES z-score, frailty and DunedinPACE were among the strongest predictors for ACM, with no association detected for HorvathEAA.

Figure 2 and **supplementary datasheet 2 (Additional File 5)** present multivariable-adjusted Cox proportional hazards models examining associations between SES, frailty, and each of five epigenetic aging metrics, where available, with all-cause mortality in NHANES, HRS and HANDLS , adjusting for age, sex, and race/ethnicity. In NHANES, all epigenetic clocks were significantly associated with increased mortality risk. GrimAgeEAA showed the strongest association (HR=1.70; 95% CI: 1.54–1.88), followed by DunedinPoAm (HR=1.40; 95% CI: 1.28–1.54), PhenoAgeEAA (HR=1.33; 95% CI: 1.20–1.47), HannumAgeEAA (HR=1.25; 95% CI: 1.13–1.38), and HorvathAgeEAA (HR=1.12; 95% CI: 1.02–1.23). In HRS, GrimAgeEAA (HR=1.73; 95% CI: 1.50–2.01), DunedinPoAm (HR=1.51; 95% CI: 1.28–1.78), PhenoAgeEAA (HR=1.37; 95% CI: 1.20–1.56), and HannumAgeEAA (HR=1.27; 95% CI: 1.11–1.45) were also significantly associated with elevated mortality risk, while HorvathAgeEAA was not (HR=1.00; 95% CI: 0.87–1.15). Frailty status (i.e. frail vs. pre-frail/robust) was associated with nearly a twofold higher mortality risk in NHANES (HR=1.99; 95% CI: 1.62–2.44) and over a two-and-a-half-fold risk in HRS (HR=2.64; 95% CI: 1.91–3.66), independently of age, sex, and race/ethnicity. These findings underscore the robust predictive value of both frailty and advanced biological aging—especially as measured by GrimAge, PhenoAge, and DunedinPoAm—for mortality across nationally representative cohorts. In HANDLS, and unlike HRS or NHANES, frailty status was no longer associated with ACM upon adjustment for age, sex and race, in contrast with DunedinPACE, HannumAgeEAA, and SES. Inclusion of Age-squared into these models did not alter our main findings.

Figure 3 and detailed **Figure S3 (Additional File 6)** compares ABN models from NHANES and HRS using the "three parents per child" specification, which allows up to three predictors for each non-exogenous variable. In both cohorts, model fit improved progressively from one to three parents per child, suggesting a more complex underlying network structure. Age and GrimAgeEAA consistently emerged as the strongest direct predictors of binary mortality risk. Female sex was associated with lower mortality, largely mediated through GrimAgeEAA or in combination with other epigenetic aging markers. SES was inversely related to biological aging as measured by DunedinPoAm in both cohorts. DunedinPoAm also showed a strong positive correlation with GrimAgeEAA, which directly predicted mortality. Notably,

frailty status was positively associated with several EAA metrics and female sex, particularly in NHANES, reinforcing the relevance of biological aging as a correlate of frailty as a multidimensional clinical syndrome. While the configuration of interconnections among biological aging markers was moderately consistent across cohorts, simpler ABN models with only one or two parents per child (**Figure S3: Additional File 6**) produced sparser and less informative networks.

In both NHANES and HRS, GSEM derived from the 3-parent limit additive Bayesian network framework demonstrated consistent patterns of associations across biological aging, social determinants, and mortality (**Table 3**). Baseline age showed a robust and direct association with mortality risk in both cohorts (NHANES: β=0.857, SE=0.043; HRS: β=1.099, SE=0.092; both $p<0.001$). GrimAgeEAA also significantly predicted mortality in NHANES (β=0.541, SE=0.054) and HRS (β=0.522, SE=0.068). Female sex was inversely associated with GrimAgeEAA, DunedinPoAm, and HorvathAgeEAA in both cohorts, indicating lower biological aging metrics in females, although it concurrently positively predicted frailty status (β=+0.848, SE=0.129 for NHANES, β=0.418, SE=0.133 for HRS). In both cohorts, higher SES predicted reduced frailty, even though frailty itself did not predict all-cause mortality in the ABN model and only marginally predicted HorvathAgeEAA in the NHANES prior to adjustment for sampling design complexity. Additionally, DunedinPoAm was strongly linked to other epigenetic clocks including GrimAgeEAA and PhenoAgeEAA, suggesting shared biological aging pathways. In both cohorts, SES predicted slower pace of aging as reflected by an inverse relationship with DunedinPoAm (e.g. β=-0.154, SE=0.026 in HRS, without survey weighting). Across both samples, consistent directionalities and statistical significance were largely retained after adjusting for sampling design complexity.

Through a series of multivariable-adjusted four-way decomposition models, and in both NHANES and HRS cohorts, frailty status was consistently associated with higher all-cause mortality risk, alternating five biological aging measures as potential mediators and/or moderators (**Figure 4, supplementary datasheet 3: Additional File 7**). Total effect risk ratios ranged from 1.72 to 1.87 in NHANES and from 2.28 to 2.36 in HRS, indicating a robust relationship between frailty and mortality. Four-way decomposition revealed that the majority of the excess mortality risk was attributable to the

controlled direct effect (CDE), accounting for over 90% of the total effect in models for 6 of 10 percentages controlled direct effects (P_CDE). Among the epigenetic clocks, GrimAgeEAA exhibited the strongest putatively mediating role in NHANES, with 33% of the association being potentially mediated (overall proportion mediated, op_m = 0.334, $p < 0.001$) under model assumptions and 38% of the effect eliminated under hypothetical intervention on the mediator (op_e = 0.385, $p < 0.001$). DunedinPoAm also demonstrated modest but statistically significant mediation effects in NHANES. In HRS, PhenoAgeEAA, DunedinPoAm and GrimAgeEAA emerged as modest mediators, with significant pure indirect effects and overall mediation (e.g., DunedinPoAm op_m = 0.089, $p = 0.040$). Conversely, HorvathEAA and HannumEAA clocks consistently showed weak or non-significant mediation effects in both cohorts. No meaningful contributions from reference or mediated interactions were detected. These findings suggest that specific epigenetic aging measures, particularly GrimAgeEAA and DunedinPoAm, may partially mediate the relationship between frailty and mortality, though the direct pathway remains predominant.

Reverse-causation models (epigenetic aging → frailty → mortality; **Figure S4: Additional File 8**) showed that second- and third-generation clocks had significant total associations with mortality, particularly GrimAge and DunedinPoAm. Frailty mediated approximately 8–18% of these associations across cohorts, with modest contributions from mediated interaction for advanced clocks. HorvathEAA showed little or no mediation. After adjustment for leukocyte composition (**Figure S4 : Additional File 8**), total effects were modestly attenuated. In NHANES, mediation for GrimAge, DunedinPoAm, and PhenoAge remained largely intact. In HRS, attenuation was more pronounced, though GrimAge mediation persisted. Overall, findings indicate partial but consistent mediation by second- and third-generation clocks, with the direct frailty–mortality pathway remaining predominant. Detailed findings can be examined in **supplementary datasheets 3** through **6 (Additional files 7, 9, 10** and **11)** , **Appendix VIII** of **Additional File 1** and on Github.

DISCUSSION

Summary of findings

In this study, we investigated the extent to which EAA may mediate or moderate the relationship between frailty and all-cause mortality using data from three large U.S. cohorts. Across NHANES, HRS, and HANDLS, frailty was consistently associated with a significantly elevated risk of mortality, independent of demographic and socioeconomic covariates. Among the five epigenetic clocks examined, GrimAge and DunedinPoAm emerged as the most salient mediators of this relationship. In NHANES, GrimAge explained approximately one-third (33%) of the total effect of frailty on mortality, while DunedinPoAm accounted for 17% of the association. In HRS, DunedinPoAm again demonstrated a modest but significant mediation effect, explaining 9% of the total effect. In contrast, Horvath and Hannum clocks showed minimal or non-significant mediation effects in both cohorts, suggesting that first-generation clocks may be less sensitive to biological changes linked to frailty and mortality. Notably, female sex was inversely associated with multiple epigenetic aging measures while being positively associated with frailty, highlighting a discordance between biological aging markers and clinical vulnerability. These findings support the hypothesis that accelerated biological aging, particularly as captured by GrimAge and DunedinPoAm, plays a partial but meaningful role in the pathway from frailty to mortality, while also suggesting that additional mechanisms beyond epigenetic aging contribute to mortality risk in frail individuals. These patterns were partly corroborated in HANDLS, despite the availability of only DunedinPACE among third-generation clocks. Overall, sensitivity analyses support the robustness of GrimAge, highlight heterogeneity across clocks, suggest partial bidirectionality, and reinforce cautious interpretation emphasizing shared biological aging processes rather than definitive mediation pathways.

Previous studies

Frailty status and mortality

Numerous studies confirm that both baseline frailty and transitions toward frailty are associated with significantly higher mortality risk (40, 41, 42). Importantly, frailty also modifies the effects of other risk factors on mortality, such as smoking (43), polypharmacy (44), and air pollution(45), suggesting a greater vulnerability to external and internal stressors. Longitudinal data highlight that improvements in frailty

status may reduce mortality risk, whereas deterioration worsens outcomes (41, 42). Findings across countries—including the U.S., Chile, China, and Europe—point to the global relevance of frailty as a strong mortality risk predictor (46, 47), with major implications for preventing premature death. In our study, frailty not emerging as a strong predictor in the ABN is likely due to shared variance that may have been absorbed by biological aging nodes, rather than being indicative of absence of association with all-cause mortality.

Association of socio-demographic and economic factors with frailty: epigenetic and other biological mechanisms

A substantial literature has established that socio-demographic and socioeconomic disadvantage is associated with frailty risk; more recent work has shifted toward understanding the biological pathways through which these effects are embedded. Lower educational attainment, income, and subjective social status are consistently linked to earlier frailty onset and progression (48, 49), largely through chronic psychosocial stress, adverse health behaviors, inflammation, and cardiometabolic dysregulation. Sex differences in these associations suggest that social support, caregiving roles, and cumulative stress exposures may differentially shape frailty trajectories in women and men (50, 51), while racial and ethnic disparities further reflect the impact of structural and cumulative disadvantage across the life course (52, 53). Importantly, Mendelian randomization and cross-national studies strengthen causal inference by demonstrating that genetically proxied socioeconomic traits—particularly educational attainment—are associated with frailty burden (54, 55). Emerging evidence indicates that epigenetic aging measures, especially clocks enriched for inflammatory and cardiometabolic pathways (e.g., GrimAge, DunedinPACE), may serve as key intermediates linking socioeconomic adversity to frailty by capturing the cumulative physiological toll of long-term disadvantage (35, 56, 57, 58). Framing socioeconomic determinants within this biological aging context advances the field beyond descriptive associations toward identifying modifiable pathways for intervention.

Across the NHANES and HRS cohorts, higher socioeconomic status (SES) was consistently associated with a slower biological pace of aging and a lower likelihood of frailty, as evidenced by the inverse

associations with DunedinPoAm and frailty risk. These findings align with a growing literature showing that socioeconomic advantage is linked to more favorable molecular aging profiles, likely through reduced chronic stress exposure, healthier behavioral patterns, and greater access to material and psychosocial resources that support physiological resilience. DunedinPoAm captures the coordinated rate of multisystem physiological decline and has been shown to be socially patterned, with faster aging observed among individuals exposed to socioeconomic disadvantage across the life course (35, 56, 57, 58). In parallel, extensive epidemiologic evidence demonstrates that lower SES is a strong predictor of frailty, reflecting the cumulative biological wear and tear associated with long-term material hardship and psychosocial adversity(59, 60). Together, these results support a model in which SES operates upstream of both molecular aging processes and clinical frailty, potentially linking social conditions to later-life vulnerability through accelerated biological aging pathways.

Association between frailty and epigenetic clocks

Emerging evidence indicates the role of epigenetic biomarkers in elucidating the biological underpinnings of frailty. Like our main findings, several studies have demonstrated that accelerated epigenetic aging, as measured by DNA methylation clocks, is significantly associated with higher frailty burden and worse clinical outcomes (61, 62, 63). Among these biomarkers, GrimAge has shown superior predictive validity for frailty and mortality compared to other clocks (64, 65), a finding that resonates with our current study. Longitudinally, epigenetic age acceleration has also been linked to transitions in frailty over time (64, 66). Mechanistic insights from systems biology suggest that frailty involves dysregulation of epigenetic pathways linked to inflammation, mitochondrial function, and oxidative stress(6, 67). These findings and others provide a promising path toward individualized risk stratification and therapeutic strategies (68), highlighting the value of biological aging measures in geriatric care. More specifically, prior work has shown that CpGs contributing to GrimAge map strongly to genes involved in inflammatory and cardiometabolic processes, while DunedinPoAm/PACE captures coordinated methylation changes reflecting the pace of multisystem physiological decline (35, 69). GrimAge and DunedinPoAm are derived from largely distinct CpG sets and were designed to capture overlapping but

non-identical dimensions of biological aging. Their interconnections in the Bayesian network likely reflect shared upstream aging processes—such as chronic inflammation, immune senescence, and metabolic dysregulation—rather than direct causal effects of one clock on another. Given evidence of bi-directionality between epigenetic aging and frailty and ABN identifies conditional dependencies rather than definitive causal directions, our findings are consistent with both frameworks: (1) frailty contributing to accelerated molecular aging and (2) molecular aging dysregulation acting as an upstream risk factor for frailty (17, 70).

Cardio-metabolic risk, frailty and multimorbidity in relation to epigenetic clocks and mortality risk: Bi-directional relationships

A growing body of evidence supports epigenetic clocks as molecular intermediaries linking cardiometabolic risk, frailty, multimorbidity, and mortality. Studies of cardiovascular health—particularly those using the American Heart Association's Life's Essential 8 (LE8)—demonstrate that more favorable cardiovascular profiles are associated with lower epigenetic age acceleration (EAA), and that second-generation clocks such as PhenoAge and GrimAge partially mediate associations between cardiovascular health and both all-cause and cardiovascular mortality (71, 72). Similarly, nonlinear associations between body mass index and survival appear to be partly explained by accelerated epigenetic aging, suggesting that DNAm-based aging metrics capture underlying metabolic dysregulation contributing to obesity-related mortality(71). In life-course analyses, Klopack et al. showed that epigenetic aging measures mediate associations between cumulative smoking exposure and later-life chronic morbidity and mortality in the HRS (73). Population-based studies further demonstrate that multiple epigenetic clocks mediate relationships between adverse lifestyle behaviors and premature death, reinforcing their role as integrative biomarkers of cumulative physiological stress (74). In clinical and aging cohorts, greater multimorbidity burden and composite indices such as the VACS Index are associated with higher EAA, which in turn predicts mortality (18). Collectively, these findings position epigenetic clocks as partial mediators

translating cardiometabolic and multisystem risk into earlier mortality, although formal tests of bidirectional mediation between epigenetic aging and multisystem morbidity remain limited.

Integrated Biological Aging Framework and Translational Implications for Frailty–Mortality Pathways

Frailty can be conceptualized as a clinical expression of multisystem physiological dysregulation, whereas epigenetic clocks such as GrimAge and DunedinPoAm represent molecular summaries of cumulative biological stress. GrimAge incorporates CpG surrogates linked to inflammatory and mortality-related pathways, and DunedinPoAm reflects the coordinated pace of multisystem decline (35, 69). Mortality, in turn, represents the downstream endpoint of accumulated vulnerability (75, 76, 77). Rather than functioning as independent predictors, frailty, epigenetic aging, and mortality likely align along shared biological axes—phenotypic vulnerability, molecular aging signatures, and clinical outcomes—consistent with geroscience frameworks proposing common mechanisms across age-related conditions (75, 76, 77). Mechanistically, chronic inflammation, immune senescence, oxidative stress, mitochondrial dysfunction, cardiometabolic dysregulation, and neuroendocrine stress signaling plausibly link these constructs (78, 79). Although GrimAge and DunedinPoAm capture overlapping dimensions of these processes, they do not directly measure discrete biological pathways. In our four-way decomposition analyses, the controlled direct effect accounted for the majority (>90% in many models) of the frailty–mortality association, with modest but significant mediation by GrimAge and DunedinPoAm and minimal interaction components. These findings suggest that epigenetic aging operates as a partial intermediary correlate rather than a dominant explanatory pathway. Stronger pathway-level inference will require longitudinal DNAm data, repeated frailty assessments, CpG-level mediation analyses, and integration with transcriptomic and proteomic profiling. Interventional studies targeting inflammatory burden or frailty trajectories will be essential to determine whether modifying biological aging processes meaningfully reduces mortality risk, thereby advancing translational relevance while maintaining appropriate causal caution.

Strengths and Limitations

This study offers several notable strengths. It investigates the association between biological aging and mortality risk in U.S. adults using three datasets. By integrating frailty, measured using standardized, harmonized instruments, alongside multiple EAA metrics, the study provides a comprehensive evaluation of how biological aging relates to mortality. The application of ABNs enhances the analysis by uncovering complex, probabilistic relationships among biological aging markers, sociodemographic characteristics, socioeconomic status, frailty, and mortality. The use of linked mortality data enables the investigation of long-term outcomes in relation to both clinical and molecular indicators of aging. Further methodological strength is added through the use of Cox regression models for survival analysis and GSEM to validate the inferred pathways.

Nonetheless, the present study has several limitations. These include cross-cohort heterogeneity in frailty and epigenetic measures (in definition, timing, and availability), reliance on primarily cross-sectional biomarker data, residual confounding due to incomplete harmonization of covariates (e.g., social relationship variables), and potential selection bias, including a healthy volunteer effect that may underestimate frailty prevalence and attenuate associations. Frailty and DNAm were measured contemporaneously (NHANES, HANDLS) or within a limited window (HRS). Although DNAm data theoretically allow derivation of multiple epigenetic biomarkers, the set of analyzable measures was constrained by cohort-specific factors, including differences in methylation arrays, CpG coverage, preprocessing pipelines, normalization procedures, and availability of calibration algorithms. For example, DunedinPACE was only available in HANDLS, whereas DunedinPoAm was available in NHANES and HRS. In addition, restricted access to raw DNAm data in NHANES and HRS, where only pre-computed epigenetic clock measures are available, limited the ability to derive alternative biomarkers. Consequently, we focused on clocks that were consistently available and harmonizable across cohorts to ensure comparability.

Furthermore, counterfactual mediation analyses rely on assumptions of no unmeasured confounding and correct temporal ordering; therefore, findings should be interpreted as consistent with intermediary processes rather than definitive causal pathways. Bidirectional relationships between frailty and epigenetic aging—supported by sensitivity analyses—further complicate causal interpretation. In this context, ABNs identify conditional dependencies but do not establish causal direction and should be viewed as hypothesis-generating.

Additional limitations include limited statistical power for cause-specific mortality and subgroup analyses, as well as the computational complexity of ABN modeling, which may affect replicability. The inability to include both frailty index (FI) and Fried frailty score (FFS) across all cohorts may have introduced additional heterogeneity; we prioritized FFS for consistency. Other differences in baseline age, clock availability, and follow-up duration may also affect cross-cohort comparability. Despite these limitations, this study provides robust, multi-cohort evidence supporting a role for epigenetic aging, particularly second- and third-generation clocks, as partial intermediaries in the frailty–mortality relationship.

Conclusions

In summary, epigenetic aging, particularly as measured by GrimAge and DunedinPoAm, explained in part the relationship between frailty and all-cause mortality, identifying potential intermediary biological processes rather than definitive causal pathways. In NHANES, GrimAge explained about one-third of the effect, while DunedinPoAm showed smaller but significant potential mediating effects in both NHANES and HRS. These clocks outperformed first-generation measures (Horvath, Hannum), which showed minimal or undetectable associations, as corroborated by DunedinPACE in the HANDLS study. Notably, female sex was inversely associated with several epigenetic aging measures yet positively associated with frailty, suggesting a divergence between biological aging markers and clinical vulnerability. Despite partial mediation, most of the association was attributable to the direct effect, indicating that additional processes also contribute. These findings underscore the importance of addressing both frailty and epigenetic aging to reduce mortality risk in older adults. Future work leveraging CpG-specific pathway

enrichment, transcriptomic integration, or locus-level mediation analyses may help elucidate the biological mechanisms underlying these associations and inform the development of frailty-sensitive or causally enriched epigenetic clocks.

DECLARATIONS

Acknowledgements

The authors would like to thank the participants, staff, and investigators of NHANES, HRS, and HANDLS for their invaluable contributions to these studies. Dr. Hind A. Beydoun and Dr. Jack Tsai worked on this manuscript outside her tour of duty at the U.S. Department of Veterans Affairs.

Consent for publication

Not applicable.

Funding

This research was supported, in part, by the Intramural Research Program of the National Institutes of Health (NIH). The contributions of the NIH author(s) were made as part of their official duties as NIH federal employees, are in compliance with agency policy requirements, and are considered Works of the United States Government. However, the findings and conclusions presented in this paper are those of the author(s) and do not necessarily reflect the views of the NIH or the U.S. Department of Health and Human Services. Funding was received under NIH Project AG000513.

Data availability

NHANES and HRS data are publicly available at: https://www.cdc.gov/nchs/nhanes/index.htm and https://hrs.isr.umich.edu/about, respectively.

HANDLS data are available upon reasonable request through a manuscript proposal process (https://handls.nih.gov/).

Code and analytic outputs supporting the findings of this study are available from the corresponding author upon reasonable request and will be made publicly available on GitHub at: https://github.com/baydounm/HRS_NHANES_HANDLS_FRAILEPIGENMORT

Authors' contributions

MAB: Conceptualization, data curation, statistical analysis, supervision, data acquisition, methodology, validation, manuscript drafting, and revision.

NNH: Conceptualization, data acquisition, methodology, resources, validation, manuscript drafting, and revision.

HAB: Conceptualization, data curation, manuscript drafting, and revision.

MFG: Conceptualization, data curation, data acquisition, methodology, validation, manuscript drafting, and revision.

JT: Conceptualization, methodology, supervision, manuscript drafting, and revision.

MKE: Conceptualization, supervision, data acquisition, resources, manuscript drafting, and revision.

ABZ: Conceptualization, data curation, supervision, data acquisition, resources, manuscript drafting, and revision.

All authors read and approved of the final manuscript.

Competing interests

The authors declare that they have no competing interests.

Ethics approval and consent to participate

NHANES protocols were approved by the National Center for Health Statistics (NCHS) Research Ethics Review Board (Protocol #98-12 for 1999–2000 and Protocol #2001-06 for 2001–2002 cycles), and all participants provided written informed consent.

The Health and Retirement Study (HRS) was approved by the University of Michigan Institutional Review Board (HUM00061128), and all participants provided informed consent.

The Healthy Aging in Neighborhoods of Diversity across the Life Span (HANDLS) study was approved by the National Institutes of Health Intramural Research Program Institutional Review Board (protocol numbers available upon request), and all participants provided written informed consent.

The present study used de-identified, publicly available (NHANES and HRS) and restricted-access (HANDLS) secondary data and was therefore exempt from additional institutional review board approval.

Table 1. Cohort characteristics and measurements

Cohort	Study Design & Years	Age Range at Baseline	Frailty Measure	Epigenetic Aging Measures	Timing of DNAm & Frailty Assessment	Mortality Follow-up Source & Period	Final Analytic Sample Size
NHANES	Nationally representative, 1999–2002	≥50 years	Fried phenotype (adapted): BMI<18.5, fatigue (DPQ), lifting difficulty, walking difficulty, low activity	Horvath, Hannum, PhenoAge, GrimAge (EAA residuals), DunedinPoAm	Baseline (1999–2002)	National Death Index, through 2019	1,537
HRS	Nationally representative, 2016 wave	≥50 years	Fried phenotype (adapted): BMI change equivalent to a weight loss of with weight loss >10 lbs/year (2014-2016), grip strength, walking difficulty, CES-D exhaustion, low activity	Horvath, Hannum, PhenoAge, GrimAge (EAA residuals), DunedinPoAm	Frailty: Mainly 2016; DNAm: 2016	NDI + Exit interviews, through 2022	1,466
HANDLS	Urban probability sample, 2004–2009	30–64 years	FRAIL scale (fatigue, resistance, ambulation, illness, weight loss)	Horvath, Hannum, PhenoAge, GrimAge, DunedinPACE	Baseline (2004–2009)	National Death Index, through 2022	455

Abbreviations: BMI = body mass index; CES-D = Center for Epidemiologic Studies–Depression scale; DNAm = DNA methylation; DPQ = Depression Questionnaire; EAA = epigenetic age acceleration; FRAIL = Fatigue, Resistance, Ambulation, Illness, and Loss of weight scale; HANDLS = Healthy Aging in Neighborhoods of Diversity across the Life Span; HRS = Health and Retirement Study; NDI = National Death Index; NHANES = National Health and Nutrition Examination Survey.

Table 2. Study characteristics and mortality risk across three cohorts (NHANES, HRS and HANDLS)

	NHANES 1999-2002	**HRS 2016**	**HANDLS 2004-2009**
	Mean (SE)	Mean (SE) or %	Mean (SE) or %
Demographics	(n=1,537)	(n=1,415)	(n=455)
Age	68.3 (0.3)	68.6 (0.4)	46.9 (0.8)***
Sex, % female	56.0	54.9	52.3
Race/ethnicity			
Non-Hispanic White	81.1	81.7	39.7***
Non-Hispanic Black	7.8	8.4	60.2
Hispanic	7.8	7.2	—
Other	3.2	2.7	—
Epigenetic age acceleration metrics	(n=1,537)	(N=1,415)	(n=455)
HorvathAgeEAA	+0.32 (0.20)	+0.08 (0.20)	+0.18 (0.36)
HannumAgeEAA	-0.11 (0.18)	+0.19 (0.15)	-0.37 (0.37)
PhenoAgeEAA	-0.10 (0.26)	-0.24 (0.23)	—
GrimAgeEAA	-0.46 (0.19)	-0.47 (0.18)	—
DunedinPoAm[1]	+1.10 (0.005)	+1.07 (0.003)	+1.05 (0.011)
SES z-score[1]	+0.352 (0.055)	+0.217 (0.044)	+0.500 (0.067)
Frailty status, %[1]	24.6	22.7	7.3
	(N=1,537)	(N=1,413)	(N=455)
Mortality rate, per 1,000 Person-years, with 95% CI	43.3 (39.8-47.0)	24.7 (21.4-28.6)	10.2 (7.6-13.8)***

Abbreviations: CI=Confidence Interval; DunedinPoAm=Dunedin Pace of Aging DNA methylation clock; GrimAgeEAA=Grim DNA methylation Epigenetic Age Acceleration; HANDLS=Healthy Aging in Neighborhoods of Diversity Across the Life Span; HannumAgeEAA=Hannum DNA methylation Age; HorvathAgeEAA=Horvath DNA methyalation Age Epigenetic Age Acceleration; HRS=Health and Retirement Study; n=unweighted sample;

NHANES=National Health and Nutrition Examination Surveys; PhenoAgeEAA=Pheno DNA methylation Age Epigenetic Age Acceleration; SE=Standard Error; SES=Socio-economic status, based on educational attainment and income level.

[1]In HANDLS, DunedinPACE was made readily available rather than DunedinPoAm. SES z-scores were not readily comparable across cohorts. Frailty was also measured differently and thus cannot be readily compared.

*P<0.05; **P<0.010; ***P<0.001 for null hypothesis of no difference in means or proportions based on a set of bivariate linear or multinomial logit regression models with Cohort as the only predictor, comparing HRS to NHANES and HANDLS to NHANES while accounting only for sampling weights.

Table 3. Generalized Structural Equations Models in NHANES, HRS and HANDLS samples based on the 3-parents/child limit Additive Bayesian Network Model solution for each cohort[a]

	Model 1[b]		**Model 2[c]**	
	β (SE)	P[d]	β (SE)	P[d]
NHANES 1999-2019 (n=1,537)				
AGE→DIED	+0.831 (0.034)	<0.001	+0.857 (0.043)	<0.001
AGE → SES	-0.142 (0.023)	<0.001	-0.134 (0.036)	<0.001
SEX→Frailty	+0.848 (0.129)	<0.001	+1.002 (0.208)	<0.001
SEX→HorvathAgeEAA	-0.204 (0.052)	<0.001	-0.187 (0.068)	<0.001
SEX→DunedinPoAm	-0.291 (0.048)	<0.001	-0.271 (0.058)	<0.001
SEX→GrimAgeEAA	-0.525 (0.033)	<0.001	-0.461 (0.039)	<0.001
NHB→SES	-0.652 (0.061)	<0.001	-0.668 (0.086)	<0.001
NHB→HannumAgeEAA	-0.429 (0.046)	<0.001	-0.317 (0.047)	<0.001
HISP→Frailty	-0.542 (0.144)	<0.001	-0.284 (0.260)	0.28
HISP→SES	-1.052 (0.052)	<0.001	-1.063 (0.107)	<0.001
HISP→ HorvathAgeEAA	-0.092 (0.054)	0.085	-0.179 (0.067)	0.012
SES→Frailty	-0.573 (0.075)	<0.001	-0.649 (0.104)	<0.001
SES→ DunedinPoAm	-0.130 (0.024)	<0.001	-0.176 (0.029)	<0.001
Frailty→ HorvathAgeEAA	+0.114 (0.061)	0.064	+0.067 (0.077)	0.39
HorvathAgeEAA→ DunedinPoAm	+0.129 (0.024)	<0.001	+0.128 (0.038)	0.002
HorvathAgeEAA→ HannumAgeEAA	+0.623 (0.019)	<0.001	+0.598 (0.033)	<0.001
HorvathAgeEAA→ PhenoAgeEAA	+0.404 (0.022)	<0.001	+0.415 (0.029)	<0.001
HannumAgeEAA→ PhenoAgeEAA	+0.301 (0.023)	<0.001	+0.276 (0.043)	<0.001
PhenoAgeEAA→ GrimAgeEAA	+0.190 (0.018)	<0.001	+0.214 (0.031)	<0.001
GrimAgeEAA→DIED	+0.423 (0.033)	<0.001	+0.541 (0.054)	<0.001
DunedinPoAm→ HannumAgeEAA	+0.131 (0.020)	<0.001	+0.152 (0.024)	<0.001
DunedinPoAm→ GrimAgeEAA	+0.558 (0.018)	<0.001	+0.567 (0.026)	<0.001

DunedinPoAm→ PhenoAgeEAA	+0.251 (0.018)	<0.001	+0.253 (0.018)	<0.001
HRS 2016-2022 (n=1,413)				
AGE→DIED	+1.035 (0.067)	<0.001	+1.099 (0.092)	<0.001
AGE→ SES	-0.211 (0.025)	<0.001	-0.253 (0.033)	<0.001
AGE→Frailty	+0.484 (0.064)	<0.001	+0.561 (0.080)	<0.001
.SEX→Frailty	+0.418 (0.133)	0.002	+0.339 (0.016)	<0.001
SEX→ HorvathAgeEAA	-0.181 (0.052)	<0.001	-0.134 (0.073)	0.072
SEX→ GrimAgeEAA	-0.515 (0.037)	<0.001	-0.508 (0.048)	<0.001
SEX→DunedinPoAM	-0.257 (0.052)	<0.001	-0.278 (0.058)	<0.001
NHB→SES	-0.631 (0.071)	<0.001	-0.701 (0.107)	<0.001
NHB→ HannumAgeEAA	-0.486 (0.062)	<0.001	-0.431 (0.087)	<0.001
HISP→SES	-1.062 (0.082)	<0.001	-1.144 (0.153)	<0.001
HISP→ HorvathAgeEAA	-0.191 (0.078)	0.016	-0.307 (0.047)	0.034
HISP→ PhenoAgeEAA	+0.280 (0.075)	<0.001	+0.327 (0.093)	0.001
SES→Frailty	-0.641 (0.070)	<0.001	-0.729 (0.106)	<0.001
SES→ DunedinPoAm	-0.154 (0.026)	<0.001	-0.180 (0.040)	<0.001
HorvathAgeEAA→HannumAgeEAA	+0.351 (0.022)	<0.001	+0.345 (0.041)	<0.001
HorvathAgeEAA→ DunedinPoAm	+0.114 (0.027)	<0.001	+0106 (0.034)	0.003
HorvathAgeEAA→PhenoAgeEAA	+0.239 (0.024)	<0.001	+0.220 (0.040)	<0.001
PhenoAgeEAA → HannumAgeEAA	+0.340 (0.023)	<0.001	+0.348 (0.039)	<0.001
PhenoAgeEAA → GrimAgeEAA	+0.179 (0.019)	<0.001	+0.180 (0.022)	<0.001
GrimAgeEAA→DIED	+0.517 (0.057)	<0.001	+0.522 (0.068)	<0.001
DunedinPoAm→ GrimAgeEAA	+0.578 (0.020)	<0.001	+0.586 (0.027)	<0.001
DunedinPoAm→ PhenoAgeEAA	+0.210 (0.024)	<0.001	+0.215 (0.028)	<0.001

Abbreviations: AGE=Baseline age; DIED=Death event (yes vs. no); DunedinPoAm=Dunedin Pace of Aging DNA methylation clock; Frailty=Frailty status; GrimAgeEAA=Grim DNA methylation Epigenetic Age Acceleration; HannumAgeEAA=Hannum DNA methylation Age, Epigenetic Age Acceleration; HISP=Hispanic;

HorvathAgeEAA=Horvath DNA methyalation Age, Epigenetic Age Acceleration; HRS=Health and Retirement Study; n=unweighted sample; NHANES=National Health and Nutrition Examination Surveys; NHB=Non-Hispanic Black; HISP=Hispanic; OTHER= Other race/ethnicities; PhenoAgeEAA=Pheno DNA methylation Age Epigenetic Age Acceleration; SE = Standard Error; SEX=Female vs. Male.

[a] Generalized structural equations models were conducted as a series of linear (most equations) and Weibull models (for the DIED outcome equation). The structure of each model was determined based on the 3-parent limit solution from ABNs for NHANES, HRS and HANDLS cohorts.

[b] Model 1 was conducted without adjustment for sampling design complexity and thus assuming a simple random sample.

[c] Model 2 adjusted for sampling design complexity by including sampling weights, PSU and strata that were most appropriate for each cohort.

[d] P-value for null hypothesis that path coefficient $\beta=0$. All $p<0.001$ passed False Discovery Rate correction.

FIGURE LEGEND

FIGURE 1. Kaplan-Meier survival curves across tertiles of SES, frailty, and markers of biological aging for the cohorts: NHANES 1999–2019, HRS 2016–2022 and HANDLS 2004-2022

Abbreviations: ACM=All-cause mortality; chi2 = Chi-square; DunedinPoAm = Dunedin Pace of Aging DNA methylation clock; GrimAgeEAA = Grim DNA methylation Epigenetic Age Acceleration; HANDLS=Healthy Aging in Neighborhoods of Diversity Across the Life Span; HannumAgeEAA = Hannum DNA methylation Age, Epigenetic Age Acceleration; HorvathAgeEAA = Horvath DNA methylation Age, Epigenetic Age Acceleration; HRS = Health and Retirement Study; NHANES = National Health and Nutrition Examination Surveys; PhenoAgeEAA = Pheno DNA methylation Age Epigenetic Age Acceleration; SES = Socio-economic Status; T1 = First tertile; T2 = Second Tertile; T3 = Third tertile.
Notes: Kaplan-Meier survival curves were conducted in all three cohorts with time on study considered as the time variable to event (all-cause death) or censoring by end of follow-up. Maximum follow-up time ranged from ~8 years for HRS to 20 years for NHANES. Median values for tertiles (T1/T2/T3) were +0.93 to 1.02 / +1.065 to 1.10 / +1.160 to +1.21 for DunedinPoAm across 3 cohorts; -4.50 to -4.38 / -0.86 to -0.75 / +4.40 to +4.56 for GrimAgeEAA across 2 cohorts; -5.38 to -4.58 / -0.054 to +0.381 / +4.48 to 5.16 for HannumAgeEAA across 3 cohorts; -4.88 to -4.30 / -0.108 to +0.272 / +4.40 to 5.45 for HorvathAgeEAA across 3 cohorts; -6.18 to -6.14/ -0.294 to -0.008 / +5.65 to +6.33 / for PhenoAgeEAA across 2 cohorts. SES z-scores have T1/T2/T3 corresponding approximately to a median of -1.12 to -0.94 / -0.083 to +0.38 /+0.84 to +1.20 for NHANES, HANDLS and HRS. Frailty status is included as a binary exposure (0=pre-frail/robust vs. 1=frail). Unweighted sample sizes were n=1,537 for NHANES, n=1,413 for HRS and n=455 for HANDLS.

FIGURE 2. Association of each biological aging metric, frailty, and SES z-scores with mortality risk adjusting for key exogenous variables: Cox proportional hazards models

Abbreviations:
DunedinPoAm = Dunedin Pace of Aging DNA methylation clock; GrimAgeEAA = Grim DNA methylation Epigenetic Age Acceleration; HANDLS=Healthy Aging in Neighborhoods of Diversity Across the Life Span HannumAgeEAA = Hannum DNA methylation Age, Epigenetic Age Acceleration; HorvathAgeEAA = Horvath DNA methylation Age, Epigenetic Age Acceleration; HRS = Health and Retirement Study; NHANES = National Health and Nutrition Examination Surveys; PhenoAgeEAA = Pheno DNA methylation Age Epigenetic Age Acceleration; SES = Socio-economic Status; z = standardized z-score.

Notes: Models are adjusted for age, sex, and race/ethnicity within each cohort. Values are Ln(hazard ratios) with 95% CI for each biological aging metric. Sampling weights were accounted for in this analysis. Unweighted sample sizes were n=1,537 for NHANES, n=1,413 for HRS and n=455 for HANDLS.

FIGURE 3. Additive Bayesian network solutions for 3 parents/child and model fit for 3 parents/child solution for associations among biological aging metrics, demographics, and mortality risk (discrete time hazards)

Abbreviations:
DunedinPoAm = Dunedin Pace of Aging DNA methylation clock; GrimAgeEAA = Grim DNA methylation Epigenetic Age Acceleration HannumAgeEAA = Hannum DNA methylation Age, Epigenetic Age Acceleration; HorvathAgeEAA = Horvath DNA methylation Age, Epigenetic Age

Acceleration; HRS = Health and Retirement Study; NHANES = National Health and Nutrition Examination Surveys; PhenoAgeEAA = Pheno DNA methylation Age Epigenetic Age Acceleration; SES = Socio-economic Status; z = standardized z-score.
Notes: This is a simplified version of the ABN solution. See **Figure S3** for more details.

Figure 4. Heatmap of four-way decomposition models for frailty status and all-cause mortality by epigenetic age acceleration measures in NHANES (1999–2002, mortality follow-up through 2019) and HRS (2016, mortality follow-up through 2022).

This figure displays standardized estimates from four-way decomposition models evaluating epigenetic age acceleration as a mediator of the association between frailty status and all-cause mortality. Rows represent epigenetic clocks and columns represent decomposition components. Color gradients reflect the magnitude and direction of effects (blue = negative; red = positive). Cell values denote point estimates, with asterisks indicating statistical significance ($P < 0.05$).

Decomposition parameters include: *tereri* (total excess relative risk); *ereri_cde* (excess relative risk due to the controlled direct effect); *ereri_pie* (excess relative risk due to the pure indirect effect); *ereri_intmed* (excess relative risk due to mediated interaction); *ereri_intref* (excess relative risk due to reference interaction); *terira* (total effect risk ratio); proportion components (*p_cde, p_pie, p_intmed, p_intref*); and overall summary measures (*op_m*, overall proportion mediated; *op_ati*, overall proportion attributable to interaction; *op_e*, overall proportion eliminated).

Models were adjusted for age, sex, race/ethnicity, and socioeconomic status index. Unweighted analytic sample sizes were n = 1,537 (NHANES) and n = 1,413 (HRS).

REFERENCES

1. Fried LP, Tangen CM, Walston J, Newman AB, Hirsch C, Gottdiener J, et al. Frailty in older adults: evidence for a phenotype. J Gerontol A Biol Sci Med Sci. 2001;56(3):M146-56.
2. Clegg A, Young J, Iliffe S, Rikkert MO, Rockwood K. Frailty in elderly people. Lancet. 2013;381(9868):752-62.
3. Theou O, Walston J, Rockwood K. Operationalizing Frailty Using the Frailty Phenotype and Deficit Accumulation Approaches. Interdiscip Top Gerontol Geriatr. 2015;41:66-73.
4. Ferrucci L, Gonzalez-Freire M, Fabbri E, Simonsick E, Tanaka T, Moore Z, et al. Measuring biological aging in humans: A quest. Aging Cell. 2020;19(2):e13080.
5. Gale CR, Marioni RE, Harris SE, Starr JM, Deary IJ. DNA methylation and the epigenetic clock in relation to physical frailty in older people: the Lothian Birth Cohort 1936. Clin Epigenetics. 2018;10(1):101.
6. Lozupone M, Solfrizzi V, Sardone R, Dibello V, Castellana F, Zupo R, et al. The epigenetics of frailty. Epigenomics. 2024;16(3):189-202.
7. Li X, Delerue T, Schottker B, Holleczek B, Grill E, Peters A, et al. Derivation and validation of an epigenetic frailty risk score in population-based cohorts of older adults. Nat Commun. 2022;13(1):5269.
8. Horvath S. DNA methylation age of human tissues and cell types. Genome Biol. 2013;14(10):R115.
9. Hannum G, Guinney J, Zhao L, Zhang L, Hughes G, Sadda S, et al. Genome-wide methylation profiles reveal quantitative views of human aging rates. Mol Cell. 2013;49(2):359-67.
10. Chen BH, Marioni RE, Colicino E, Peters MJ, Ward-Caviness CK, Tsai PC, et al. DNA methylation-based measures of biological age: meta-analysis predicting time to death. Aging (Albany NY). 2016;8(9):1844-65.
11. Marioni RE, Shah S, McRae AF, Chen BH, Colicino E, Harris SE, et al. DNA methylation age of blood predicts all-cause mortality in later life. Genome Biol. 2015;16(1):25.
12. Phyo AZZ, Wu Z, Espinoza SE, Murray AM, Fransquet PD, Wrigglesworth J, et al. Epigenetic age acceleration and cognitive performance over time in older adults. Alzheimers Dement (Amst). 2024;16(3):e70010.
13. Savin MJ, Wang H, Pei H, Aiello AE, Assuras S, Caspi A, et al. Association of a pace of aging epigenetic clock with rate of cognitive decline in the Framingham Heart Study Offspring Cohort. Alzheimers Dement (Amst). 2024;16(4):e70038.
14. Beydoun MA, Shaked D, Tajuddin SM, Weiss J, Evans MK, Zonderman AB. Accelerated epigenetic age and cognitive decline among urban-dwelling adults. Neurology. 2020;94(6):e613-e25.
15. Joyce BT, Gao T, Zheng Y, Ma J, Hwang SJ, Liu L, et al. Epigenetic Age Acceleration Reflects Long-Term Cardiovascular Health. Circ Res. 2021;129(8):770-81.
16. Mendelson MM. Epigenetic Age Acceleration: A Biological Doomsday Clock for Cardiovascular Disease? Circ Genom Precis Med. 2018;11(3):e002089.
17. Lin X, Hu Z, Tang L, Zhan Y. Association between frailty index and epigenetic aging acceleration in older adults: Evidence from the health and retirement study. Exp Gerontol. 2025;205:112765.
18. Oursler KK, Marconi VC, Wang Z, Xu K, Montano M, So-Armah K, et al. Epigenetic Age Acceleration Markers Are Associated With Physiologic Frailty and All-Cause Mortality in People With Human Immunodeficiency Virus. Clin Infect Dis. 2023;76(3):e638-e44.

19. Koller D, & Friedman, N. Probabilistic Graphical Models: Principles and Techniques. : MIT Press; 2009.
20. Calderon A, Baik SY, Ng MHS, Fitzsimmons-Craft EE, Eisenberg D, Wilfley DE, et al. Machine learning and Bayesian network analyses identifies associations with insomnia in a national sample of 31,285 treatment-seeking college students. BMC Psychiatry. 2024;24(1):656.
21. Calderon A, Baik SY, Ng MHS, Fitzsimmons-Craft EE, Eisenberg D, Wilfley DE, et al. Machine Learning and Bayesian Network Analyses Identifies Psychiatric Disorders and Symptom Associations with Insomnia in a national sample of 31,285 Treatment-Seeking College Students. Res Sq. 2024.
22. Tarabeih N, Kalinkovich A, Ashkenazi S, Cherny SS, Shalata A, Livshits G. Analysis of the Associations of Measurements of Body Composition and Inflammatory Factors with Cardiovascular Disease and Its Comorbidities in a Community-Based Study. Biomedicines. 2024;12(5).
23. Discacciati A, Bellavia A, Lee JJ, Mazumdar M, Valeri L. Med4way: a Stata command to investigate mediating and interactive mechanisms using the four-way effect decomposition. Int J Epidemiol. 2018.
24. Yu W, Gao C, Zhao X, Li C, Fan B, Lv J, et al. Four-way decomposition of effect of cigarette smoking and body mass index on serum lipid profiles. PLoS One. 2022;17(8):e0270486.
25. Beydoun MA, Beydoun HA, Noren Hooten N, Li Z, Hu YH, Georgescu MF, et al. Plasma proteomic biomarkers as mediators or moderators for the association between poor cardiovascular health and white matter microstructural integrity: The UK Biobank study. Alzheimers Dement. 2025;21(2):e14507.
26. Zipf G, Chiappa M, Porter KS, Ostchega Y, Lewis BG, Dostal J. National health and nutrition examination survey: plan and operations, 1999-2010. Vital Health Stat 1. 2013(56):1-37.
27. Sonnega A, Faul JD, Ofstedal MB, Langa KM, Phillips JW, Weir DR. Cohort Profile: the Health and Retirement Study (HRS). Int J Epidemiol. 2014;43(2):576-85.
28. Evans MK, Lepkowski JM, Powe NR, LaVeist T, Kuczmarski MF, Zonderman AB. Healthy aging in neighborhoods of diversity across the life span (HANDLS): overcoming barriers to implementing a longitudinal, epidemiologic, urban study of health, race, and socioeconomic status. Ethn Dis. 2010;20(3):267-75.
29. Griffin FR, Mode NA, Ejiogu N, Zonderman AB, Evans MK. Frailty in a racially and socioeconomically diverse sample of middle-aged Americans in Baltimore. PLoS One. 2018;13(4):e0195637.
30. Beydoun MA, Noren Hooten N, Fanelli-Kuczmaski MT, Maino Vieytes CA, Georgescu MF, Beydoun HA, et al. Growth Differentiation Factor 15 and Diet Quality Trajectory Interact to Determine Frailty Incidence among Middle-Aged Urban Adults. J Nutr. 2024;154(5):1652-64.
31. Kuczmarski MF, Beydoun MA, Georgescu MF, Noren Hooten N, Mode NA, Evans MK, et al. Pro-Inflammatory Diets Are Associated with Frailty in an Urban Middle-Aged African American and White Cohort. Nutrients. 2023;15(21).
32. Beydoun MA, Noren Hooten N, Asefa NG, Georgescu MF, Song M, Beydoun HA, et al. Telomere Length, Epigenetic Age Acceleration, and Mortality Risk in US Adult Populations: An Additive Bayesian Network Analysis. Aging Cell. 2025;24(9):e70159.
33. Beydoun MA, Beydoun HA, Noren Hooten N, Maldonado AI, Weiss J, Evans MK, et al. Epigenetic clocks and their association with trajectories in perceived discrimination and

depressive symptoms among US middle-aged and older adults. Aging (Albany NY). 2022;14(13):5311-44.
34. Beydoun MA, Hossain S, Chitrala KN, Tajuddin SM, Beydoun HA, Evans MK, et al. Association between epigenetic age acceleration and depressive symptoms in a prospective cohort study of urban-dwelling adults. J Affect Disord. 2019;257:64-73.
35. Belsky DW, Caspi A, Corcoran DL, Sugden K, Poulton R, Arseneault L, et al. DunedinPACE, a DNA methylation biomarker of the pace of aging. Elife. 2022;11.
36. U.S. Department of Health and Human Services. Annual update of the HHS poverty guidelines. 2004 [Available from: https://www.federalregister.gov/documents/2004/02/13/04-3329/annual-update-of-the-hhs-poverty-guidelines.
37. StataCorp Stata Statistical Software: Release 18, College Station, TX: StataCorp LLC. 2023.
38. R Core Team. R: A Language and Environment for Statistical Computing. R Foundation for Statistical Computing, Vienna, Austria. URL https://www.R-project.org/. 2024.
39. VanderWeele TJ, Shrier I. Sufficient Cause Representation of the Four-way Decomposition for Mediation and Interaction. Epidemiology. 2016;27(5):e32-3.
40. Cespedes Feliciano EM, Hohensee C, Rosko AE, Anderson GL, Paskett ED, Zaslavsky O, et al. Association of Prediagnostic Frailty, Change in Frailty Status, and Mortality After Cancer Diagnosis in the Women's Health Initiative. JAMA Netw Open. 2020;3(9):e2016747.
41. Li CM, Lin CH, Li CI, Liu CS, Lin WY, Li TC, et al. Frailty status changes are associated with healthcare utilization and subsequent mortality in the elderly population. BMC Public Health. 2021;21(1):645.
42. Wang Z, Ruan H, Li L, Song N, He S. Association of changes in frailty status with the risk of all-cause mortality and cardiovascular death in older people: results from the Chinese Longitudinal Healthy Longevity Survey (CLHLS). BMC Geriatr. 2024;24(1):96.
43. Patiño-Hernández D, Pérez-Bautista Ó G, Pérez-Zepeda MU, Cano-Gutiérrez C. Does the association between smoking and mortality differ due to frailty status? A secondary analysis from the Mexican Health and Aging Study. Age Ageing. 2022;51(12).
44. Midão L, Brochado P, Almada M, Duarte M, Paúl C, Costa E. Frailty Status and Polypharmacy Predict All-Cause Mortality in Community Dwelling Older Adults in Europe. Int J Environ Res Public Health. 2021;18(7).
45. Gerber Y, Myers V, Broday DM, Steinberg DM, Yuval, Koton S, et al. Frailty status modifies the association between air pollution and post-myocardial infarction mortality: a 20-year follow-up study. J Am Coll Cardiol. 2014;63(16):1698-9.
46. Molina N, Wehinger S, Marrugat J, Subirana I, Fuentes E, Palomo I. Effect of frailty status on mortality risk among chilean community-dwelling older adults. Geriatr Nurs. 2024;57:154-62.
47. Zhao X, Zhu R, Chen Q, He J. Effect of frailty status on mortality risk among Chinese community-dwelling older adults: a prospective cohort study. BMC Geriatr. 2023;23(1):150.
48. Hanlon P, Politis M, Wightman H, Kirkpatrick S, Jones C, Khan M, et al. Frailty and socioeconomic position: A systematic review of observational studies. Ageing Res Rev. 2024;100:102420.
49. Van der Linden BWA, Cheval B, Sieber S, Orsholits D, Guessous I, Stringhini S, et al. Life Course Socioeconomic Conditions and Frailty at Older Ages. J Gerontol B Psychol Sci Soc Sci. 2020;75(6):1348-57.

50. Dong P, Zhang XQ, Yin WQ, Li ZY, Li XN, Gao M, et al. The relationship among socioeconomic status, social support and frailty: is there a gender difference? Aging Clin Exp Res. 2025;37(1):111.
51. Wang HY, Zhang M, Sun X. Sex-Specific Association Between Socioeconomic Status, Lifestyle, and the Risk of Frailty Among the Elderly in China. Front Med (Lausanne). 2021;8:775518.
52. Majid Z, Welch C, Davies J, Jackson T. Global frailty: The role of ethnicity, migration and socioeconomic factors. Maturitas. 2020;139:33-41.
53. Wu AH, Setiawan VW, Stram DO, Crimmins EM, Tseng CC, Lim U, et al. Racial, Ethnic, and Socioeconomic Differences in a Deficit Accumulation Frailty Index in the Multiethnic Cohort Study. J Gerontol A Biol Sci Med Sci. 2023;78(7):1246-57.
54. Huang J, Gui Y, Wu J, Xie Y. Causal effects of socioeconomic traits on frailty: a Mendelian randomization study. Front Med (Lausanne). 2024;11:1344217.
55. Wilkie RZ, Ailshire JA. Socioeconomic Inequalities in Frailty Distribution: A Cross-National Comparison of the United States and England. J Gerontol B Psychol Sci Soc Sci. 2024;79(11).
56. Harris KM, Levitt B, Gaydosh L, Martin C, Meyer JM, Mishra AA, et al. Sociodemographic and Lifestyle Factors and Epigenetic Aging in US Young Adults: NIMHD Social Epigenomics Program. JAMA Netw Open. 2024;7(7):e2427889.
57. Schmitz LL, Opsasnick LA, Ratliff SM, Faul JD, Zhao W, Hughes TM, et al. Epigenetic biomarkers of socioeconomic status are associated with age-related chronic diseases and mortality in older adults. PNAS Nexus. 2025;4(4):pgaf121.
58. Willems YE, Rezaki AD, Aikins M, Bahl A, Wu Q, Belsky DW, et al. Social determinants of health and epigenetic clocks: Meta-analysis of 140 studies. medRxiv. 2025.
59. Geronimus AT, Hicken M, Keene D, Bound J. "Weathering" and age patterns of allostatic load scores among blacks and whites in the United States. Am J Public Health. 2006;96(5):826-33.
60. Braveman P, Gottlieb L. The social determinants of health: it's time to consider the causes of the causes. Public Health Rep. 2014;129 Suppl 2(Suppl 2):19-31.
61. Kuiper LM, Polinder-Bos HA, Bizzarri D, Vojinovic D, Vallerga CL, Beekman M, et al. Epigenetic and metabolomic biomarkers for biological age: a comparative analysis of mortality and frailty risk. The Journals of Gerontology: Series A. 2023;78(10):1753-62.
62. Lin X, Hu Z, Tang L, Zhan Y. Association between frailty index and epigenetic aging acceleration in older adults: Evidence from the health and retirement study. Experimental Gerontology. 2025:112765.
63. Verschoor CP, Lin DT, Kobor MS, Mian O, Ma J, Pare G, et al. Epigenetic age is associated with baseline and 3-year change in frailty in the Canadian Longitudinal Study on Aging. Clinical epigenetics. 2021;13:1-10.
64. Mak JK, Karlsson IK, Tang B, Wang Y, Pedersen NL, Hägg S, et al. Temporal dynamics of epigenetic aging and frailty from midlife to old age. The Journals of Gerontology: Series A. 2024;79(10):glad251.
65. McCrory C, Fiorito G, Hernandez B, Polidoro S, O'Halloran AM, Hever A, et al. GrimAge outperforms other epigenetic clocks in the prediction of age-related clinical phenotypes and all-cause mortality. The Journals of Gerontology: Series A. 2021;76(5):741-9.

66. Hillstedt E, Wahlin RR, Castegren M, Sandblom G, Kane A. SCOPING REVIEW OF CLINICAL STUDIES EXPLORING THE ASSOCIATION BETWEEN EPIGENETIC AGE AND FRAILTY. Innovation in Aging. 2023;7(Suppl 1):1115.
67. Gomez-Verjan J, Ramírez-Aldana R, Pérez-Zepeda M, Quiroz-Baez R, Luna-López A, Gutierrez Robledo L. Systems biology and network pharmacology of frailty reveal novel epigenetic targets and mechanisms. Scientific reports. 2019;9(1):10593.
68. García-Giménez JL, Mena-Molla S, Tarazona-Santabalbina FJ, Viña J, Gomez-Cabrera MC, Pallardó FV. Implementing precision medicine in human frailty through epigenetic biomarkers. International journal of environmental research and public health. 2021;18(4):1883.
69. Lu AT, Quach A, Wilson JG, Reiner AP, Aviv A, Raj K, et al. DNA methylation GrimAge strongly predicts lifespan and healthspan. Aging (Albany NY). 2019;11(2):303-27.
70. Mak JKL, Karlsson IK, Tang B, Wang Y, Pedersen NL, Hagg S, et al. Temporal Dynamics of Epigenetic Aging and Frailty From Midlife to Old Age. J Gerontol A Biol Sci Med Sci. 2024;79(10).
71. Carbonneau M, Li Y, Prescott B, Liu C, Huan T, Joehanes R, et al. Epigenetic Age Mediates the Association of Life's Essential 8 With Cardiovascular Disease and Mortality. J Am Heart Assoc. 2024;13(11):e032743.
72. Zhao Y, Yang H, Jiao R, Wang Y, Xiao M, Song M, et al. Phenotypic age mediates effects of Life's Essential 8 on reduced mortality risk in US adults. Precis Clin Med. 2024;7(3):pbae019.
73. Ler P, Jylhava J, Hagg S, Finkel D, Dahl Aslan AK, Ploner A, et al. The mediating role of epigenetic ageing in the nonlinear association between body mass index and survival: a prospective cohort analysis of the US Health and Retirement Study. EBioMedicine. 2025;119:105883.
74. Chen XL, Zhao QQ, Lin SR, He XL, Zhang XJ, Li SJ, et al. Epigenetic clocks as mediators of health behaviors and mortality in middle-aged and older adults. J Nutr Health Aging. 2025;29(7):100602.
75. Lopez-Otin C, Blasco MA, Partridge L, Serrano M, Kroemer G. The hallmarks of aging. Cell. 2013;153(6):1194-217.
76. Lopez-Otin C, Blasco MA, Partridge L, Serrano M, Kroemer G. Hallmarks of aging: An expanding universe. Cell. 2023;186(2):243-78.
77. Kennedy BK, Berger SL, Brunet A, Campisi J, Cuervo AM, Epel ES, et al. Geroscience: linking aging to chronic disease. Cell. 2014;159(4):709-13.
78. Franceschi C, Garagnani P, Parini P, Giuliani C, Santoro A. Inflammaging: a new immune-metabolic viewpoint for age-related diseases. Nat Rev Endocrinol. 2018;14(10):576-90.
79. Ferrucci L, Fabbri E. Inflammageing: chronic inflammation in ageing, cardiovascular disease, and frailty. Nat Rev Cardiol. 2018;15(9):505-22.

Additional Files

Additional File 1: Supplementary Appendices I–VIII
This file contains detailed methodological and supporting materials. Appendix I describes cohort design, sampling, and documentation for NHANES, HRS, and HANDLS. Appendix II details harmonized frailty definitions and algorithms across cohorts. Appendix III summarizes epigenetic clock derivation and age acceleration measures. Appendix IV outlines discrete-time hazard modeling. Appendix V describes the additive Bayesian network (ABN) framework and workflow. Appendix VI presents generalized structural equation modeling (GSEM) specifications. Appendix VII details four-way decomposition methods and assumptions, including sensitivity analyses with leukocyte adjustment. Appendix VIII summarizes sensitivity analysis findings across primary and reverse-causation models.

Additional File 2: Figures S1
Fig. S1 – Participant flowcharts for NHANES (1999–2002), HRS (2016), and HANDLS (2004–2009), showing sample selection and exclusions.

Additional File 3: Figure S2
Fig. S2 – Pearson correlation matrices and kernel density plots of frailty scores across NHANES, HRS, and HANDLS, illustrating relationships among SES, frailty, and epigenetic aging measures.

Additional File 4: Supplementary Datasheet 1
Supplementary Datasheet 1 – Correlation matrices and descriptive statistics for SES, frailty, and epigenetic aging measures across cohorts.

Additional File 5: Supplementary Datasheet 2
Supplementary Datasheet 2 – Multivariable Cox regression results for associations between SES, frailty, epigenetic clocks, and all-cause mortality across NHANES, HRS, and HANDLS.

Additional File 6: Figure S3
Fig. S3 – Additive Bayesian network (ABN) models for NHANES and HRS under varying parent limits (1–3 parents per node), including final network structures and model fit comparisons across specifications.

Additional File 7: Supplementary Datasheet 3
Supplementary Datasheet 3 – Detailed four-way decomposition results (primary models) for NHANES and HRS, including total effects and component estimates.

Additional File 8: Figure S4
Fig. S4 – Heatmaps summarizing four-way decomposition results for frailty–epigenetic aging–mortality pathways across primary and sensitivity analyses, including leukocyte-adjusted and reverse-causation models.

Additional File 9: Supplementary Datasheet 4
Supplementary Datasheet 4 – Four-way decomposition results with leukocyte (WBC) adjustment across NHANES and HRS.

Additional File 10: Supplementary Datasheet 5
Supplementary Datasheet 5 – Reverse-causation four-way decomposition results (epigenetic aging → frailty → mortality).

Additional File 11: Supplementary Datasheet 6
Supplementary Datasheet 6 – Reverse-causation four-way decomposition results with additional leukocyte (WBC) adjustment.

(A) NHANES 1999-2002; follow-up until 2019

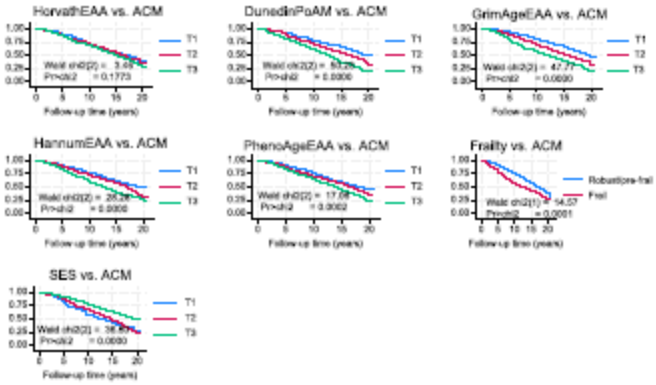

(B) HRS 2016, follow-up until 2022

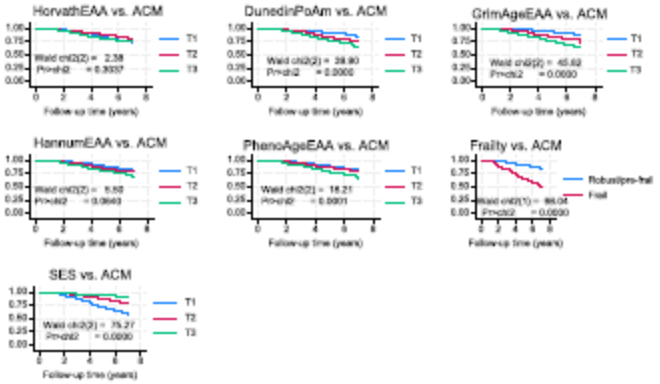

(C) HANDLS 2004-2009, follow-up until 2022

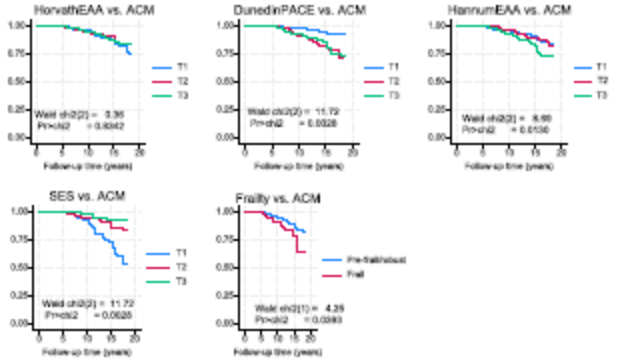

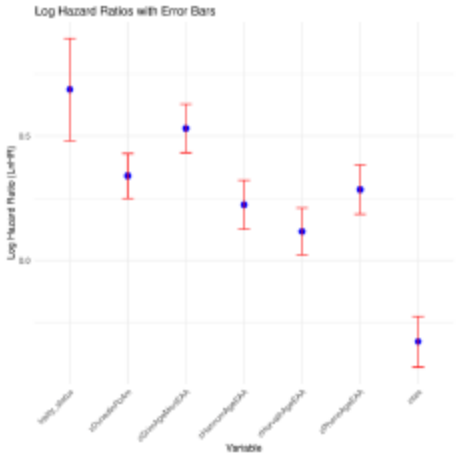

(A) NHANES 1999–2019

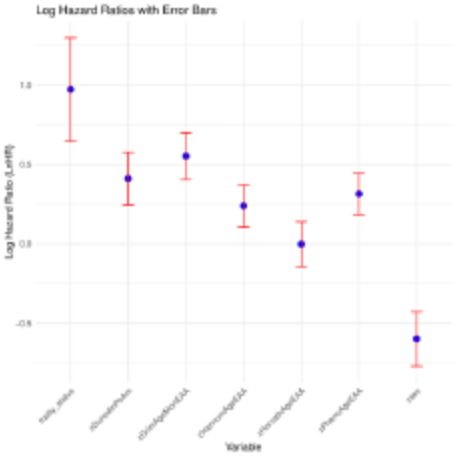

(B) HRS 2016–2022

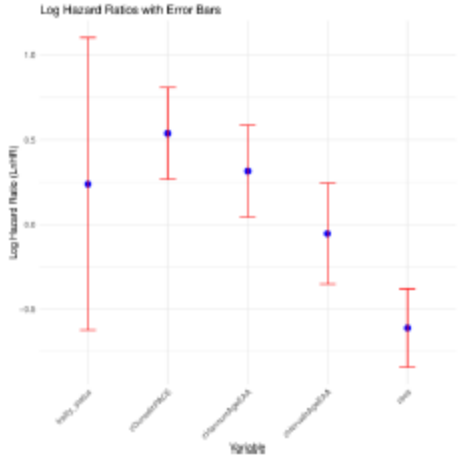

(C) HANDLS 2004–2022

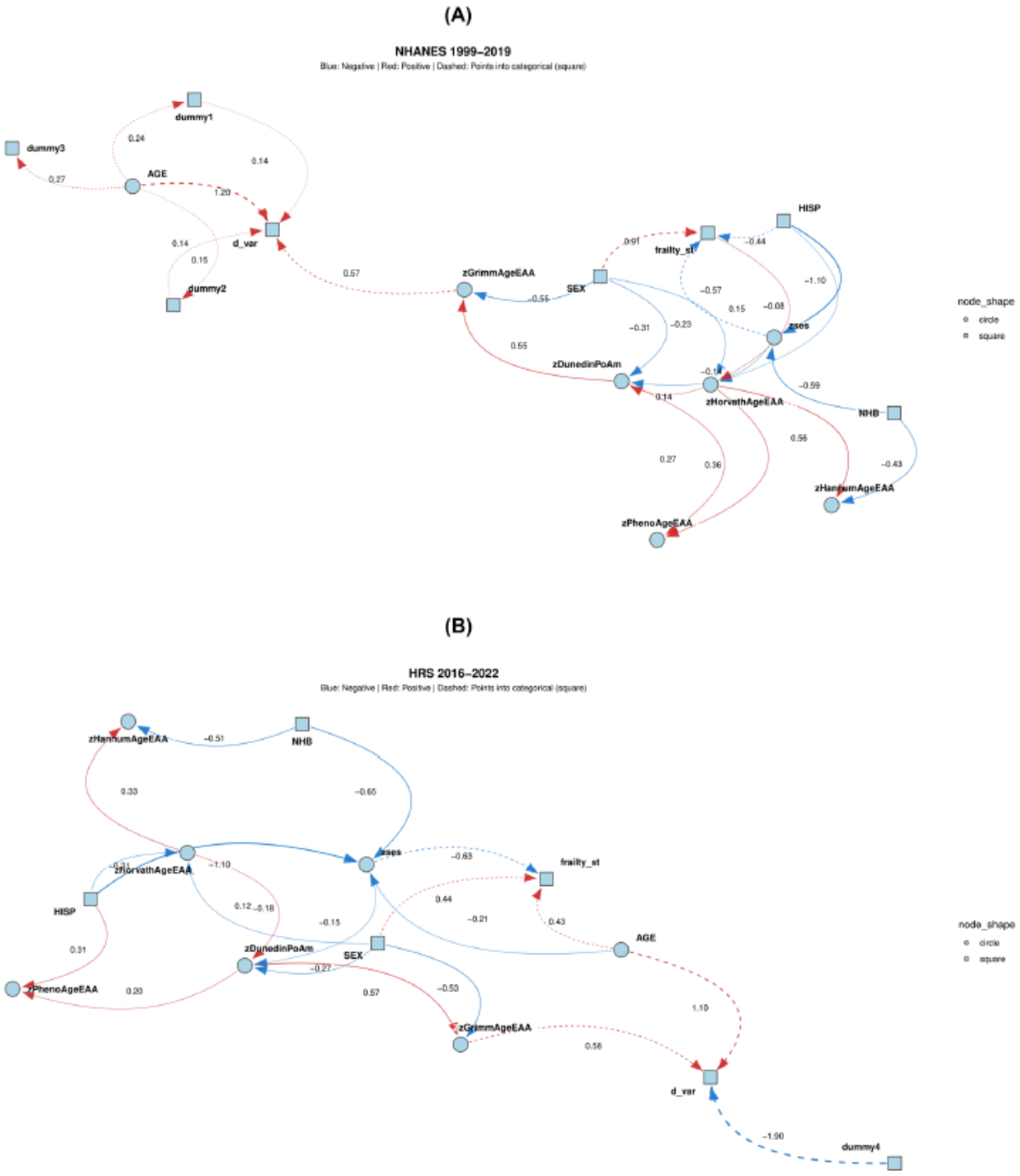
(A)
NHANES 1999–2019
Blue: Negative | Red: Positive | Dashed: Points into categorical (square)
dummy1
dummy3
AGE
d_var
dummy2
zGrimmAgeEAA
SEX
frailty_st
HISP
zses
zDunedinPoAm
zHorvathAgeEAA
NHB
zHannumAgeEAA
zPhenoAgeEAA
node_shape
circle
square
(B)
HRS 2016–2022
Blue: Negative | Red: Positive | Dashed: Points into categorical (square)
zHannumAgeEAA
NHB
zHorvathAgeEAA
zses
frailty_st
HISP
zDunedinPoAm
SEX
AGE
zPhenoAgeEAA
zGrimmAgeEAA
d_var
dummy4
node_shape
circle
square

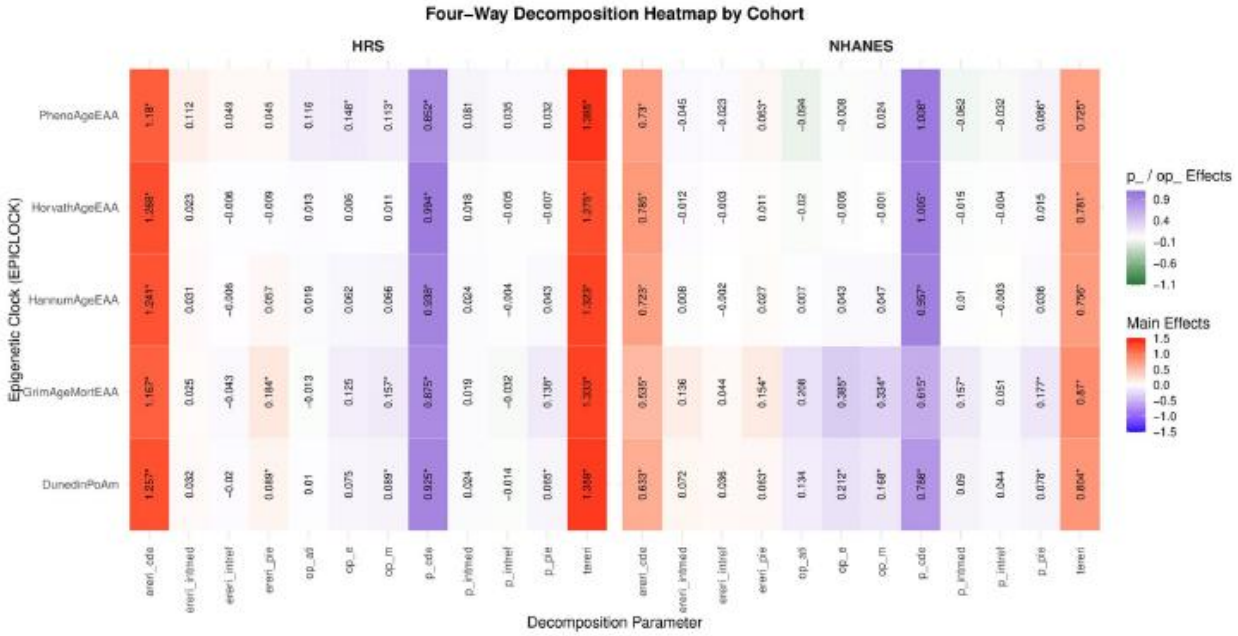

SUPPLEMENTARY MATERIALS

APPENDIX I. DATABASES AND DETAILED STUDY DESIGN DOCUMENTATION

1) NHANES:

The CDC's NHANES website provides comprehensive resources to support data interpretation, including documentation on survey methodology, sample design, estimation procedures, and analytical strategies. These materials are regularly updated to reflect changes in survey structure and advances in statistical methods. Key components of NHANES analytic resources include the Plan and Operations Reports, Sample Design Documentation, Estimation and Weighting Procedures, and overarching Analytic Standards. The Analytic Guidelines for 1999–2010 offer detailed instructions for analyzing data from that period, while the Analytic Guidance for the 2017–March 2020 Pre-pandemic Data Files addresses challenges encountered during the COVID-19 pandemic and provides guidance for combining multiple survey cycles to produce nationally representative estimates.
For the present study, we used demographic data from the 1999–2000 and 2001–2002 cycles, which were merged with additional serum biomarker data to generate epigenetic clock measures. Although the demographic files cover individuals aged 0 to 85+, our analysis was restricted to participants aged 50 years and older, consistent with the availability of DNA methylation (DNAm) data. Most analyses employed a two-cycle weighting scheme, using four-year sample weights adjusted to account for the subset of participants with available epigenetic measures.

Source: https://wwwn.cdc.gov/nchs/nhanes/analyticguidelines.aspx

2) HRS:

The Health and Retirement Study (HRS) offers extensive documentation on its survey design and methodology. The Data Collection Path Table provides a historical overview of HRS data initiatives, with links to detailed information on each dataset. The longitudinal cohort sample design illustrates how the HRS integrates successive birth cohorts over time, maintaining a steady-state sampling approach by refreshing the study population with younger cohorts every six years. Detailed tables summarize sample sizes and interview response rates by survey wave, panel, race/ethnicity, and cohort. Survey weights are provided to ensure nationally representative estimates.
To support data management and analysis, resources such as An Elementary Cookbook of Data Management using HRS Data with SPSS, SAS, and Stata Examples offer practical guidance across statistical software. Technical reports elaborate on survey design, including the use of unfolding brackets to reduce item nonresponse and the imputation methods used across waves. Administrative materials cover IRB protocols and other governance-related considerations.
For this project, we used the 2020 HRS RAND FAT FILE, V1.A, released in May 2024, and the Cross-Wave Tracker File, updated in November 2024, which includes data through early 2022. The Tracker File provides a unique record per respondent and is used here to determine death dates and follow-up time for survival analyses. RAND and Tracker File resources are accessible at:

- RAND HRS: https://hrsdata.isr.umich.edu/data-products/rand
- Tracker File: https://hrsdata.isr.umich.edu/data-products/cross-wave-tracker-file

Source: https://hrs.isr.umich.edu/documentation/survey-design

3) HANDLS

The Healthy Aging in Neighborhoods of Diversity across the Life Span (HANDLS) study is a population-based, prospective cohort launched by the National Institute on Aging Intramural Research Program (NIA/IRP) in 2004. Its primary goal is to investigate the interplay between race, socioeconomic status (SES), and health disparities across the life course, particularly in urban environments. The HANDLS cohort comprises 3,720 community-dwelling adults aged 30–64 years at baseline, recruited from 13 neighborhoods in Baltimore, Maryland. Participants were selected using an area probability sampling strategy across a factorial design of sex, race (Black and White), age group, and poverty status (above or below 125% of the federal poverty level), ensuring diverse representation.

Source: https://handls.nih.gov/

APPENDIX II. FRAILTY ALGORITHM AND DOCUMENTATION

Frailty was initially operationalized using the Fried frailty phenotype, a widely used clinical model that characterizes frailty as a biological syndrome resulting from cumulative declines across multiple physiological systems. This model defines frailty based on the presence of three or more of the following five criteria, originally proposed by Fried et al. (2001) (1):

1. Unintentional weight loss (shrinking): Self-reported unintentional weight loss of >10 pounds (4.5 kg) in the past year, or a significant decline in body mass index (BMI), operationalized here as an annualized BMI decrease of ≥ 1.5 kg/m².
2. Weakness: Assessed via handgrip strength, defined as being in the lowest 20th percentile, adjusted for sex and body mass index.
3. Exhaustion: Based on self-reported items from the Center for Epidemiologic Studies Depression (CES-D) scale, indicating a frequent feeling of effort or inability to get going.
4. Slowness: Measured via gait speed or walking time over a specified distance (e.g., 2.5 or 4 meters), with the slowest 20% adjusted for sex and height considered frail.
5. Low physical activity: Determined using questionnaire data on weekly energy expenditure or frequency of engagement in moderate or vigorous activities, with thresholds based on sex-specific cut-points.

Both NHANES and HRS used a modified version of the Fried frailty phenotype. In HANDLS, another definition was used as described in a later section.

Other source: https://my.clevelandclinic.org/health/diseases/frailty

1) NHANES

We operationalized the Fried frailty phenotype based on five domains—shrinking, weakness, slowness, low physical activity, and fatigue—using available proxy variables from NHANES 1999–2000 and 2001–2002. The analysis combined relevant datasets across cycles, generated indicators for each frailty component, and constructed a summary frailty score and categorical frailty status. Below is a summary of the procedure:

Data Preparation and Merging

1. **Import and Append Data Files:**
    - The following NHANES data files were extracted and appended across cycles: *BMX (Body Measures)*, *PAQ (Physical Activity)*, *PFQ (Physical Functioning)*, and *DEMO (Demographics)*.
    - Each dataset was appended across cycles 1 (1999–2000) and 2 (2001–2002) after tagging them with a cycle variable.
    - The final working dataset was generated by sequentially merging DEMO with BMX, PAQ, and PFQ using SEQN as the key.

Frailty Component Definitions

Each frailty component was operationalized using available NHANES variables as follows:

1. Shrinking
   Proxy: Body Mass Index (BMI)
   Variable: BMXBMI
   Definition: Participants with BMI < 18.5 were coded as frail for shrinking.
2. Weakness
   Proxy: Self-reported difficulty lifting or carrying 10 pounds
   Variable: PFQ060E
   Definition: Responses of "some difficulty", "much difficulty", or "unable to do" were coded as frail.
3. Slowness
   Proxy: Difficulty walking a quarter mile
   Variable: PFQ060B
   Definition: Same response scheme as weakness; difficulty of any kind coded as frail.
4. Low Physical Activity
   Proxies: Engagement in vigorous or moderate physical activity in the past 30 days
   Variables: PAD200 (vigorous), PAD320 (moderate)
   Definition: Respondents answering "no" or "unable to do" for both items were classified as having low activity.
5. Fatigue
   Proxy: Difficulty walking up ten steps without resting
   Variable: PFQ060C
   Definition: Any reported difficulty (some, much, or unable) coded as frail.

Score Construction

- Each domain was scored as 1 (frail) or 0 (not frail).
- A frailty score was computed by summing the five components (range: 0–5).
- A frailty status categorical variable was then generated:
    - 0 = Robust (score = 0)
    - 0 = Pre-frail (score = 1–2)
    - 1 = Frail (score ≥ 3)

Final Output

The resulting dataset FRAILTY_NHANES.dta includes:

- Component variables (e.g., frail_weakness, frail_activity)
- The continuous frailty score (frailty_score)
- Categorical frailty status (frailty_status)

All analyses were conducted in Stata using syntax for data import (import sasxport5), appending, merging, recoding, and labeling consistent with NHANES documentation.

2) HRS

We constructed the Fried frailty score using data from the 2016 wave of the Health and Retirement Study (HRS), combining the RAND longitudinal file with the 2016 core physical measures (H16I_R) and psychosocial (H16LB_R) datasets. Data were preprocessed and merged using the unique household-person identifier (HHIDPN).
Fried frailty components were operationalized as follows:

1. Shrinking (Unintentional Weight Loss or being underweight): Calculated from BMI change between 2014 and 2016, with weight loss >10 lbs/year coded as 1 or being underweight in 2016 with BMI<18.5 $kg.m^{-2}$.
2. Weakness: Average grip strength across four trials (PI816, PI851–853); weakness was defined as being in the lowest sex-specific quintile (≤27.1 kg for men, ≤16.6 kg for women).
3. Slowness: Proxy based on self-reported difficulty walking several blocks (r13walksa).
4. Exhaustion: Derived from two CES-D items: "felt everything was an effort" (PLB018G) and "could not get going" (PLB018J); endorsement of either item (agree/strongly agree) classified as exhaustion.
5. Low Physical Activity: Defined as low frequency of vigorous or moderate physical activity (≤3 times per month or never, based on r13vgactx and r13mdactx).

Each component was coded as 1 (present) or 0 (absent), and summed to create the Fried frailty score (range 0–5). Based on established thresholds:

- 0 = Robust
- 1–2 = Pre-frail
- 3–5 = Frail

The final analytic dataset (hrs2016_friedfrailty_final.dta) includes individual component variables, total frailty score, and frailty status label. This approach aligns with prior research applying Fried's criteria in aging cohorts and facilitates integration with other HRS biomarker and epigenetic data.

3) HANDLS

The FRAIL scale comprises five domains: fatigue, resistance (ability to climb stairs), ambulation (ability to walk a specific distance), number of illnesses, and weight loss. We followed the original operationalization described by Morley et al., with the exception of the weight loss domain, which was adapted according to Theou et al.. Fatigue was assessed using item 20 from the Center for Epidemiologic Studies Depression Scale (CES-D), which asks: "During the past week, did you feel you could not get going?" Fatigue was coded as present if participants reported experiencing this feeling occasionally (3–4 days per week) or most of the time (5–7 days per week). Resistance was defined by self-reported difficulty climbing 10 stairs without resting. Ambulation was determined by whether participants reported difficulty walking a quarter of a mile. Illness burden was assessed based on self-reported physician diagnoses of 11 conditions: hypertension, diabetes, cancer, chronic lung disease, myocardial infarction, congestive heart failure, angina, asthma, arthritis, stroke, and kidney disease. The presence of five or more conditions was coded as meeting the illness criterion. Weight loss was assessed via item 2 of the CES-D: "During the past week, did you not feel like eating or have a poor appetite?" This domain was considered present if participants reported the symptom occasionally (3–4 days) or most of the time (5–7 days). Each present domain contributed one point to the total FRAIL score, resulting in a range from 0 (no components present) to 5 (all components present). Scores were categorized as follows: frail (3–5), pre-frail (1–2), and not frail (0). For binary classification, individuals with scores of 3 or higher were considered frail, while those with scores of 0–2 were considered not frail. Inclusion in the analytic sample required complete data on at least three of the five FRAIL components, consistent with criteria used in the frailty phenotype framework.

APPENDIX III. EPIGENEITC AGE ACCELERATION

Health and Retirement Study (HRS)

Epigenetic data were obtained from a subsample of 4,018 HRS participants, with high-quality DNA methylation (DNAm) profiles successfully generated for over 97% of samples. DNAm was assessed using the Illumina Infinium MethylationEPIC BeadChip array. To align with NHANES and other cohort studies, five widely used epigenetic clocks were selected: Horvath, Hannum, Levine PhenoAge, GrimAge, and Dunedin Pace of Aging (DunedinPoAM). For the first four clocks, epigenetic age acceleration (EAA) was calculated by regressing DNAm age on chronological age using a linear model, with the residuals representing the component of biological age not explained by chronological age. These residuals capture accelerated or decelerated aging and may range from fractions of a year to several years. As DunedinPoAm directly quantifies the pace of aging, no transformation was applied. All five clock-derived measures were standardized (z-scored), and extreme outliers were excluded prior to analysis.

Sources: https://hrsdata.isr.umich.edu/data-products/epigenetic-clocks and (2)

National Health and Nutrition Examination Survey (NHANES)

Detailed documentation for DNAm and epigenetic clock data in NHANES is available at: https://wwwn.cdc.gov/nchs/nhanes/dnam/. DNAm was measured using the Illumina MethylationEPIC BeadChip array among adults aged 50 years and older from diverse demographic backgrounds, with data available for the 1999–2000 and 2001–2002 waves. The DNAm data underwent extensive preprocessing and normalization, including quality control procedures to remove sample outliers and mismatches. Available datasets include normalized methylation matrices, biomarker data, and estimated blood cell proportions. As in HRS, we selected five clocks—Horvath, Hannum, PhenoAge, GrimAge, and DunedinPoAm—and applied the same residual-based method to calculate EAA for the first four clocks, while using DunedinPoAm as-is to capture aging rate.

Source: https://wwwn.cdc.gov/nchs/nhanes/dnam/

Healthy Aging in Neighborhoods of Diversity across the Life Span (HANDLS)

In the HANDLS study, DNAm was measured from peripheral blood samples using the Illumina Infinium MethylationEPIC BeadChip, consistent with the platforms used in HRS and NHANES. Epigenetic age was estimated using the Horvath and Hannum clocks, and EAA was derived by comparing the predicted DNAm age to chronological age using the residual approach. These residuals served as indicators of accelerated or decelerated biological aging. Additionally, HANDLS implemented the DunedinPACE clock to directly assess the pace of aging, in place of DunedinPoAm. This harmonized approach facilitated cross-cohort comparisons of biological aging trajectories.

Sources: (3, 4, 5, 6)

APPENDIX IV. DISCRETE TIME HAZARD MODEL:

Discrete-time hazard models are statistical methods used to analyze time-to-event data when time is measured in distinct intervals (e.g., years, months, or days). These models are particularly valuable in fields like public health, social sciences, and education, where time is often recorded in discrete units. A key feature of discrete-time hazard models is their reliance on a binary logistic regression framework, allowing for flexible incorporation of time-varying covariates and straightforward estimation using standard regression software. These models offer several advantages, including effective handling of tied

event times, adaptability to varying covariate values across time, and compatibility with widely used software platforms such as R, Stata, and SAS.
In implementation, the data must be structured in a person-period format, where each individual contributes multiple records—one for each time interval at risk. The model involves defining discrete time periods, specifying a baseline hazard function (often using time dummies), and incorporating relevant covariates. Importantly, discrete-time hazard models align well with additive Bayesian network (ABN) frameworks, which support Gaussian, binomial, and Poisson distributions (see Appendix V). However, limitations include the need to discretize continuous time, potential loss of information with wide intervals, and the assumption of constant risk within each interval.

$$\log\left(\frac{h_t}{1-h_t}\right) = \beta_0 + \sum_{i=1}^{p} \beta_i X_i$$

Sources: (7)

APPENDIX V. ADDITIVE BAYESIAN NETWORKS:

A) Theoretical framework

Additive Bayesian Networks (ABNs) are a class of probabilistic graphical models that represent conditional dependencies among variables using a directed acyclic graph (DAG). They offer key benefits such as multivariate analysis, potential for causal inference, and adaptability to various data types and distributions. In ABNs, each node's distribution is modeled locally—typically using linear regression for continuous variables and logistic regression for binary outcomes. Central to ABNs is Bayes' Theorem, which guides the estimation of posterior distributions by combining the likelihood from observed data with prior distributions. The model selection process involves a scoring function, often incorporating the Bayesian Information Criterion (BIC), to balance fit and complexity. ABNs are widely applied in disciplines like epidemiology, genetics, and the social sciences to examine complex inter-variable relationships and uncover potential causal pathways.

Sources: (8, 9)

The following set of equations are used in this method:

(Eq. 1.1) *Linear regression*: $Y = \beta_0 + \sum_{i=1}^{k} \beta_i X_i + \varepsilon$

(Eq. 1.2) *Logistic regression*: $logit\big(P(Y = 1|X_1, \dots, X_k)\big) = \beta_0 + \sum_{i=1}^{k} \beta_i X_i$

(Eq. 1.3) *Likelihood Function*: $\boldsymbol{L(\theta|D)} = \prod_{i=1}^{n} \boldsymbol{P(X_i \mid Parents(X_i), \theta_i)}$

(Eq. 1.4) *Bayesian Posterior*: $\boldsymbol{P(\theta|D)} = \frac{P(\boldsymbol{D}|\boldsymbol{\theta})P(\boldsymbol{\theta})}{\boldsymbol{P(D)}}$

(Eq. 3.5) *BIC for Model Selection*: $\boldsymbol{BIC = -2log\big(L(\theta|D)\big) + p \times log(n)}$

B) Additive Bayesian Network workflow

The R code, available on GitHub and applied to both NHANES and HRS datasets, provides a comprehensive framework for conducting ABN analysis. This includes steps for software installation, data preprocessing, specification of structural constraints, model fitting, and iterative model refinement. To determine the optimal number of parent nodes for each child node, the study assessed the stabilization of the log marginal likelihood in relation to model complexity across key variables. Given the high computational demands of ABN modeling and the large analytic sample (e.g., over 18,000 person-period observations in NHANES 1999–2019), the maximum number of parents per child node was limited to three. A two-parent configuration was only retained when the log marginal likelihood showed clear stabilization compared to the three-parent model.

Source: https://r-bayesian-networks.org/

APPENDIX VI. GENERALIZED STRUCTURAL EQUATIONS MODELS

Stata's Generalized Structural Equation Modeling (gsem) framework provides a versatile approach for modeling both linear and nonlinear relationships among variables. It supports a wide range of outcome types and allows for the inclusion of random effects. Estimation is conducted using Maximum Likelihood or Quasi-Maximum Likelihood methods, and model fit is assessed through various goodness-of-fit statistics and tests. The framework also enables users to generate linear predictions, compute residuals, and evaluate both linear and nonlinear combinations of model parameters.

Probability density function for Weibull distribution

$$f(t;\delta,k) = \frac{k}{\delta}(\frac{t}{\delta})^{k-1}e^{-(\frac{t}{\delta})^k}, t \geq 0$$

Where:

- *t is the time or random variable of interst.*
- *δ>0 is the scale parameter*
- *k>0 is the shape parameter*

Cumulative distribution function (CDF) and survival function (complement of CDF) for Weibull distribution

$$F(t;\delta,k) = 1 - e^{-(\frac{t}{\delta})^k}, t \geq 0$$

$$S(t;\delta,k) = e^{-(\frac{t}{\delta})^k}, t \geq 0$$

Hazard function for Weibull distribution

$$h(t;\delta,k) = \frac{f(t;\delta,k)}{S(t;\delta,k)} = \frac{k}{\delta}\left(\frac{t}{\delta}\right)^{k-1}, t \geq 0$$

Source: https://www.stata.com/manuals/semgsem.pdf

APPENDIX VII. Four-way decomposition models

Causal mediation analysis seeks to quantify the pathways through which an exposure affects an outcome, distinguishing between direct and indirect effects. Traditional approaches often assume no interaction between the exposure and the mediator. To overcome these limitations, four-way decomposition extends mediation analysis by accounting for both mediation and exposure–mediator interaction, partitioning the total effect into four components:

1. Controlled Direct Effect (CDE): The portion of the effect of the exposure on the outcome that is not mediated and not due to interaction.
2. Pure Indirect Effect (PIE): The effect that is solely mediated by the mediator, assuming no interaction.
3. Mediated Interaction (INTmed): The component attributable to both mediation and interaction—i.e., the mediator influences the outcome, and its effect depends on exposure.
4. Reference Interaction (INTref): The component that arises solely due to interaction between the exposure and mediator, assuming the mediator is fixed at a reference level.

To estimate these components, we used the med4way command in Stata with the *fulloutput* option. This provided the following parameters:

- tereri: *Total Excess Relative Risk* — the excess relative risk (RR - 1) comparing exposed vs. unexposed.
- terira: *Total Effect Risk Ratio* — the RR comparing the exposed group to the unexposed.
- ereri_cde: *Excess RR due to Controlled Direct Effect* — portion of the effect not explained by mediation or interaction.
- ereri_pie: *Excess RR due to Pure Indirect Effect* — mediated effect assuming no interaction.
- ereri_intmed: *Excess RR due to Mediated Interaction* — effect due to joint mediation and interaction.
- ereri_intref: *Excess RR due to Reference Interaction* — effect due solely to interaction with the mediator fixed at the reference level.

We also report proportions:

- p_cde: Proportion of the total effect attributable to the controlled direct effect (ereri_cde / tereri).
- p_pie: Proportion due to the pure indirect effect.
- p_intmed: Proportion due to mediated interaction.
- p_intref: Proportion due to reference interaction.

Global effect summaries include:

- op_m: *Overall Proportion Mediated* — the combined proportion mediated through PIE and INTmed.
- op_ati: *Overall Proportion Attributable to Interaction* — combined contribution of INTmed and INTref.
- op_e: *Overall Proportion Eliminated* — the proportion of the total effect that would be removed if the mediator were fixed at the reference level.

Assumptions

This decomposition relies on several key assumptions:

- No unmeasured confounding between exposure–outcome, exposure–mediator, and mediator–outcome paths.
- Correct model specification for both outcome and mediator.
- Positivity (non-zero probability of all covariate combinations).

- Consistency (observed data reflect counterfactual outcomes under the same conditions).

1. Counterfactual notation
Let:

- $A \in \{0,1\}$= exposure
- $M \in \{0,1\}$= mediator
- Y= outcome
- $Y_{a,m}$= potential outcome if $A = a, M = m$
- M_a= mediator value if $A = a$

Total effect (risk ratio scale):

$$RR_{TE} = \frac{E[Y_{1,M_1}]}{E[Y_{0,M_0}]}$$

Excess relative risk:

$$TERERI = RR_{TE} - 1$$

2. Four-way decomposition (Excess RR scale)
The total excess relative risk decomposes as:

$$TERERI = ERERI_{CDE} + ERERI_{PIE} + ERERI_{INTmed} + ERERI_{INTref}$$

(1) Controlled Direct Effect (CDE)
Mediator fixed at reference level $m = 0$:

$$ERERI_{CDE} = \frac{E[Y_{1,0}]}{E[Y_{0,0}]} - 1$$

(2) Pure Indirect Effect (PIE)
Effect of mediator under no interaction:

$$ERERI_{PIE} = \frac{E[Y_{0,M_1}]}{E[Y_{0,M_0}]} - 1$$

(3) Mediated Interaction (INTmed)
Joint mediation and interaction component:

$$ERERI_{INTmed} = \frac{E[Y_{1,M_1}] - E[Y_{1,M_0}] - E[Y_{0,M_1}] + E[Y_{0,M_0}]}{E[Y_{0,M_0}]}$$

(4) Reference Interaction (INTref)
Interaction when mediator fixed at reference:

$$ERERI_{INTref} = \frac{E[Y_{1,M_0}] - E[Y_{0,M_0}] - \left(E[Y_{1,M_1}] - E[Y_{0,M_1}]\right)}{E[Y_{0,M_0}]}$$

3. Total Effect Risk Ratio

$$TERIRA = RR_{TE} = \frac{E[Y_{1,M_1}]}{E[Y_{0,M_0}]}$$
$$TERERI = TERIRA - 1$$

4. Proportions

$$p_{CDE} = \frac{ERERI_{CDE}}{TERERI}$$
$$p_{PIE} = \frac{ERERI_{PIE}}{TERERI}$$
$$p_{INTmed} = \frac{ERERI_{INTmed}}{TERERI}$$
$$p_{INTref} = \frac{ERERI_{INTref}}{TERERI}$$

5. Global summaries

Overall Proportion Mediated

$$op_m = \frac{ERERI_{PIE} + ERERI_{INTmed}}{TERERI}$$

Overall Proportion Attributable to Interaction

$$op_{ati} = \frac{ERERI_{INTmed} + ERERI_{INTref}}{TERERI}$$

Overall Proportion Eliminated (if mediator fixed at reference)

$$op_e = \frac{ERERI_{PIE} + ERERI_{INTmed} + ERERI_{INTref}}{TERERI}$$

Assumptions (formalized)

1. No unmeasured confounding

$$Y_{a,m} \perp A \mid C$$
$$M_a \perp A \mid C$$
$$Y_{a,m} \perp M \mid A, C$$

2. Positivity

$$0 < P(A = a \mid C) < 1$$

3. Consistency

$$Y = Y_{a,m} \text{ if } A = a, M = m$$

4. Correct model specification

Outcome and mediator models correctly specified.

Implementation
Models were specified using Cox regression for time-to-event outcomes and linear regression for continuous mediators. Confidence intervals were computed using the delta method. The results provide nuanced causal insights, distinguishing how much of the effect is mediated biologically (e.g., through epigenetic age acceleration) and how much is due to direct or interactive pathways.

Sources: (10, 11)

Sensitivity analyses controlling for WBC composition:

For harmonized analyses of leukocyte composition, comparable complete blood count (CBC) variables are available from NHANES 1999–2002 and the Health and Retirement Study (HRS) 2016 Venous Blood Study (VBS). NHANES CBC documentation is available at:
1999–2000: https://wwwn.cdc.gov/Nchs/Data/Nhanes/Public/1999/DataFiles/LAB25.htm
2001–2002: https://wwwn.cdc.gov/Nchs/Data/Nhanes/Public/2001/DataFiles/L25_B.htm

In NHANES 1999–2002, venous whole blood was collected in Mobile Examination Centers and analyzed using standardized automated hematology analyzers under strict quality-control protocols. The CBC panel includes total white blood cell (WBC) count and a five-part differential reported as both percentages and absolute counts. The percentage variables include neutrophils, lymphocytes, monocytes, eosinophils, and basophils (each expressed as percent of total WBC). Absolute counts for each subtype (cells $\times 10^3/\mu L$) are also provided. For harmonization focused on leukocyte composition adjustment, the key variables are the five differential percentages and total WBC count, which together capture circulating immune cell distribution independent of red cell or platelet parameters. These measures are widely used to control for immune heterogeneity in analyses of inflammation, epigenetic aging, gene expression, and other molecular phenotypes.

The HRS 2016 Venous Blood Study (VBS) provides directly comparable venous-based CBC measures collected by trained phlebotomists during in-home visits and analyzed in certified laboratories using automated hematology platforms. Documentation is available through the HRS biomarker and VBS data description pages: https://hrsdata.isr.umich.edu/documentation (see 2016 Venous Blood Study files). The HRS VBS CBC includes total WBC count and a five-part differential, reported as both percentages and absolute counts for neutrophils, lymphocytes, monocytes, eosinophils, and basophils. Because both NHANES and HRS VBS use venous blood and automated differential counting, the percentage distributions of leukocyte subtypes are conceptually and methodologically comparable across studies. For harmonized modeling, the primary shared variables are: total WBC count and percent neutrophils, percent lymphocytes, percent monocytes, percent eosinophils, and percent basophils. These percentage measures provide a standardized representation of leukocyte composition suitable for covariate adjustment to reduce confounding due to variation in circulating immune cell mixtures. Using percentages rather than absolute counts further enhances cross-cohort comparability when laboratory platforms or calibration standards differ slightly between surveys.

Thus, as sensitivity analysis and in both NHANES 1999-2002 and HRS 2016, WBC composition was entered into the four-way composition models by including several common WBC percentage by sub-type into the model as exogenous variables in addition to the covariates that were originally entered into

the model. The exact list of covariates that is finally included in the sensitivity analyses is provided in the main methods section.

Sensitivity analyses for bi-directional relationships: Epigenetic aging → Frailty → mortality

To evaluate potential reverse or bi-directional pathways, we conducted sensitivity analyses specifying epigenetic aging as the exposure, frailty as the mediator, and mortality as the outcome. This framework tests whether accelerated biological aging increases mortality risk indirectly through increased frailty burden, while also allowing for exposure–mediator interaction. Using the same four-way decomposition approach implemented via the *med4way* command in Stata, we partitioned the total effect of epigenetic age acceleration on mortality into the Controlled Direct Effect (CDE), Pure Indirect Effect (PIE), Mediated Interaction (INTmed), and Reference Interaction (INTref). This allowed us to distinguish whether frailty functions primarily as a downstream pathway linking epigenetic aging to mortality, or whether the mortality risk associated with epigenetic aging operates largely independently of frailty status.

Models were specified consistently with the primary analysis, using Cox regression for mortality and linear regression for frailty indices, adjusting for demographic, socioeconomic, and health-related covariates. We compared the overall proportion mediated (op_m) and proportion attributable to interaction (op_ati) across forward and reverse models to assess directional robustness. If the mediated proportion remained substantial under this reversed specification, it would support a bidirectional feedback mechanism between biological aging and clinical vulnerability. Conversely, attenuation of the mediated component would suggest that epigenetic aging more plausibly operates downstream of frailty rather than as its upstream determinant.

Below are the **equations rewritten explicitly for the reverse-causation specification**:

- **Exposure:** epigenetic aging metric A(continuous; for interpretation you can set $A = a_1$vs $A = a_0$, e.g., +1 SD vs 0)
- **Mediator:** frailty index M(continuous)
- **Outcome:** mortality time-to-event T(Cox model), with effect summarized on an **RR/HR scale** (as in med4way output)

1) Counterfactual definitions (reverse model)

Let:

- M_a= frailty burden that would be observed if epigenetic aging were set to $A = a$
- $Y_{a,m}$= potential mortality outcome if $A = a$ and frailty were set to $M = m$
  (with $E[Y.]$interpreted as a **risk** or **hazard-based risk ratio** target used by med4way)

Total effect (epigenetic aging → mortality, through all pathways including frailty):

$$RR_{TE} \equiv TERIRA = \frac{E\left[Y_{a_1, M_{a_1}}\right]}{E\left[Y_{a_0, M_{a_0}}\right]}$$

Total excess relative risk:

$$TERERI = TERIRA - 1$$

2) Four-way decomposition (reverse model; Excess RR scale)

$$TERERI = ERERI_{CDE} + ERERI_{PIE} + ERERI_{INTmed} + ERERI_{INTref}$$

Choose a **reference frailty level** m(often $m = 0$ if $M$is centered/standardized; otherwise a meaningful baseline).

(1) Controlled Direct Effect (CDE)

Effect of epigenetic aging on mortality **holding frailty fixed** at m :

$$ERERI_{CDE} = \frac{E\left[Y_{a_1, m}\right]}{E\left[Y_{a_0, m}\right]} - 1$$

(2) Pure Indirect Effect (PIE)

Effect of epigenetic aging on mortality **only through changing frailty**, evaluated at baseline exposure a_0:

$$ERERI_{PIE} = \frac{E\left[Y_{a_0, M_{a_1}}\right]}{E\left[Y_{a_0, M_{a_0}}\right]} - 1$$

(3) Mediated Interaction (INTmed)

Portion due to **both** mediation and exposure–mediator interaction:

$$ERERI_{INTmed} = \frac{E\left[Y_{a_1, M_{a_1}}\right] - E\left[Y_{a_1, M_{a_0}}\right] - E\left[Y_{a_0, M_{a_1}}\right] + E\left[Y_{a_0, M_{a_0}}\right]}{E\left[Y_{a_0, M_{a_0}}\right]}$$

(4) Reference Interaction (INTref)

Portion due to **interaction only**, when frailty is set to what it would be under a_0:

$$ERERI_{INTref} = \left(\frac{E\left[Y_{a_1, M_{a_0}}\right]}{E\left[Y_{a_0, M_{a_0}}\right]} - \frac{E\left[Y_{a_1, m}\right]}{E\left[Y_{a_0, m}\right]}\right)$$

(Equivalent to "interaction contribution beyond the CDE" on the excess-RR scale.)

3) Proportions (reverse model)

$$p_{CDE} = \frac{ERERI_{CDE}}{TERERI}, p_{PIE} = \frac{ERERI_{PIE}}{TERERI}, p_{INTmed} = \frac{ERERI_{INTmed}}{TERERI}, p_{INTref} = \frac{ERERI_{INTref}}{TERERI}$$

4) Global summaries used for directionality checks

Overall proportion mediated (frailty-mediated share):

$$op_m = \frac{ERERI_{PIE} + ERERI_{INTmed}}{TERERI}$$

Overall proportion attributable to interaction (synergism share):

$$op_{ati} = \frac{ERERI_{INTmed} + ERERI_{INTref}}{TERERI}$$

Overall proportion eliminated if frailty were fixed at m:

$$op_e = \frac{ERERI_{PIE} + ERERI_{INTmed} + ERERI_{INTref}}{TERERI}$$

Interpretation in **reverse causation** language:

- **Large** op_m⇒ epigenetic aging affects mortality partly through increasing frailty burden (supporting an upstream role of biological aging).

- Large op_{ati}⇒ synergism: the mortality effect of frailty differs by epigenetic aging level (or vice versa).
- Attenuated op_mrelative to the forward model ⇒ frailty is less plausible as a downstream mediator of epigenetic aging (more consistent with epigenetic aging operating downstream of frailty or reflecting shared causes).

5) Model specification
Mediator model (logistic regression):

Let Abe the epigenetic aging metric (continuous, e.g., SD units), $M \in \{0,1\}$be **frailty status**, and Ccovariates.

$$\text{logit}\{P(M = 1 \mid A, C)\} = \alpha_0 + \alpha_A A + \alpha_C^\top C$$

Equivalently,

$$P(M = 1 \mid A, C) = \frac{\exp(\alpha_0 + \alpha_A A + \alpha_C^\top C)}{1 + \exp(\alpha_0 + \alpha_A A + \alpha_C^\top C)}$$

Outcome model (Cox with interaction):

Mortality hazard given A, M, and C:

$$h(t \mid A, M, C) = h_0(t)\exp(\beta_A A + \beta_M M + \beta_{AM}(A \cdot M) + \beta_C^\top C)$$

This implies the **hazard ratio for a one-unit increase in** Adepends on frailty status:

- Among non-frail ($M = 0$):

$$HR_{A|M=0} = \exp(\beta_A)$$

- Among frail ($M = 1$):

$$HR_{A|M=1} = \exp(\beta_A + \beta_{AM})$$

And the **effect of frailty on mortality** depends on epigenetic aging:

$$HR_{M|A} = \exp(\beta_M + \beta_{AM} A)$$

6) Assumptions (reverse model; stated for this direction)
No unmeasured confounding (conditional on covariates C):

$$Y_{a,m} \perp A \mid C, M_a \perp A \mid C, Y_{a,m} \perp M \mid A, C$$

Positivity:

$$0 < f(A \mid C) \text{ on the support used (e.g., } a_0, a_1)$$

Consistency:

$$M = M_a \text{ if } A = a, Y = Y_{a,m} \text{ if } A = a, M = m$$

Correct specification of the mediator and Cox models.

APPENDIX VIII. Sensitivity analysis findings

Sensitivity analysis 1: adjustment for WBC composition

NHANES

In NHANES, the primary analysis (frailty → mortality, EAA as mediator) shows that the total effect (TE) of frailty on mortality remains statistically significant across clocks and is only modestly attenuated after WBC adjustment. Mediation is clock-specific: Horvath and Hannum show little evidence of a pure indirect effect (PIE), whereas DunedinPoAm, PhenoAge, and especially GrimAge demonstrate significant mediation that persists after WBC adjustment, although somewhat attenuated. GrimAge consistently exhibits the largest mediated component. The controlled direct effect (CDE) remains the dominant contributor to the TE across models, indicating that frailty's association with mortality is largely independent of epigenetic aging.

Interaction components (INTmed and INTref) are generally small. INTmed is modestly positive for DunedinPoAm, PhenoAge, and GrimAge, suggesting limited amplification when frailty and accelerated aging co-occur, while INTref is negligible. Importantly, these interaction patterns are not materially altered by WBC adjustment. However, caution is warranted in interpreting differences between WBC-adjusted and unadjusted models because WBC-adjusted analyses rely on smaller analytic samples. Some attenuation of mediation or interaction components may reflect reduced statistical power rather than true biological change.

HRS

In HRS, patterns are broadly similar but more sensitive to WBC adjustment. In primary models (frailty → mortality, EAA mediates), TE remains significant across clocks but attenuates more noticeably after WBC adjustment. GrimAge shows the most consistent mediation signal, remaining significant after adjustment. DunedinPoAm mediation weakens substantially with WBC adjustment, and PhenoAge, Hannum, and Horvath show minimal mediation. The CDE accounts for most of the TE in all models. Interaction components are generally small and unstable. INTmed is occasionally positive for GrimAge and DunedinPoAm in unadjusted models but attenuates after WBC adjustment. INTref remains minimal. However, these differences must be interpreted cautiously because WBC-adjusted models are based on smaller subsamples, reducing precision and potentially obscuring modest mediated or interaction effects.

Sensitivity analysis 2A: reverse causation

In NHANES reverse-causation models (epigenetic aging → frailty → mortality), second- and third-generation clocks showed the most consistent evidence of mediation. Horvath EAA demonstrated minimal total effect and no meaningful mediation. Hannum and PhenoAge showed significant pure indirect effects, though the overall proportion mediated was modest and borderline for PhenoAge. DunedinPoAm showed a stronger total association (RR≈1.39), with approximately 10% mediated through frailty and evidence of positive mediated interaction. GrimAge exhibited the largest total effect (RR≈1.66), with roughly 11% mediated and some contribution from interaction components. Overall, frailty explained about 7–11% of the total association for more advanced clocks.

In HRS, findings were similar but generally stronger. Horvath again showed no meaningful total effect or mediation. In contrast, Hannum, PhenoAge, DunedinPoAm (RR≈1.51), and GrimAge demonstrated significant total effects, with approximately 8–18% of associations mediated through frailty. Interaction components contributed modestly for DunedinPoAm and GrimAge. Across cohorts, frailty accounted for a consistent but partial share of the epigenetic aging–mortality association.

Sensitivity analysis 2B: reverse causation + WBC adjustment

NHANES

In reverse-causation models (EAA → mortality, frailty mediates), TE remains significant for second-generation clocks and is only slightly attenuated after WBC adjustment. Frailty mediation persists for DunedinPoAm, PhenoAge, and GrimAge, though some weakening (e.g., Hannum) is observed. Interaction effects remain small. Overall, NHANES findings appear relatively robust to WBC adjustment, but sample-size differences between models necessitate cautious comparison, particularly for marginal mediation effects.

HRS

In reverse-causation models (EAA → mortality, frailty mediates), TE remains significant for Hannum, DunedinPoAm, PhenoAge, and GrimAge, though attenuated after WBC adjustment. Frailty mediation persists most consistently for GrimAge (and often PhenoAge), whereas mediation for Hannum and DunedinPoAm becomes non-significant after adjustment. Given the smaller WBC-adjusted sample, loss of statistical significance may reflect limited power rather than elimination of mediation. Overall, HRS results suggest robustness primarily for GrimAge, but comparisons between adjusted and unadjusted models should be made with caution due to sample-size differences.

SUPPLEMENTARY REFRENCES

1. Fried LP, Tangen CM, Walston J, Newman AB, Hirsch C, Gottdiener J, et al. Frailty in older adults: evidence for a phenotype. J Gerontol A Biol Sci Med Sci. 2001;56(3):M146-56.
2. Beydoun MA, Beydoun HA, Noren Hooten N, Maldonado AI, Weiss J, Evans MK, et al. Epigenetic clocks and their association with trajectories in perceived discrimination and depressive symptoms among US middle-aged and older adults. Aging (Albany NY). 2022;14(13):5311-44.
3. Evans MK, Lepkowski JM, Powe NR, LaVeist T, Kuczmarski MF, Zonderman AB. Healthy aging in neighborhoods of diversity across the life span (HANDLS): overcoming barriers to implementing a longitudinal, epidemiologic, urban study of health, race, and socioeconomic status. Ethn Dis. 2010;20(3):267-75.
4. Beydoun MA, Hossain S, Chitrala KN, Tajuddin SM, Beydoun HA, Evans MK, et al. Association between epigenetic age acceleration and depressive symptoms in a prospective cohort study of urban-dwelling adults. J Affect Disord. 2019;257:64-73.
5. Beydoun MA, Shaked D, Tajuddin SM, Weiss J, Evans MK, Zonderman AB. Accelerated epigenetic age and cognitive decline among urban-dwelling adults. Neurology. 2020;94(6):e613-e25.
6. Belsky DW, Caspi A, Corcoran DL, Sugden K, Poulton R, Arseneault L, et al. DunedinPACE, a DNA methylation biomarker of the pace of aging. Elife. 2022;11.
7. Kvamme H, Borgan O. Continuous and discrete-time survival prediction with neural networks. Lifetime Data Anal. 2021;27(4):710-36.
8. Lewis FI, Ward MP. Improving epidemiologic data analyses through multivariate regression modelling. Emerg Themes Epidemiol. 2013;10(1):4.
9. Scutari M, Denis, J.-B.,. Bayesian Networks With Examples in R. Boca Raton, FL: CRC Press; 2022.
10. VanderWeele TJ, Shrier I. Sufficient Cause Representation of the Four-way Decomposition for Mediation and Interaction. Epidemiology. 2016;27(5):e32-3.

11. Discacciati A, Bellavia A, Lee JJ, Mazumdar M, Valeri L. Med4way: a Stata command to investigate mediating and interactive mechanisms using the four-way effect decomposition. Int J Epidemiol. 2018.

FIGURE S1. Participant flowcharts for NHANES, HRS and HANDLS samples

(A) NHANES 1999-2002

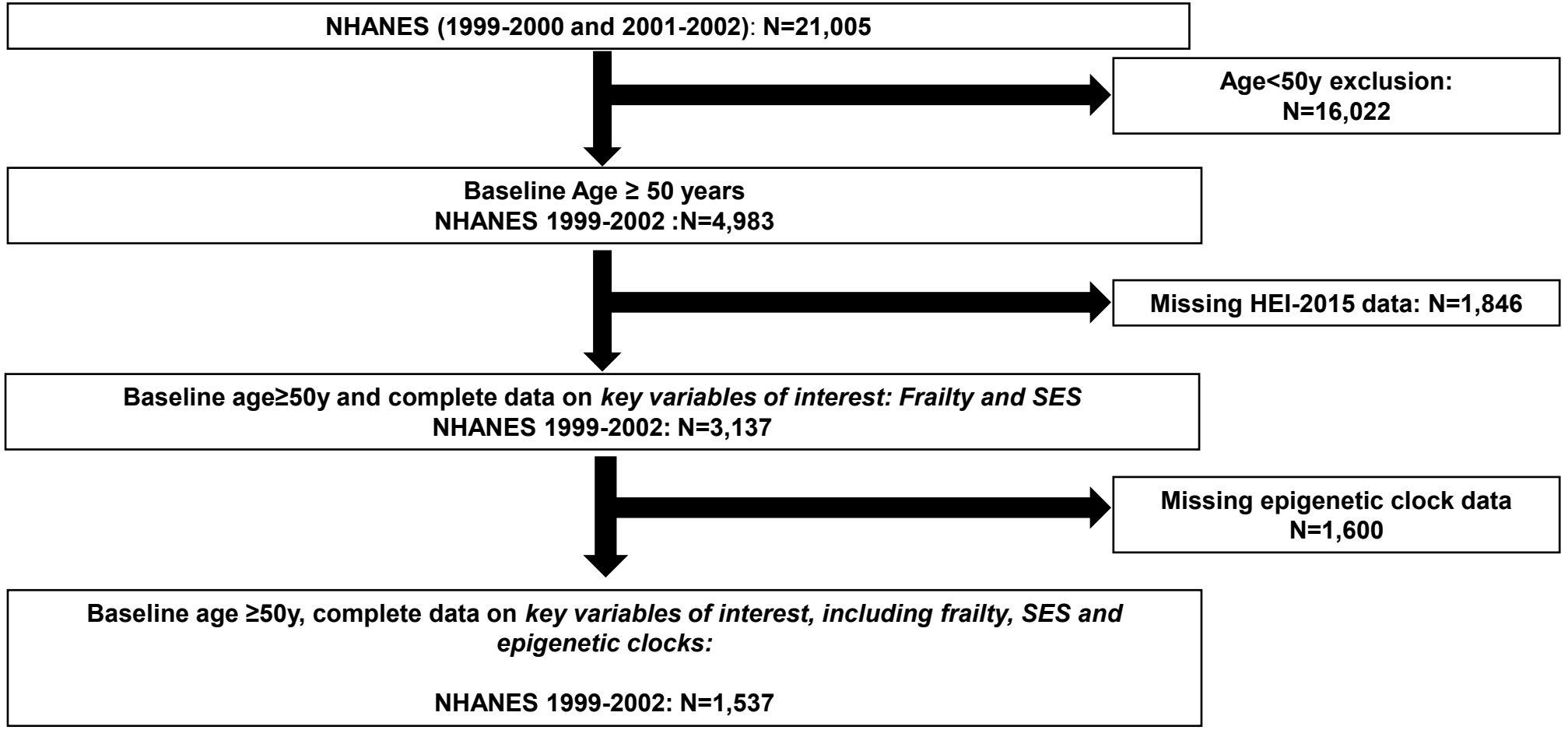

(B) HRS 2016

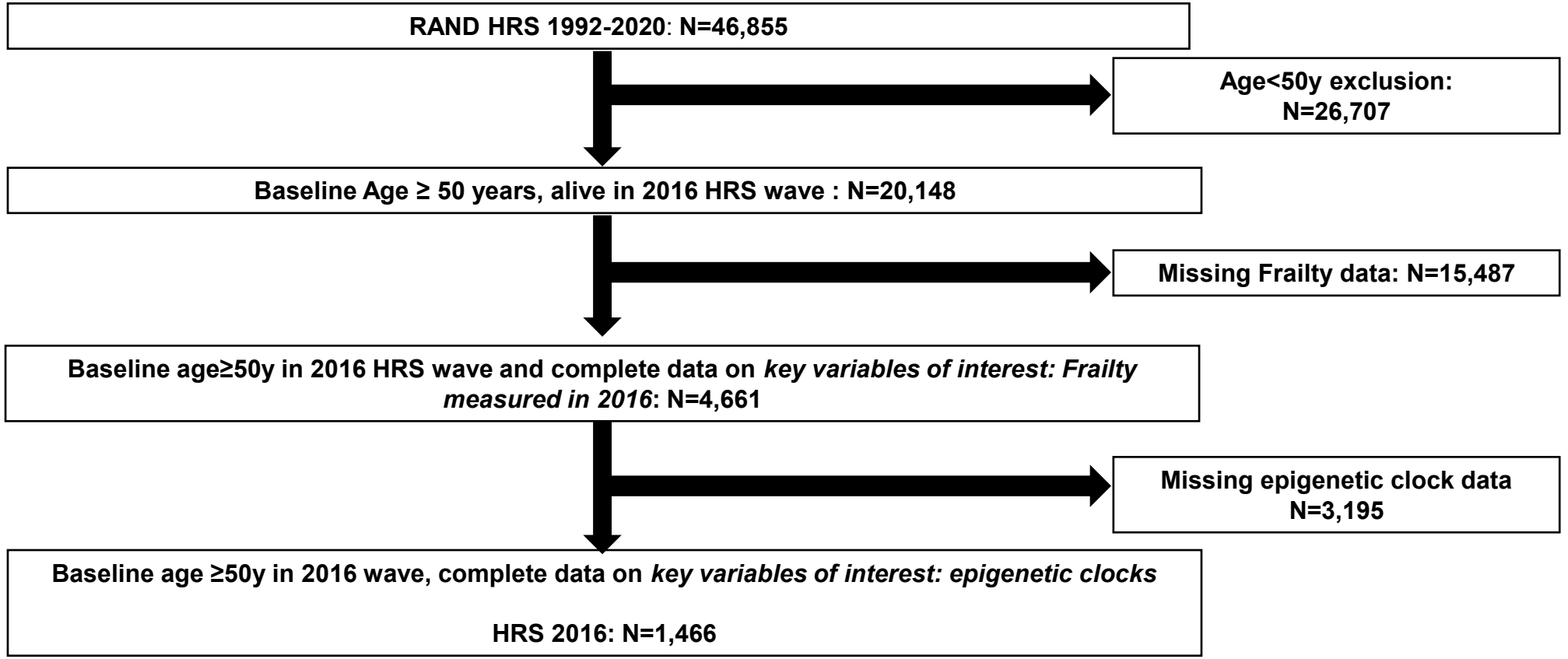
RAND HRS 1992-2020: N=46,855
Age<50y exclusion: N=26,707
Baseline Age ≥ 50 years, alive in 2016 HRS wave : N=20,148
Missing Frailty data: N=15,487
Baseline age≥50y in 2016 HRS wave and complete data on key variables of interest: Frailty measured in 2016: N=4,661
Missing epigenetic clock data N=3,195
Baseline age ≥50y in 2016 wave, complete data on key variables of interest: epigenetic clocks
HRS 2016: N=1,466

(C) HANDLS 2004-2009

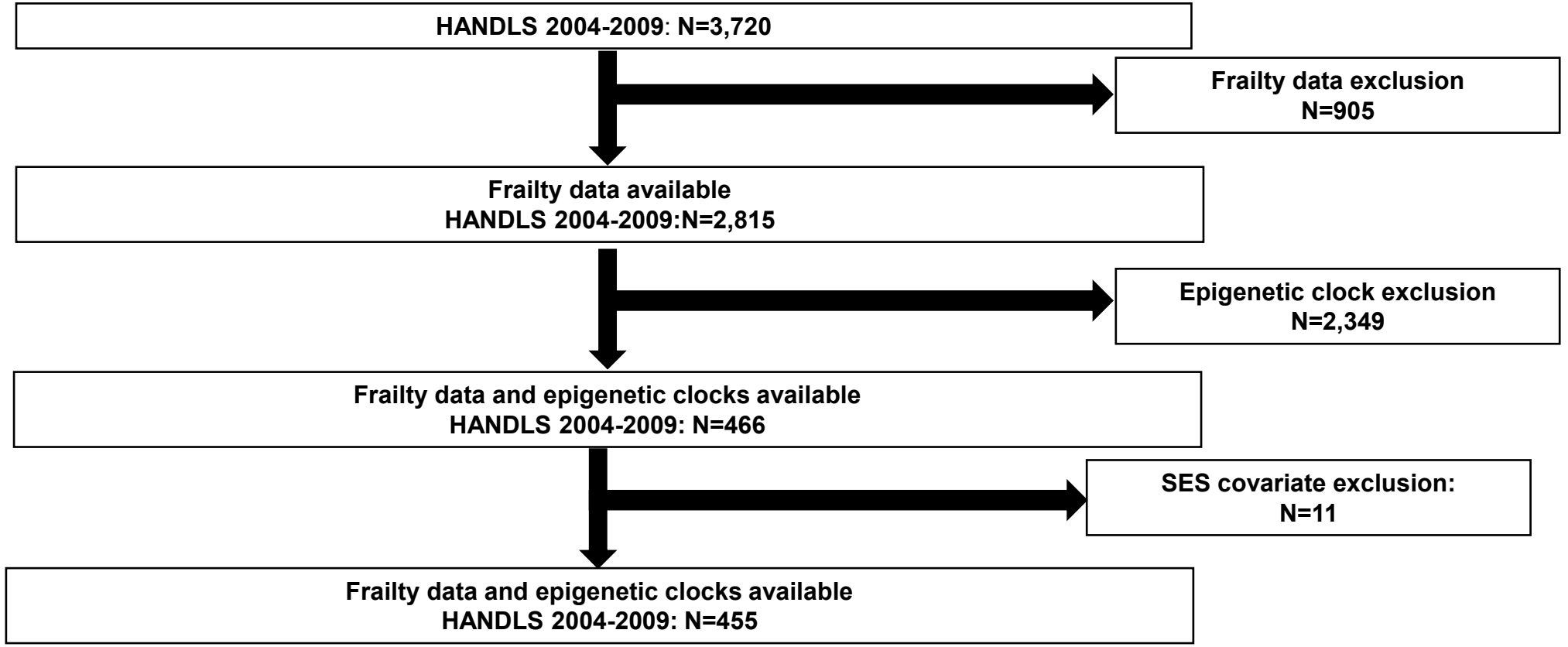

Abbreviations: HANDLS=Healthy Aging in Neighborhoods of Diversity across the Life Span; HRS=Health and Retirement Study; NHANES=National Health and Nutrition Examination Surveys.

FIGURE S2. Pearson's correlation matrix between SES, frailty, and epigenetic clock metrics and kernel smoothed distribution of the frailty score: NHANES 1999–2002, HRS 2016 and HANDLS 2004-2009

(A) NHANES 1999-2002

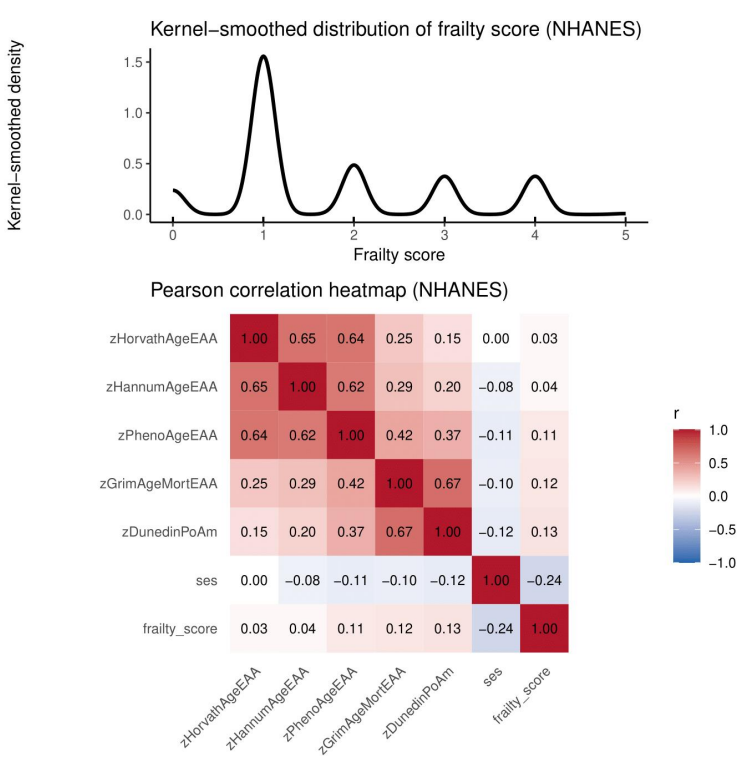

(B) HRS 2016

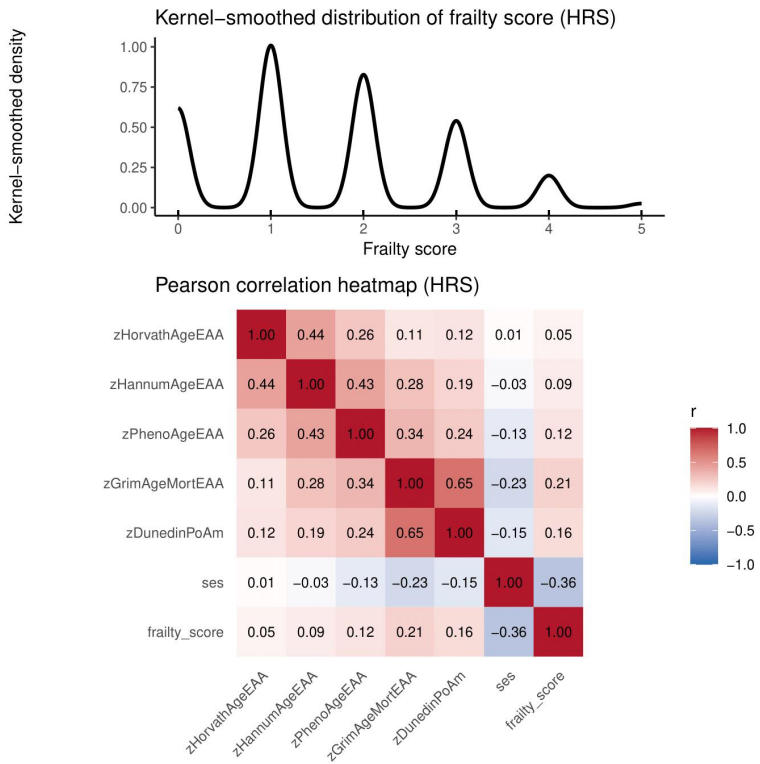

(C) HANDLS 2004-2009

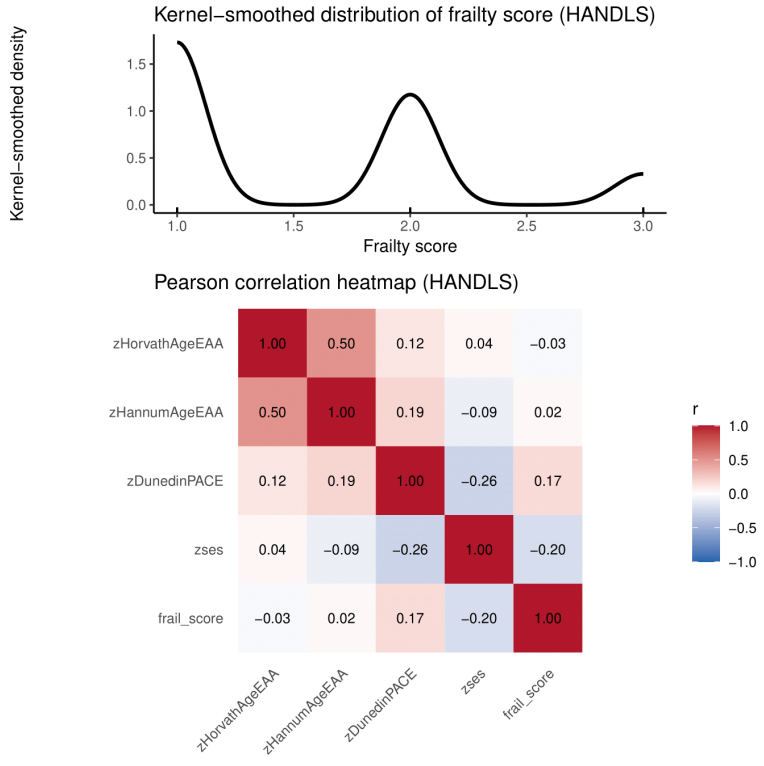

Abbreviations:
DunedinPoAm = Dunedin Pace of Aging DNA methylation clock; GrimAgeEAA = Grim DNA methylation Epigenetic Age Acceleration; HANDLS=Healthy Aging in Neighborhoods of Diversity Across the Life Span; HannumAgeEAA = Hannum DNA methylation Age, Epigenetic Age Acceleration; HorvathAgeEAA = Horvath DNA methylation Age, Epigenetic Age Acceleration; HRS = Health and Retirement Study; NHANES = National Health and Nutrition Examination Surveys; PhenoAgeEAA = Pheno DNA methylation Age Epigenetic Age Acceleration; SES = Socio-economic Status; z = standardized z-score.
Notes: Sampling weights were not accounted for in this analysis. Unweighted sample sizes were n=1,537 for NHANES, n=1,413 for HRS and n=455 for HANDLS.

Supplementary Datasheet 1. Cross-cohort correlation matrices of epigenetic age acceleration, socioeconomic status, and frailty in NHANES, HRS, and HANDLS.
This datasheet presents cohort-specific Pearson correlation matrices among standardized epigenetic age acceleration (EAA) measures, socioeconomic status (SES), and frailty indices in NHANES, HRS, and HANDLS. EAA metrics were z-standardized within cohort. Frailty and SES were harmonized using cohort-specific measures.
Diagonal elements equal 1.00; off-diagonal values are Pearson correlation coefficients (r), describing pairwise associations among biological aging measures and social/clinical factors prior to multivariable analyses.

	zHorvathAgeEAA	zHannumAgeEAA	zPhenoAgeEAA	zGrimAgeMortEAA	zDunedinPoAm
zHorvathAgeEAA	1	0.65242195	0.64016199	0.25495821	0.14831309
zHannumAgeEAA	0.65242195	1	0.61701632	0.29419559	0.20491162
zPhenoAgeEAA	0.64016199	0.61701632	1	0.41604084	0.36596066
zGrimAgeMortEAA	0.25495821	0.29419559	0.41604084	1	0.6740154
zDunedinPoAm	0.14831309	0.20491162	0.36596066	0.6740154	1
frailty_score	0.029399686	0.038167827	0.10618085	0.11515809	0.12609491
ses	0.00138552	-0.079700097	-0.11101422	-0.10025715	-0.12000751

frailty_score	ses
0.029399686	0.00138552
0.038167827	-0.079700097
0.10618085	-0.11101422
0.11515809	-0.10025715
0.12609491	-0.12000751
1	-0.24024588
-0.24024588	1

	zHorvathAgeEAA	zHannumAgeEAA	zPhenoAgeEAA	zGrimAgeMortEAA	zDunedinPoAm
zHorvathAgeEAA	1	0.43653053	0.25978586	0.11417771	0.12423234
zHannumAgeEAA	0.43653053	1	0.42545348	0.28371906	0.1877277
zPhenoAgeEAA	0.25978586	0.42545348	1	0.33919132	0.23936777
zGrimAgeMortEAA	0.11417771	0.28371906	0.33919132	1	0.65341711
zDunedinPoAm	0.12423234	0.1877277	0.23936777	0.65341711	1
ses	0.009521559	-0.034989238	-0.12721166	-0.23159505	-0.14620583
fried_sum	0.053811591	0.089202948	0.12356342	0.20981404	0.16117696

ses	fried_sum
0.009521559	0.053811591
-0.034989238	0.089202948
-0.12721166	0.12356342
-0.23159505	0.20981404
-0.14620583	0.16117696
1	-0.35817996
-0.35817996	1

	zHorvathAgeEAA	zHannumAgeEAA	zDunedinPACE	zses	frail_score
zHorvathAgeEAA	1	0.50369805	0.11534224	0.03628926	-0.029448243
zHannumAgeEAA	0.50369805	1	0.18618332	-0.092729867	0.023523092
zDunedinPACE	0.11534224	0.18618332	1	-0.25992414	0.1678929
zses	0.03628926	-0.092729867	-0.25992414	1	-0.19849512
frail_score	-0.029448243	0.023523092	0.1678929	-0.19849512	1

Supplementary Datasheet 2. Multivariable associations between socioeconomic status, frailty, and epigenetic age accelerat NHANES, HRS, and HANDLS.
This datasheet presents cohort-specific multivariable regression models examining associations of socioeconomic status (SES) a standardized epigenetic age acceleration (EAA) measures in NHANES, HRS, and HANDLS. EAA metrics were z-standardized within

	LnHR	SE	HR	LCL	UCL
zHorvathAgeEAA	0.116	0.0485	1.12299587213325	1.02116078015259	1.23498645202558
zHannumAgeEAA	0.224	0.05	1.25107101942836	1.13428216828303	1.37988477595725
zPhenoAgeEAA	0.285	0.0503	1.32976202812147	1.20491858458467	1.46754069034735
zGrimAgeMortEAA	0.531	0.05	1.70063209067655	1.54187622070063	1.87573390717751
zDunedinPoAm	0.34	0.0458	1.40494759056359	1.28432334514278	1.53690092117029
frailty_status	0.687	0.105	1.98774334939826	1.61801485551466	2.44195756893729
zses	-0.326	0.0519	0.721805187431716	0.651991339577694	0.799094553833793

	LnHR	SE	HR	LCL	UCL
zHorvathAgeEAA	-0.00283	0.0723	0.99717400067514	0.865422025741286	1.14898391541484
zHannumAgeEAA	0.239	0.068	1.26997853658384	1.11151060996046	1.45103921539804
zPhenoAgeEAA	0.314	0.0661	1.36888973654738	1.20254963661959	1.55823847412422
zGrimAgeMortEAA	0.551	0.0752	1.73498713780072	1.49721692287517	2.01051719516592
zDunedinPoAm	0.41	0.084	1.50681778511285	1.27808133967744	1.77649087506859
frail_status	0.972	0.166	2.6432256276808	1.90911541257306	3.65962249993683
zses	-0.599	0.0874	0.54936072222743	0.462872333731201	0.652009595590785

	LnHR	SE	HR	LCL	UCL
zHorvathAgeEAA	-0.0534	0.152	0.948000736337591	0.703758515094511	1.27700820213298
zHannumAgeEAA	0.316	0.138	1.37163025562604	1.04657193584335	1.79764953914296
zDunedinPACE	0.539	0.137	1.71429171304018	1.31059338460165	2.24234008192514
frailty_status	0.24	0.441	1.2712491503214	0.535604105478173	3.01729278335181
zses	-0.612	0.118	0.542265253313983	0.430296832632559	0.683369206212066

FIGURE S3. ABN findings using discrete time hazards models, for 1 and 2 parents/child limits

(A) NHANES 1999-2002, follow-up till 2019

1 parent/child

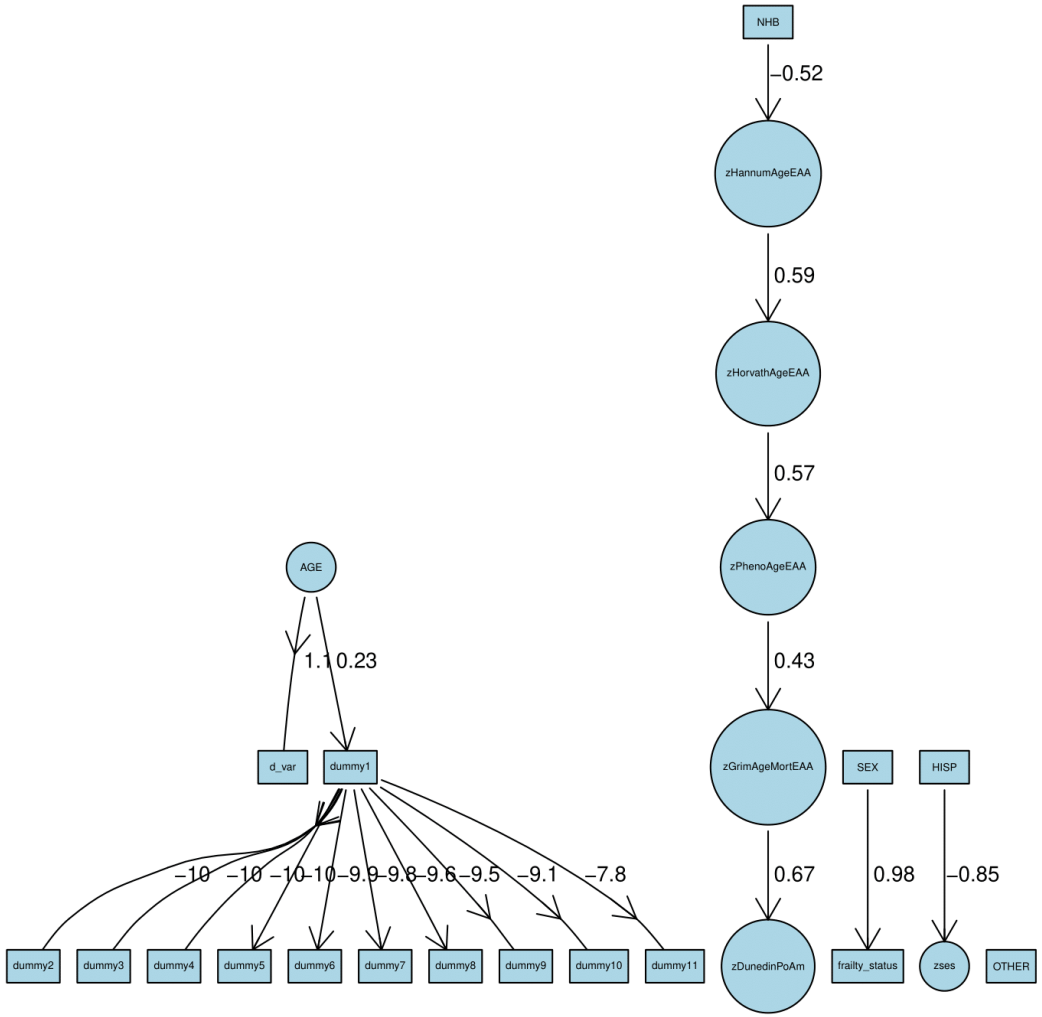

2 parents/child

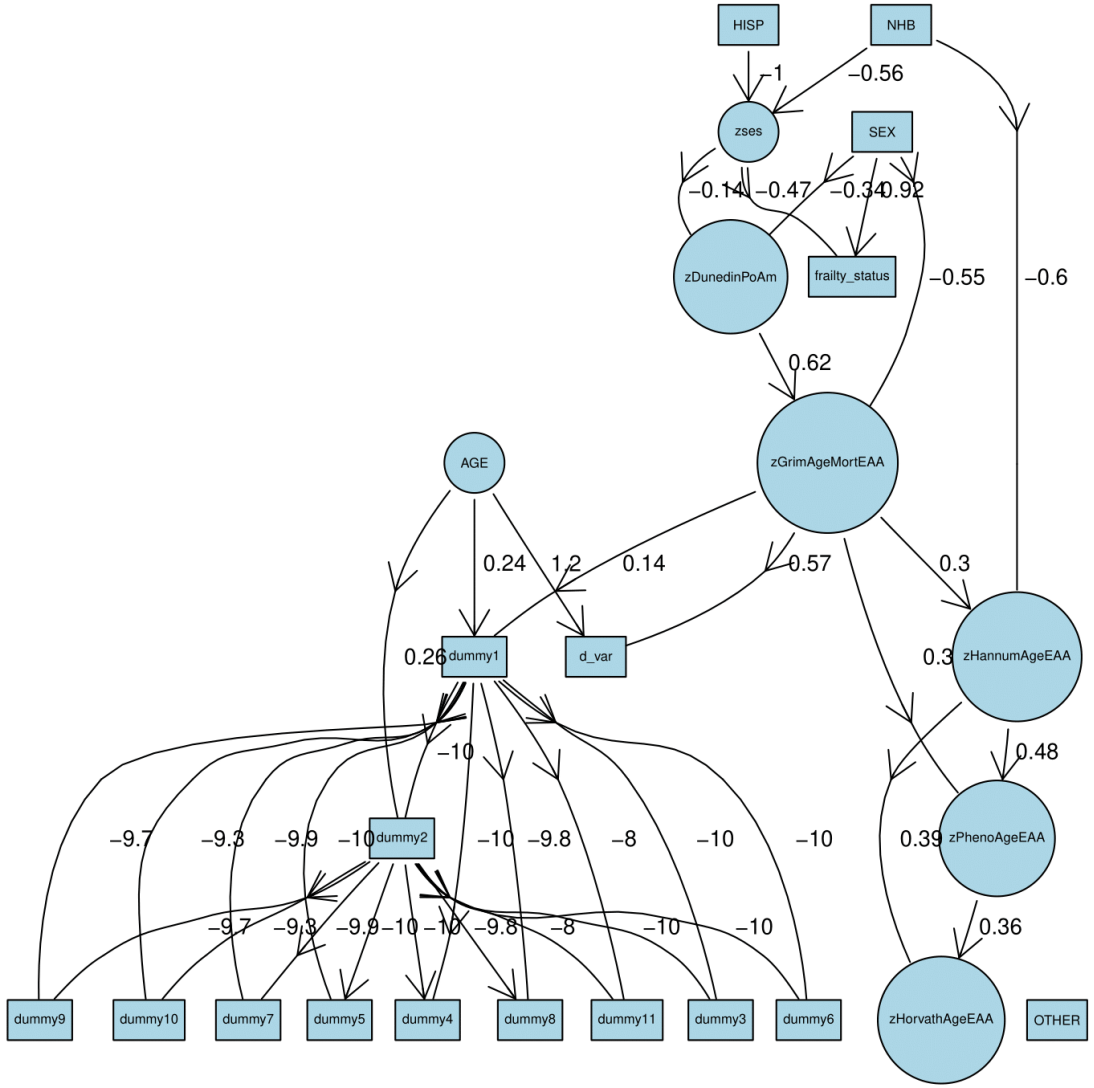

NHANES 1999-2019: Final solution

3 parents/child solution

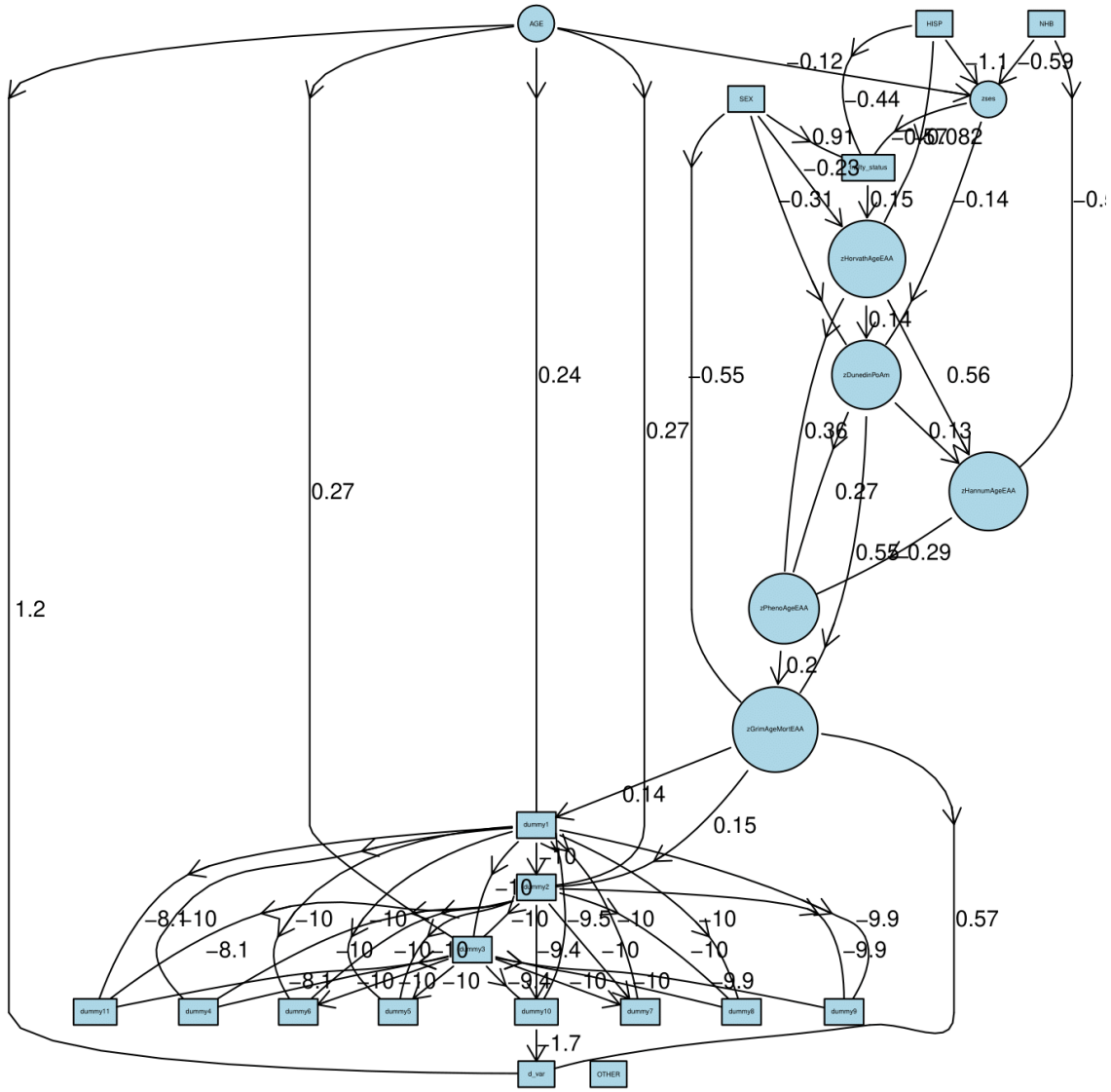

Model fit for 1-3 parents/child

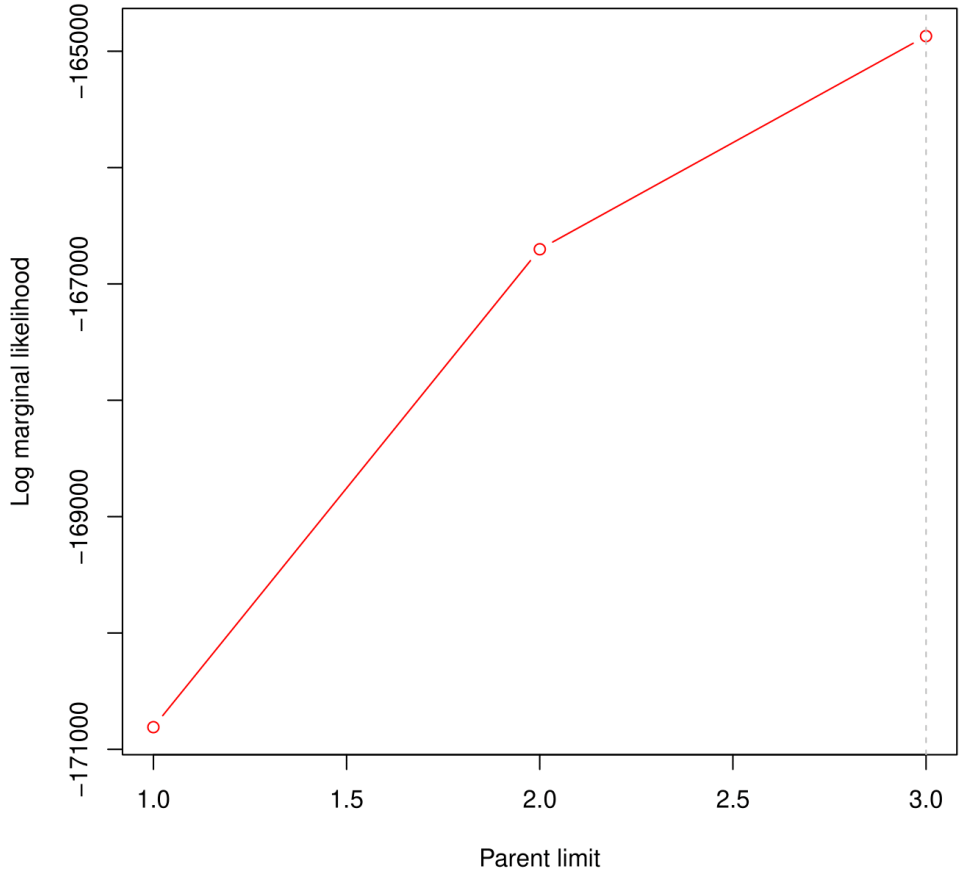

(B) HRS 2016, follow-up till 2022

1 parent/child

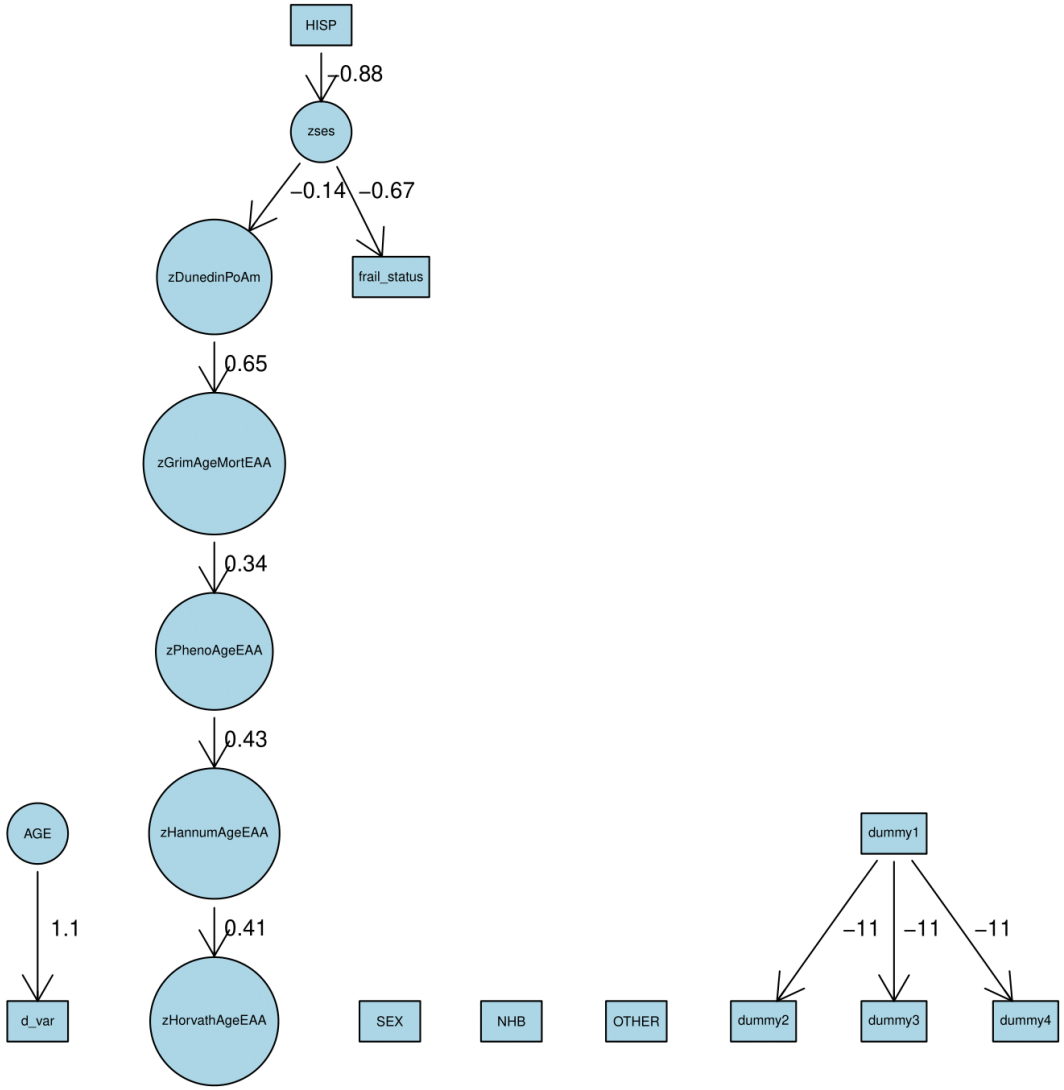

2 parents/child

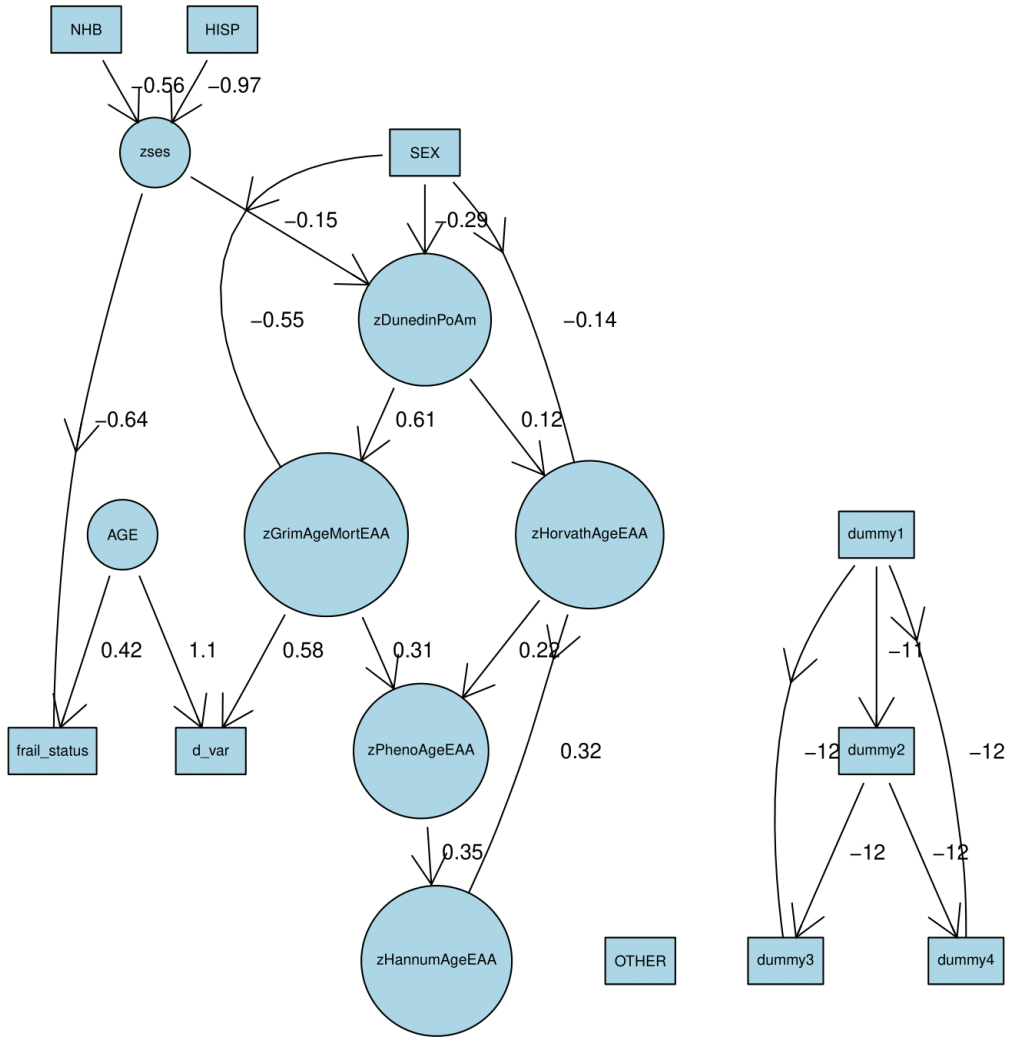

HRS 2016-2022: Final solution

3 parents/child solution

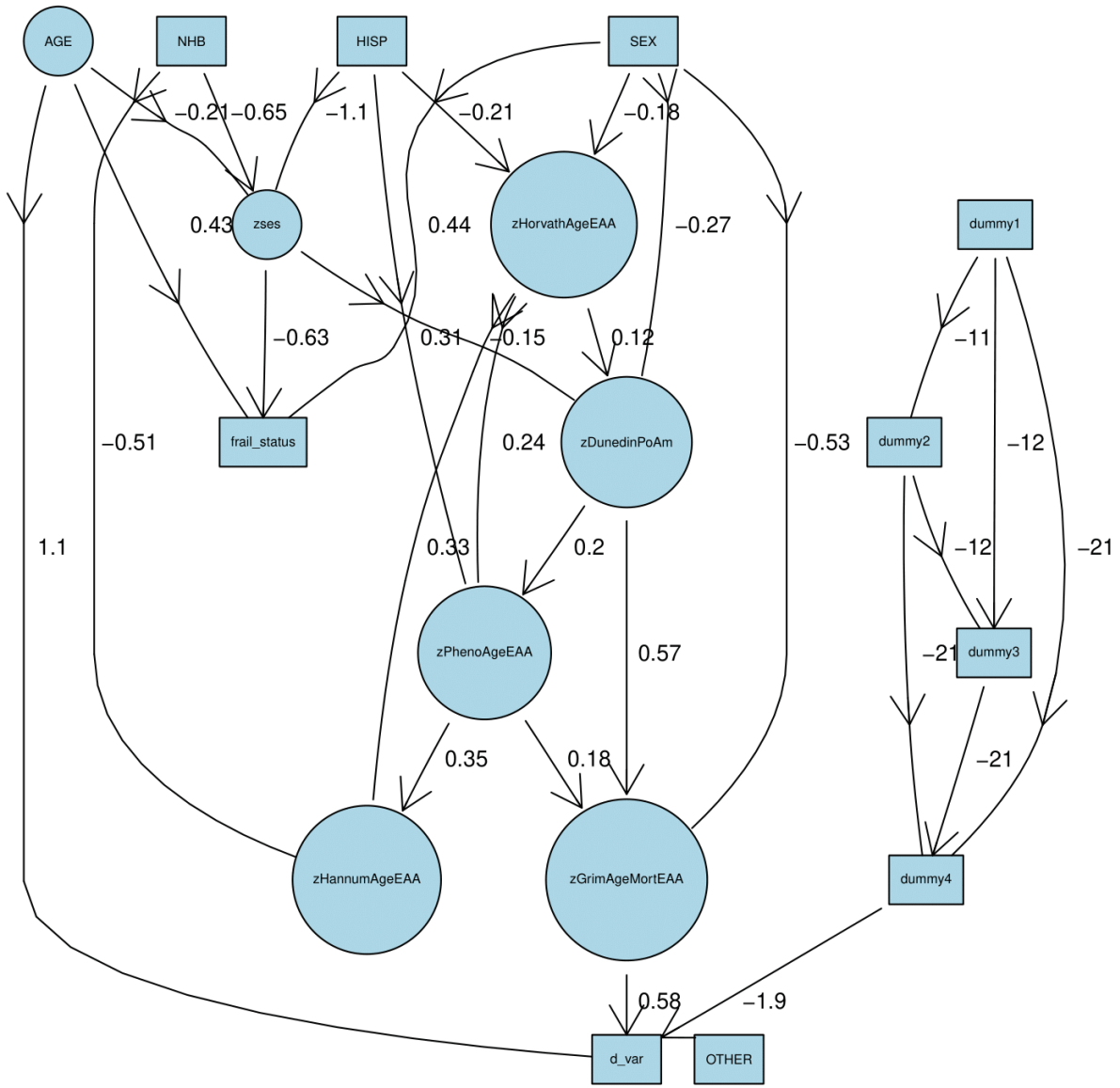

Model fit for 1-3 parents/child

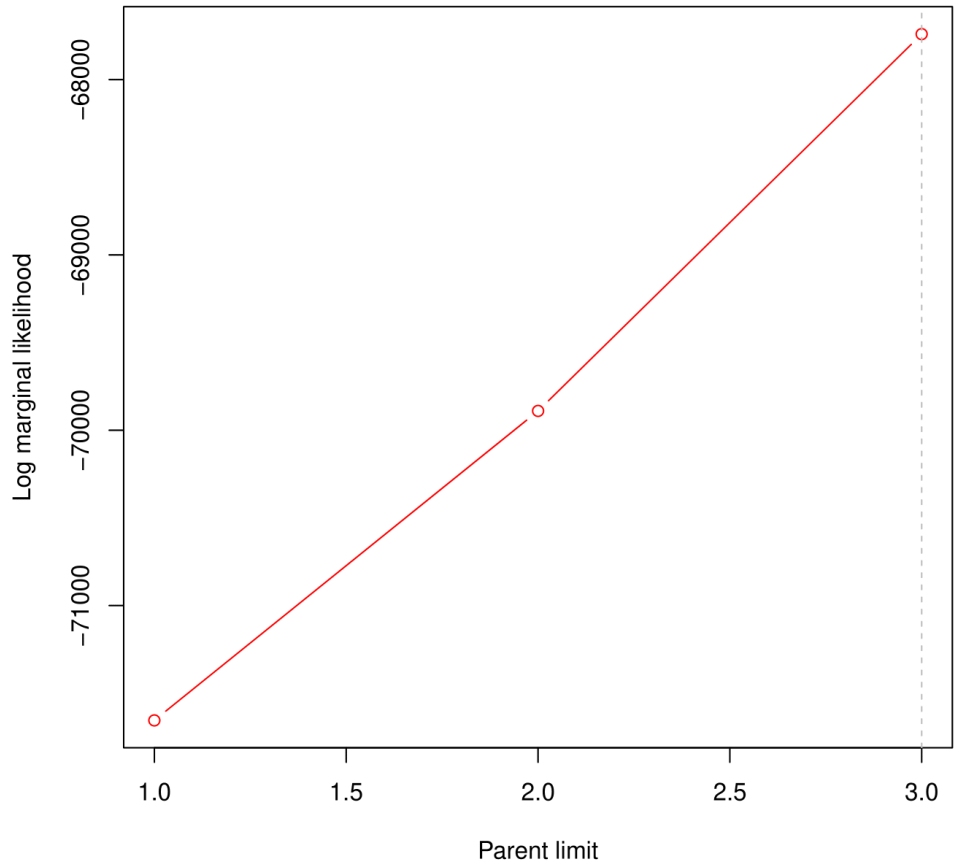

Notes: Details for R code used for this analysis described in **Appendix VI** and provided on Github. This code provides a comprehensive pipeline for conducting ABN analysis, including installation, data preprocessing, constraint specification, model fitting, and iterative optimization. It involves installing R versions 4.4 or higher, data preparation, data wrangling, defining variable groups, setting constraints, optimizing across parent limits, building the additive Bayesian network, and generating visual representations. The optimal number of parents of a child is determined based on levelling off the log marginal likelihood and desired complexity between key variables. Unweighted sample sizes were n=1,537 for NHANES, n=1,415 for HRS.

Abbreviations: DunedinPoAm=Dunedin Pace of Aging DNA methylation clock; frail_status: Frail=1, Pre-frail/Robust=0; GrimAgeEAA=Grim DNA methylation Epigenetic Age Acceleration; HannumAgeEAA=Hannum DNA methylation Age, Epigenetic Age Acceleration; HorvathAgeEAA=Horvath DNA methyalation Age, Epigenetic Age Acceleration; HRS=Health and Retirement Study; NHANES=National Health and Nutrition Examination Surveys; PhenoAgeEAA=Pheno DNA methylation Age Epigenetic Age Acceleration; SES=Socio-economic Status; z=standardized *z*-score.

Supplementary Datasheet 3. Four-way decomposition of the associations between frailty, epigenetic age acceleration, and m
NHANES and HRS

This datasheet presents cohort-specific four-way decomposition analyses partitioning the total effect of frailty on all-cause morta
direct effects, reference interaction, mediated interaction, and pure indirect effects through standardized epigenetic age accelera

Estimates include effect sizes with 95% confidence intervals and p-values, derived from counterfactual-based mediation models
demographic and relevant covariates. Results quantify the relative contributions of mediation and interaction pathways linking fra
through biological aging markers.

Parameter	Coefficient	Std. err.	z	P>z	LCL
tereri	0.7808444	0.189146	4.13	0	0.4101251
ereri_cde	0.7849575	0.1890235	4.15	0	0.4144782
ereri_intref	-0.003484	0.0080815	-0.43	0.666	-0.0193234
ereri_intmed	-0.0120152	0.0210535	-0.57	0.568	-0.0532793
ereri_pie	0.0113861	0.0092069	1.24	0.216	-0.0066592
terira	1.780844	0.189146	9.42	0	1.410125
p_cde	1.005267	0.0192199	52.3	0	0.9675973
p_intref	-0.0044618	0.0104221	-0.43	0.669	-0.0248887
p_intmed	-0.0153874	0.0273402	-0.56	0.574	-0.0689733
p_pie	0.0145817	0.0123465	1.18	0.238	-0.009617
op_m	-0.0008057	0.0242033	-0.03	0.973	-0.0482433
op_ati	-0.0198492	0.0244569	-0.81	0.417	-0.0677839
op_e	-0.0052675	0.0192198	-0.27	0.784	-0.0429377
tereri	0.7558041	0.1913635	3.95	0	0.3807386
ereri_cde	0.723035	0.1867134	3.87	0	0.3570835
ereri_intref	-0.002429	0.0160649	-0.15	0.88	-0.0339157
ereri_intmed	0.0077857	0.0246535	0.32	0.752	-0.0405342
ereri_pie	0.0274124	0.0146803	1.87	0.062	-0.0013604
terira	1.755804	0.1913635	9.18	0	1.380739
p_cde	0.9566434	0.0519116	18.43	0	0.8548986
p_intref	-0.0032139	0.0213854	-0.15	0.881	-0.0451285
p_intmed	0.0103012	0.0320485	0.32	0.748	-0.0525127
p_pie	0.0362692	0.0213588	1.7	0.089	-0.0055931
op_m	0.0465705	0.0352717	1.32	0.187	-0.0225608
op_ati	0.0070874	0.05307	0.13	0.894	-0.0969278
op_e	0.0433566	0.0519116	0.84	0.404	-0.0583882
tereri	0.8036325	0.1958896	4.1	0	0.419696
ereri_cde	0.6333866	0.1829444	3.46	0.001	0.2748221
ereri_intref	0.0356042	0.0371824	0.96	0.338	-0.037272
ereri_intmed	0.0720735	0.0439134	1.64	0.101	-0.0139951
ereri_pie	0.0625682	0.0215054	2.91	0.004	0.0204185
terira	1.803633	0.1958896	9.21	0	1.419696
p_cde	0.7881545	0.0934426	8.43	0	0.6050104
p_intref	0.0443041	0.0456298	0.97	0.332	-0.0451287
p_intmed	0.0896846	0.0488185	1.84	0.066	-0.0059979
p_pie	0.0778568	0.0311947	2.5	0.013	0.0167162
op_m	0.1675414	0.0603551	2.78	0.006	0.0492476
op_ati	0.1339887	0.0896545	1.49	0.135	-0.0417309
op_e	0.2118455	0.0934426	2.27	0.023	0.0287013
tereri	0.7247697	0.1874413	3.87	0	0.3573916
ereri_cde	0.7304074	0.1904086	3.84	0	0.3572133

ereri_intref	-0.0231793	0.0142252	-1.63	0.103	-0.0510601
ereri_intmed	-0.0450337	0.0385492	-1.17	0.243	-0.1205887
ereri_pie	0.0625754	0.023366	2.68	0.007	0.0167789
terira	1.72477	0.1874413	9.2	0	1.357392
p_cde	1.007779	0.048621	20.73	0	0.912483
p_intref	-0.0319816	0.0220497	-1.45	0.147	-0.0751982
p_intmed	-0.0621352	0.0552446	-1.12	0.261	-0.1704127
p_pie	0.0863383	0.0394656	2.19	0.029	0.0089871
op_m	0.0242031	0.0468078	0.52	0.605	-0.0675385
op_ati	-0.0941168	0.0652054	-1.44	0.149	-0.2219169
op_e	-0.0077785	0.048621	-0.16	0.873	-0.1030739
tereri	0.8699394	0.2211501	3.93	0	0.4364931
ereri_cde	0.5354044	0.1697276	3.15	0.002	0.2027444
ereri_intref	0.0442704	0.0467035	0.95	0.343	-0.0472667
ereri_intmed	0.1363182	0.077928	1.75	0.08	-0.0164178
ereri_pie	0.1539463	0.0349839	4.4	0	0.0853791
terira	1.869939	0.2211501	8.46	0	1.436493
p_cde	0.6154503	0.1104231	5.57	0	0.399025
p_intref	0.0508891	0.0494594	1.03	0.304	-0.0460495
p_intmed	0.1566985	0.0671113	2.33	0.02	0.0251628
p_pie	0.1769621	0.0557828	3.17	0.002	0.0676299
op_m	0.3336606	0.0761098	4.38	0	0.1844881
op_ati	0.2075876	0.1129067	1.84	0.066	-0.0137054
op_e	0.3845497	0.1104231	3.48	0	0.1681244

UCL	EPICLOCK
1.151564	HorvathAgeEAA
1.155437	HorvathAgeEAA
0.0123554	HorvathAgeEAA
0.029249	HorvathAgeEAA
0.0294314	HorvathAgeEAA
2.151564	HorvathAgeEAA
1.042938	HorvathAgeEAA
0.015965	HorvathAgeEAA
0.0381985	HorvathAgeEAA
0.0387805	HorvathAgeEAA
0.0466319	HorvathAgeEAA
0.0280854	HorvathAgeEAA
0.0324027	HorvathAgeEAA
1.13087	HannumAgeEAA
1.088986	HannumAgeEAA
0.0290576	HannumAgeEAA
0.0561057	HannumAgeEAA
0.0561852	HannumAgeEAA
2.13087	HannumAgeEAA
1.058388	HannumAgeEAA
0.0387007	HannumAgeEAA
0.0731152	HannumAgeEAA
0.0781316	HannumAgeEAA
0.1157017	HannumAgeEAA
0.1111026	HannumAgeEAA
0.1451014	HannumAgeEAA
1.187569	DunedinPoAm
0.9919511	DunedinPoAm
0.1084804	DunedinPoAm
0.1581421	DunedinPoAm
0.104718	DunedinPoAm
2.187569	DunedinPoAm
0.9712987	DunedinPoAm
0.1337368	DunedinPoAm
0.1853672	DunedinPoAm
0.1389974	DunedinPoAm
0.2858352	DunedinPoAm
0.3097083	DunedinPoAm
0.3949896	DunedinPoAm
1.092148	PhenoAgeEAA
1.103601	PhenoAgeEAA

0.0047015	PhenoAgeEAA
0.0305213	PhenoAgeEAA
0.1083718	PhenoAgeEAA
2.092148	PhenoAgeEAA
1.103074	PhenoAgeEAA
0.011235	PhenoAgeEAA
0.0461423	PhenoAgeEAA
0.1636895	PhenoAgeEAA
0.1159446	PhenoAgeEAA
0.0336834	PhenoAgeEAA
0.0875169	PhenoAgeEAA
1.303386	GrimAgeMortEAA
0.8680645	GrimAgeMortEAA
0.1358075	GrimAgeMortEAA
0.2890543	GrimAgeMortEAA
0.2225134	GrimAgeMortEAA
2.303386	GrimAgeMortEAA
0.8318756	GrimAgeMortEAA
0.1478277	GrimAgeMortEAA
0.2882343	GrimAgeMortEAA
0.2862943	GrimAgeMortEAA
0.4828331	GrimAgeMortEAA
0.4288807	GrimAgeMortEAA
0.600975	GrimAgeMortEAA

Parameter	Coefficient	Std. err.	z	P>z	LCL
tereri	1.275483	0.3695509	3.45	0.001	0.5511766
ereri_cde	1.26827	0.3698083	3.43	0.001	0.5434585
ereri_intref	-0.0062902	0.0198533	-0.32	0.751	-0.045202
ereri_intmed	0.0228537	0.024834	0.92	0.357	-0.0258201
ereri_pie	-0.00935	0.0135544	-0.69	0.49	-0.0359161
terira	2.275483	0.3695509	6.16	0	1.551177
p_cde	0.9943445	0.0225494	44.1	0	0.9501485
p_intref	-0.0049317	0.0156759	-0.31	0.753	-0.0356559
p_intmed	0.0179177	0.0202655	0.88	0.377	-0.0218019
p_pie	-0.0073305	0.0109594	-0.67	0.504	-0.0288105
op_m	0.0105872	0.0139948	0.76	0.449	-0.0168421
op_ati	0.0129861	0.0208692	0.62	0.534	-0.0279167
op_e	0.0056555	0.0225494	0.25	0.802	-0.0385405
tereri	1.322959	0.3799252	3.48	0	0.578319
ereri_cde	1.240849	0.3691501	3.36	0.001	0.5173278
ereri_intref	-0.0056191	0.0228035	-0.25	0.805	-0.050313
ereri_intmed	0.0311695	0.0544339	0.57	0.567	-0.0755191
ereri_pie	0.0565596	0.033586	1.68	0.092	-0.0092678
terira	2.322959	0.3799252	6.11	0	1.578319
p_cde	0.9379345	0.0480653	19.51	0	0.8437282
p_intref	-0.0042474	0.0172785	-0.25	0.806	-0.0381126
p_intmed	0.0235604	0.0399316	0.59	0.555	-0.054704
p_pie	0.0427524	0.0274852	1.56	0.12	-0.0111176
op_m	0.0663128	0.0369387	1.8	0.073	-0.0060856
op_ati	0.0193131	0.0564212	0.34	0.732	-0.0912705
op_e	0.0620655	0.0480653	1.29	0.197	-0.0321409
tereri	1.35893	0.3836593	3.54	0	0.6069712
ereri_cde	1.257178	0.3585782	3.51	0	0.5543778
ereri_intref	-0.0195367	0.0655323	-0.3	0.766	-0.1479776
ereri_intmed	0.032481	0.0576011	0.56	0.573	-0.080415
ereri_pie	0.088807	0.0393015	2.26	0.024	0.0117774
terira	2.35893	0.3836593	6.15	0	1.606971
p_cde	0.9251239	0.079642	11.62	0	0.7690284
p_intref	-0.0143765	0.0491714	-0.29	0.77	-0.1107507
p_intmed	0.0239019	0.0398865	0.6	0.549	-0.0542742
p_pie	0.0653507	0.0328634	1.99	0.047	0.0009397
op_m	0.0892526	0.0433566	2.06	0.04	0.0042752
op_ati	0.0095254	0.0880668	0.11	0.914	-0.1630824
op_e	0.0748761	0.079642	0.94	0.347	-0.0812194
tereri	1.385189	0.3955504	3.5	0	0.6099246
ereri_cde	1.17955	0.35224	3.35	0.001	0.4891719

ereri_intref	0.0486129	0.0532071	0.91	0.361	-0.055671
ereri_intmed	0.1120292	0.0731028	1.53	0.125	-0.0312496
ereri_pie	0.0449975	0.0290765	1.55	0.122	-0.0119913
terira	2.385189	0.3955504	6.03	0	1.609925
p_cde	0.8515441	0.0728741	11.69	0	0.7087134
p_intref	0.0350948	0.0363216	0.97	0.334	-0.0360942
p_intmed	0.0808765	0.0450817	1.79	0.073	-0.007482
p_pie	0.0324847	0.0224243	1.45	0.147	-0.0114662
op_m	0.1133612	0.045551	2.49	0.013	0.0240828
op_ati	0.1159712	0.0763547	1.52	0.129	-0.0336813
op_e	0.1484559	0.0728741	2.04	0.042	0.0056253
tereri	1.332651	0.3874949	3.44	0.001	0.5731754
ereri_cde	1.166633	0.3639936	3.21	0.001	0.4532191
ereri_intref	-0.0426051	0.0426797	-1	0.318	-0.1262558
ereri_intmed	0.0248822	0.0902681	0.28	0.783	-0.15204
ereri_pie	0.1837409	0.0513828	3.58	0	0.0830324
terira	2.332651	0.3874949	6.02	0	1.573175
p_cde	0.8754228	0.0888053	9.86	0	0.7013676
p_intref	-0.0319702	0.0341482	-0.94	0.349	-0.0988995
p_intmed	0.0186712	0.06575	0.28	0.776	-0.1101964
p_pie	0.1378762	0.053853	2.56	0.01	0.0323262
op_m	0.1565474	0.06708	2.33	0.02	0.025073
op_ati	-0.0132989	0.0988361	-0.13	0.893	-0.2070142
op_e	0.1245772	0.0888053	1.4	0.161	-0.049478

UCL	EPICLOCK
1.999789	HorvathAgeEAA
1.993081	HorvathAgeEAA
0.0326216	HorvathAgeEAA
0.0715276	HorvathAgeEAA
0.0172162	HorvathAgeEAA
2.999789	HorvathAgeEAA
1.03854	HorvathAgeEAA
0.0257926	HorvathAgeEAA
0.0576374	HorvathAgeEAA
0.0141495	HorvathAgeEAA
0.0380164	HorvathAgeEAA
0.0538889	HorvathAgeEAA
0.0498515	HorvathAgeEAA
2.067598	HannumAgeEAA
1.96437	HannumAgeEAA
0.0390749	HannumAgeEAA
0.137858	HannumAgeEAA
0.1223871	HannumAgeEAA
3.067598	HannumAgeEAA
1.032141	HannumAgeEAA
0.0296179	HannumAgeEAA
0.1018249	HannumAgeEAA
0.0966224	HannumAgeEAA
0.1387113	HannumAgeEAA
0.1298966	HannumAgeEAA
0.1562718	HannumAgeEAA
2.110888	DunedinPoAm
1.959979	DunedinPoAm
0.1089043	DunedinPoAm
0.145377	DunedinPoAm
0.1658365	DunedinPoAm
3.110888	DunedinPoAm
1.081219	DunedinPoAm
0.0819977	DunedinPoAm
0.1020781	DunedinPoAm
0.1297617	DunedinPoAm
0.17423	DunedinPoAm
0.1821332	DunedinPoAm
0.2309716	DunedinPoAm
2.160454	PhenoAgeEAA
1.869927	PhenoAgeEAA

0.1528968	PhenoAgeEAA
0.255308	PhenoAgeEAA
0.1019863	PhenoAgeEAA
3.160454	PhenoAgeEAA
0.9943747	PhenoAgeEAA
0.1062838	PhenoAgeEAA
0.1692349	PhenoAgeEAA
0.0764356	PhenoAgeEAA
0.2026395	PhenoAgeEAA
0.2656238	PhenoAgeEAA
0.2912866	PhenoAgeEAA
2.092127	GrimAgeMortEAA
1.880048	GrimAgeMortEAA
0.0410457	GrimAgeMortEAA
0.2018045	GrimAgeMortEAA
0.2844493	GrimAgeMortEAA
3.092127	GrimAgeMortEAA
1.049478	GrimAgeMortEAA
0.0349592	GrimAgeMortEAA
0.1475388	GrimAgeMortEAA
0.2434261	GrimAgeMortEAA
0.2880218	GrimAgeMortEAA
0.1804163	GrimAgeMortEAA
0.2986324	GrimAgeMortEAA

Figure S4. Combined heatmaps of four-way decomposition models across primary and sensitivity analyses.

This figure presents four heatmaps summarizing four-way decomposition components for the frailty–epigenetic aging–mortality pathway across NHANES and HRS. Panels include: (A) primary analysis ; (B) primary analysis additionally adjusted for leukocyte composition (WBC) ; (C) reverse causation model (epigenetic aging → frailty → mortality) ; and (D) reverse causation model with additional WBC adjustment .

Rows represent epigenetic clocks (EPICLOCK), and columns represent four-way decomposition parameters, including the controlled direct effect (CDE), pure indirect effect (PIE), mediated interaction (INTmed), reference interaction (INTref), and total effect (TE), as well as corresponding proportion parameters (p_ and op_).

Color gradients indicate the magnitude and direction of standardized coefficients (blue = negative; red = positive for main effects; green–purple scale for proportion parameters). Values within cells denote coefficients rounded to three decimals; asterisks indicate statistical significance ($P < 0.05$).

Comparative visualization allows assessment of robustness to leukocyte adjustment and evaluation of directional consistency between primary and reverse causation frameworks.

(A) Primary analysis: Frailty → Epigenetic aging → Mortality

(B) Sensitivity analysis: Frailty → Epigenetic aging → Mortality: + WBC adjustment

(C) Sensitivity analysis: Epigenetic aging →Frailty→ Mortality

(D) Sensitivity analysis: Epigenetic aging →Frailty→ Mortality: + WBC adjustment

Parameter	Coefficient	Std. err.	z	P>z	LCL	UCL
tereri	0.089617	0.0573483	1.56	0.118	-0.0227836	0.2020176
ereri_cde	0.1028479	0.0554039	1.86	0.063	-0.0057418	0.2114375
ereri_intref	-0.0227863	0.0358412	-0.64	0.525	-0.0930338	0.0474612
ereri_intmed	-0.0018227	0.0031159	-0.58	0.559	-0.0079298	0.0042843
ereri_pie	0.0113781	0.0079881	1.42	0.154	-0.0042782	0.0270345
terira	1.089617	0.0573483	19	0	0.9772164	1.202018
p_cde	1.147638	0.4828775	2.38	0.017	0.2012156	2.09406
p_intref	-0.254263	0.4855993	-0.52	0.601	-1.20602	0.6974941
p_intmed	-0.0203392	0.040667	-0.5	0.617	-0.100045	0.0593665
p_pie	0.1269642	0.1144389	1.11	0.267	-0.097332	0.3512603
op_m	0.1066249	0.093745	1.14	0.255	-0.0771118	0.2903617
op_ati	-0.2746022	0.5240789	-0.52	0.6	-1.301778	0.7525736
op_e	-0.1476381	0.4828775	-0.31	0.76	-1.09406	0.7987844
tereri	0.2042071	0.0629383	3.24	0.001	0.0808502	0.3275639
ereri_cde	0.1760586	0.0641338	2.75	0.006	0.0503587	0.3017585
ereri_intref	0.0097913	0.0340506	0.29	0.774	-0.0569465	0.0765292
ereri_intmed	0.0012595	0.0044167	0.29	0.776	-0.0073972	0.0099161
ereri_pie	0.0170976	0.0086599	1.97	0.048	0.0001245	0.0340708
terira	1.204207	0.0629383	19.13	0	1.08085	1.327564
p_cde	0.8621575	0.1864177	4.62	0	0.4967855	1.227529
p_intref	0.0479481	0.1634142	0.29	0.769	-0.2723378	0.368234
p_intmed	0.0061675	0.0211703	0.29	0.771	-0.0353255	0.0476606
p_pie	0.0837269	0.0472837	1.77	0.077	-0.0089474	0.1764012
op_m	0.0898944	0.0518217	1.73	0.083	-0.0116743	0.1914631
op_ati	0.0541157	0.1844177	0.29	0.769	-0.3073364	0.4155678
op_e	0.1378425	0.1864177	0.74	0.46	-0.2275294	0.5032145
tereri	0.3872667	0.0663553	5.84	0	0.2572126	0.5173207
ereri_cde	0.2794759	0.0645351	4.33	0	0.1529896	0.4059623
ereri_intref	0.0693694	0.03898	1.78	0.075	-0.00703	0.1457688
ereri_intmed	0.0141854	0.0089256	1.59	0.112	-0.0033084	0.0316792
ereri_pie	0.0242359	0.0092972	2.61	0.009	0.0060136	0.0424582
terira	1.387267	0.0663553	20.91	0	1.257213	1.517321
p_cde	0.7216628	0.114503	6.3	0	0.4972411	0.9460845
p_intref	0.1791256	0.0933042	1.92	0.055	-0.0037472	0.3619985
p_intmed	0.0366296	0.0212166	1.73	0.084	-0.0049543	0.0782134
p_pie	0.062582	0.0254319	2.46	0.014	0.0127364	0.1124275
op_m	0.0992115	0.0368662	2.69	0.007	0.0269551	0.171468
op_ati	0.2157552	0.1121794	1.92	0.054	-0.0041123	0.4356227
op_e	0.2783372	0.114503	2.43	0.015	0.0539155	0.5027589
tereri	0.2479352	0.0652432	3.8	0	0.1200609	0.3758095
ereri_cde	0.2720799	0.0730824	3.72	0	0.128841	0.4153188

ereri_intref	-0.0419944	0.0320484	-1.31	0.19	-0.1048081	0.0208192
ereri_intmed	-0.0080717	0.0066274	-1.22	0.223	-0.0210612	0.0049179
ereri_pie	0.0259215	0.0098626	2.63	0.009	0.0065911	0.0452519
terira	1.247935	0.0652432	19.13	0	1.120061	1.37581
p_cde	1.097383	0.1577579	6.96	0	0.7881832	1.406583
p_intref	-0.1693767	0.1400442	-1.21	0.226	-0.4438584	0.105105
p_intmed	-0.0325556	0.0283879	-1.15	0.251	-0.0881949	0.0230837
p_pie	0.1045493	0.048325	2.16	0.031	0.009834	0.1992646
op_m	0.0719937	0.042349	1.7	0.089	-0.0110087	0.1549961
op_ati	-0.2019323	0.1668842	-1.21	0.226	-0.5290193	0.1251546
op_e	-0.097383	0.1577579	-0.62	0.537	-0.4065829	0.2118169
tereri	0.6598406	0.0957194	6.89	0	0.472234	0.8474472
ereri_cde	0.493992	0.0822025	6.01	0	0.332878	0.655106
ereri_intref	0.0922895	0.0507962	1.82	0.069	-0.0072693	0.1918483
ereri_intmed	0.0349476	0.0202252	1.73	0.084	-0.004693	0.0745882
ereri_pie	0.0386116	0.0131003	2.95	0.003	0.0129354	0.0642877
terira	1.659841	0.0957194	17.34	0	1.472234	1.847447
p_cde	0.7486535	0.0960884	7.79	0	0.5603238	0.9369832
p_intref	0.1398663	0.0679823	2.06	0.04	0.0066234	0.2731093
p_intmed	0.0529637	0.0270498	1.96	0.05	-0.000053	0.1059803
p_pie	0.0585165	0.0207282	2.82	0.005	0.0178899	0.0991431
op_m	0.1114802	0.0361891	3.08	0.002	0.0405509	0.1824094
op_ati	0.19283	0.0936182	2.06	0.039	0.0093417	0.3763183
op_e	0.2513465	0.0960884	2.62	0.009	0.0630168	0.4396762

EPICLOCK
HorvathAgeEAA
HorvathAgeEAA
HorvathAgeEAA
HorvathAgeEAA
HorvathAgeEAA
HorvathAgeEAA
HorvathAgeEAA
HorvathAgeEAA
HorvathAgeEAA
HorvathAgeEAA
HorvathAgeEAA
HorvathAgeEAA
HorvathAgeEAA
HorvathAgeEAA
HannumAgeEAA
HannumAgeEAA
HannumAgeEAA
HannumAgeEAA
HannumAgeEAA
HannumAgeEAA
HannumAgeEAA
HannumAgeEAA
HannumAgeEAA
HannumAgeEAA
HannumAgeEAA
HannumAgeEAA
DunedinPoAm
DunedinPoAm
DunedinPoAm
DunedinPoAm
DunedinPoAm
DunedinPoAm
DunedinPoAm
DunedinPoAm
DunedinPoAm
DunedinPoAm
DunedinPoAm
DunedinPoAm
DunedinPoAm
PhenoAgeEAA
PhenoAgeEAA

PhenoAgeEAA
PhenoAgeEAA
PhenoAgeEAA
PhenoAgeEAA
PhenoAgeEAA
PhenoAgeEAA
PhenoAgeEAA
PhenoAgeEAA
PhenoAgeEAA
PhenoAgeEAA
PhenoAgeEAA
GrimAgeMortEAA
GrimAgeMortEAA
GrimAgeMortEAA
GrimAgeMortEAA
GrimAgeMortEAA
GrimAgeMortEAA
GrimAgeMortEAA
GrimAgeMortEAA
GrimAgeMortEAA
GrimAgeMortEAA
GrimAgeMortEAA
GrimAgeMortEAA
GrimAgeMortEAA

Parameter	Coefficient	Std. err.	z	P>z	LCL
tereri	-0.014654	0.0792694	-0.18	0.853	-0.1700191
ereri_cde	-0.078038	0.094016	-0.83	0.407	-0.2623059
ereri_intref	0.0447619	0.0374726	1.19	0.232	-0.0286831
ereri_intmed	0.0031276	0.0034761	0.9	0.368	-0.0036855
ereri_pie	0.0154944	0.0118782	1.3	0.192	-0.0077864
terira	0.985346	0.0792694	12.43	0	0.8299809
p_cde	5.325367	23.23851	0.23	0.819	-40.22128
p_intref	-3.054587	16.25194	-0.19	0.851	-34.90781
p_intmed	-0.21343	1.172685	-0.18	0.856	-2.51185
p_pie	-1.05735	5.911732	-0.18	0.858	-12.64413
op_m	-1.27078	7.071981	-0.18	0.857	-15.13161
op_ati	-3.268017	17.41513	-0.19	0.851	-37.40104
op_e	-4.325367	23.2385	-0.19	0.852	-49.87199
tereri	0.2702294	0.097622	2.77	0.006	0.0788938
ereri_cde	0.1985599	0.1142667	1.74	0.082	-0.0253988
ereri_intref	0.0229132	0.04294	0.53	0.594	-0.0612476
ereri_intmed	0.0046596	0.008827	0.53	0.598	-0.0126409
ereri_pie	0.0440966	0.0161031	2.74	0.006	0.012535
terira	1.270229	0.097622	13.01	0	1.078894
p_cde	0.7347828	0.2280942	3.22	0.001	0.2877264
p_intref	0.0847917	0.1654222	0.51	0.608	-0.2394299
p_intmed	0.0172433	0.0338509	0.51	0.61	-0.0491033
p_pie	0.1631822	0.0747869	2.18	0.029	0.0166026
op_m	0.1804254	0.0905261	1.99	0.046	0.0029975
op_ati	0.102035	0.1989784	0.51	0.608	-0.2879555
op_e	0.2652172	0.2280942	1.16	0.245	-0.1818392
tereri	0.5123834	0.1292355	3.96	0	0.2590864
ereri_cde	0.4361911	0.142079	3.07	0.002	0.1577213
ereri_intref	0.0321454	0.0622981	0.52	0.606	-0.0899566
ereri_intmed	0.0053986	0.0106116	0.51	0.611	-0.0153998
ereri_pie	0.0386483	0.0154857	2.5	0.013	0.0082968
terira	1.512383	0.1292355	11.7	0	1.259086
p_cde	0.8512982	0.1470508	5.79	0	0.5630839
p_intref	0.062737	0.121472	0.52	0.606	-0.1753438
p_intmed	0.0105363	0.0206386	0.51	0.61	-0.0299147
p_pie	0.0754285	0.0326478	2.31	0.021	0.0114401
op_m	0.0859648	0.0411189	2.09	0.037	0.0053732
op_ati	0.0732733	0.1418509	0.52	0.605	-0.2047494
op_e	0.1487018	0.1470508	1.01	0.312	-0.1395125
tereri	0.3180987	0.1004666	3.17	0.002	0.1211878
ereri_cde	0.1672866	0.1042682	1.6	0.109	-0.0370753

ereri_intref	0.0954809	0.0561981	1.7	0.089	-0.0146654
ereri_intmed	0.0173858	0.0115473	1.51	0.132	-0.0052465
ereri_pie	0.0379455	0.0148346	2.56	0.011	0.0088702
terira	1.318099	0.1004666	13.12	0	1.121188
p_cde	0.5258952	0.2280566	2.31	0.021	0.0789124
p_intref	0.3001612	0.1790901	1.68	0.094	-0.050849
p_intmed	0.0546553	0.0353237	1.55	0.122	-0.0145778
p_pie	0.1192883	0.0515754	2.31	0.021	0.0182023
op_m	0.1739436	0.0745241	2.33	0.02	0.0278791
op_ati	0.3548165	0.2107098	1.68	0.092	-0.0581671
op_e	0.4741048	0.2280566	2.08	0.038	0.0271221
tereri	0.6300358	0.1319048	4.78	0	0.3715071
ereri_cde	0.5389832	0.1316992	4.09	0	0.2808575
ereri_intref	0.0117959	0.0583433	0.2	0.84	-0.102555
ereri_intmed	0.0041793	0.0206851	0.2	0.84	-0.0363627
ereri_pie	0.0750775	0.0232766	3.23	0.001	0.0294562
terira	1.630036	0.1319048	12.36	0	1.371507
p_cde	0.8554803	0.1255945	6.81	0	0.6093196
p_intref	0.0187225	0.0914572	0.2	0.838	-0.1605303
p_intmed	0.0066334	0.0324191	0.2	0.838	-0.0569068
p_pie	0.1191638	0.0430939	2.77	0.006	0.0347013
op_m	0.1257972	0.0507071	2.48	0.013	0.0264131
op_ati	0.0253559	0.1238573	0.2	0.838	-0.2173999
op_e	0.1445197	0.1255945	1.15	0.25	-0.101641

UCL	EPICLOCK
0.1407111	HorvathAgeEAA
0.10623	HorvathAgeEAA
0.118207	HorvathAgeEAA
0.0099407	HorvathAgeEAA
0.0387752	HorvathAgeEAA
1.140711	HorvathAgeEAA
50.87201	HorvathAgeEAA
28.79864	HorvathAgeEAA
2.08499	HorvathAgeEAA
10.52943	HorvathAgeEAA
12.59005	HorvathAgeEAA
30.86501	HorvathAgeEAA
41.22126	HorvathAgeEAA
0.461565	HannumAgeEAA
0.4225186	HannumAgeEAA
0.107074	HannumAgeEAA
0.0219602	HannumAgeEAA
0.0756582	HannumAgeEAA
1.461565	HannumAgeEAA
1.181839	HannumAgeEAA
0.4090133	HannumAgeEAA
0.0835898	HannumAgeEAA
0.3097618	HannumAgeEAA
0.3578534	HannumAgeEAA
0.4920255	HannumAgeEAA
0.7122736	HannumAgeEAA
0.7656804	DunedinPoAm
0.7146608	DunedinPoAm
0.1542474	DunedinPoAm
0.026197	DunedinPoAm
0.0689998	DunedinPoAm
1.76568	DunedinPoAm
1.139512	DunedinPoAm
0.3008178	DunedinPoAm
0.0509872	DunedinPoAm
0.139417	DunedinPoAm
0.1665563	DunedinPoAm
0.351296	DunedinPoAm
0.4369161	DunedinPoAm
0.5150096	PhenoAgeEAA
0.3716484	PhenoAgeEAA

0.2056272	PhenoAgeEAA
0.040018	PhenoAgeEAA
0.0670207	PhenoAgeEAA
1.51501	PhenoAgeEAA
0.9728779	PhenoAgeEAA
0.6511714	PhenoAgeEAA
0.1238884	PhenoAgeEAA
0.2203743	PhenoAgeEAA
0.3200082	PhenoAgeEAA
0.7678001	PhenoAgeEAA
0.9210876	PhenoAgeEAA
0.8885645	GrimAgeMortEAA
0.7971089	GrimAgeMortEAA
0.1261467	GrimAgeMortEAA
0.0447213	GrimAgeMortEAA
0.1206987	GrimAgeMortEAA
1.888565	GrimAgeMortEAA
1.101641	GrimAgeMortEAA
0.1979754	GrimAgeMortEAA
0.0701736	GrimAgeMortEAA
0.2036263	GrimAgeMortEAA
0.2251813	GrimAgeMortEAA
0.2681118	GrimAgeMortEAA
0.3906804	GrimAgeMortEAA

Supplementary Datasheet 4. Four-way decomposition of the associations between epigenetic age acceleration, frailty and m NHANES and HRS
This datasheet presents cohort-specific four-way decomposition analyses partitioning the total effect of frailty on all-cause morta direct effects, reference interaction, mediated interaction, and pure indirect effects through standardized epigenetic age accelera
Estimates include effect sizes with 95% confidence intervals and p-values, derived from counterfactual-based mediation models demographic and relevant covariates. Results quantify the relative contributions of mediation and interaction pathways linking bio mortality through frailty.

Parameter	Coefficient	Std. err.	z	P>z	LCL	UCL
tereri	0.8215497	0.1912193	4.3	0	0.4467668	1.196333
ereri_cde	0.819018	0.190484	4.3	0	0.4456761	1.19236
ereri_intref	-0.0036466	0.0055222	-0.66	0.509	-0.01447	0.0071768
ereri_intmed	-0.004148	0.0186128	-0.22	0.824	-0.0406284	0.0323324
ereri_pie	0.0103263	0.0089361	1.16	0.248	-0.0071882	0.0278408
terira	1.82155	0.1912193	9.53	0	1.446767	2.196333
p_cde	0.9969184	0.0253333	39.35	0	0.947266	1.046571
p_intref	-0.0044387	0.0068609	-0.65	0.518	-0.0178859	0.0090084
p_intmed	-0.005049	0.0227866	-0.22	0.825	-0.0497099	0.039612
p_pie	0.0125693	0.0112803	1.11	0.265	-0.0095398	0.0346784
op_m	0.0075203	0.0219146	0.34	0.731	-0.0354315	0.0504722
op_ati	-0.0094877	0.0275544	-0.34	0.731	-0.0634934	0.044518
op_e	0.0030816	0.0253333	0.12	0.903	-0.0465708	0.052734
tereri	0.8048085	0.1926713	4.18	0	0.4271796	1.182437
ereri_cde	0.7733471	0.188806	4.1	0	0.4032941	1.1434
ereri_intref	-0.000487	0.0156625	-0.03	0.975	-0.0311849	0.0302108
ereri_intmed	0.009493	0.0228641	0.42	0.678	-0.0353198	0.0543057
ereri_pie	0.0224555	0.0134745	1.67	0.096	-0.0039541	0.048865
terira	1.804808	0.1926713	9.37	0	1.42718	2.182437
p_cde	0.9609082	0.0465586	20.64	0	0.869655	1.052161
p_intref	-0.0006052	0.0194796	-0.03	0.975	-0.0387844	0.0375741
p_intmed	0.0117953	0.0278644	0.42	0.672	-0.0428178	0.0664084
p_pie	0.0279016	0.0179527	1.55	0.12	-0.0072851	0.0630883
op_m	0.0396969	0.0314741	1.26	0.207	-0.0219911	0.1013849
op_ati	0.0111901	0.0468443	0.24	0.811	-0.0806231	0.1030034
op_e	0.0390918	0.0465586	0.84	0.401	-0.0521615	0.130345
tereri	0.7962042	0.1946428	4.09	0	0.4147113	1.177697
ereri_cde	0.6782407	0.1881845	3.6	0	0.3094058	1.047076
ereri_intref	0.0277774	0.0305811	0.91	0.364	-0.0321605	0.0877153
ereri_intmed	0.0481977	0.0317529	1.52	0.129	-0.0140369	0.1104323
ereri_pie	0.0419884	0.0178072	2.36	0.018	0.0070869	0.0768899
terira	1.796204	0.1946428	9.23	0	1.414711	2.177697
p_cde	0.8518426	0.0762277	11.17	0	0.7024391	1.001246
p_intref	0.0348873	0.0386302	0.9	0.366	-0.0408265	0.1106011
p_intmed	0.0605343	0.0371942	1.63	0.104	-0.012365	0.1334337
p_pie	0.0527357	0.0245303	2.15	0.032	0.0046571	0.1008143
op_m	0.1132701	0.04994	2.27	0.023	0.0153894	0.2111507
op_ati	0.0954217	0.0706381	1.35	0.177	-0.0430265	0.2338698
op_e	0.1481574	0.0762277	1.94	0.052	-0.0012462	0.2975609
tereri	0.7813524	0.1907035	4.1	0	0.4075804	1.155124
ereri_cde	0.7873863	0.1936141	4.07	0	0.4079096	1.166863

ereri_intref	-0.018382	0.0131028	-1.4	0.161	-0.044063	0.0072989
ereri_intmed	-0.0326242	0.0314688	-1.04	0.3	-0.0943019	0.0290534
ereri_pie	0.0449724	0.020023	2.25	0.025	0.005728	0.0842167
terira	1.781352	0.1907035	9.34	0	1.40758	2.155124
p_cde	1.007722	0.0368869	27.32	0	0.9354255	1.080019
p_intref	-0.0235259	0.0182756	-1.29	0.198	-0.0593455	0.0122936
p_intmed	-0.0417536	0.0409716	-1.02	0.308	-0.1220565	0.0385494
p_pie	0.0575571	0.0294032	1.96	0.05	-0.0000722	0.1151864
op_m	0.0158035	0.0354908	0.45	0.656	-0.0537572	0.0853642
op_ati	-0.0652795	0.0486073	-1.34	0.179	-0.1605481	0.0299892
op_e	-0.0077224	0.0368869	-0.21	0.834	-0.0800194	0.0645746
tereri	0.8652604	0.2163942	4	0	0.4411355	1.289385
ereri_cde	0.5734151	0.1741009	3.29	0.001	0.2321836	0.9146466
ereri_intref	0.0382367	0.0432328	0.88	0.376	-0.046498	0.1229713
ereri_intmed	0.1201897	0.070218	1.71	0.087	-0.0174351	0.2578144
ereri_pie	0.1334189	0.0324273	4.11	0	0.0698626	0.1969752
terira	1.86526	0.2163942	8.62	0	1.441136	2.289385
p_cde	0.6627082	0.1061453	6.24	0	0.4546672	0.8707492
p_intref	0.0441909	0.0468226	0.94	0.345	-0.0475798	0.1359616
p_intmed	0.1389058	0.0631669	2.2	0.028	0.015101	0.2627105
p_pie	0.1541951	0.0500152	3.08	0.002	0.0561671	0.2522231
op_m	0.2931009	0.0731901	4	0	0.149651	0.4365508
op_ati	0.1830967	0.1063798	1.72	0.085	-0.0254038	0.3915972
op_e	0.3372918	0.1061453	3.18	0.001	0.1292508	0.5453328

EPICLOCK
HorvathAgeEAA
HorvathAgeEAA
HorvathAgeEAA
HorvathAgeEAA
HorvathAgeEAA
HorvathAgeEAA
HorvathAgeEAA
HorvathAgeEAA
HorvathAgeEAA
HorvathAgeEAA
HorvathAgeEAA
HorvathAgeEAA
HorvathAgeEAA
HorvathAgeEAA
HannumAgeEAA
HannumAgeEAA
HannumAgeEAA
HannumAgeEAA
HannumAgeEAA
HannumAgeEAA
HannumAgeEAA
HannumAgeEAA
HannumAgeEAA
HannumAgeEAA
HannumAgeEAA
HannumAgeEAA
DunedinPoAm
DunedinPoAm
DunedinPoAm
DunedinPoAm
DunedinPoAm
DunedinPoAm
DunedinPoAm
DunedinPoAm
DunedinPoAm
DunedinPoAm
DunedinPoAm
DunedinPoAm
DunedinPoAm
PhenoAgeEAA
PhenoAgeEAA

PhenoAgeEAA
PhenoAgeEAA
PhenoAgeEAA
PhenoAgeEAA
PhenoAgeEAA
PhenoAgeEAA
PhenoAgeEAA
PhenoAgeEAA
PhenoAgeEAA
PhenoAgeEAA
PhenoAgeEAA
GrimAgeMortEAA
GrimAgeMortEAA
GrimAgeMortEAA
GrimAgeMortEAA
GrimAgeMortEAA
GrimAgeMortEAA
GrimAgeMortEAA
GrimAgeMortEAA
GrimAgeMortEAA
GrimAgeMortEAA
GrimAgeMortEAA
GrimAgeMortEAA
GrimAgeMortEAA

Parameter	Coefficient	Std. err.	z	P>z	LCL
tereri	0.8899401	0.3164489	2.81	0.005	0.2697117
ereri_cde	0.8665131	0.313809	2.76	0.006	0.2514588
ereri_intref	0.0121443	0.0440722	0.28	0.783	-0.0742357
ereri_intmed	0.0142465	0.0383431	0.37	0.71	-0.0609046
ereri_pie	-0.0029637	0.008846	-0.34	0.738	-0.0203015
terira	1.88994	0.3164489	5.97	0	1.269712
p_cde	0.9736757	0.0577153	16.87	0	0.8605558
p_intref	0.0136462	0.0493584	0.28	0.782	-0.0830945
p_intmed	0.0160084	0.0429541	0.37	0.709	-0.0681801
p_pie	-0.0033303	0.0099844	-0.33	0.739	-0.0228993
op_m	0.0126781	0.0340415	0.37	0.71	-0.054042
op_ati	0.0296546	0.0599905	0.49	0.621	-0.0879246
op_e	0.0263243	0.0577153	0.46	0.648	-0.0867956
tereri	0.9459764	0.3274355	2.89	0.004	0.3042146
ereri_cde	0.8294845	0.3094034	2.68	0.007	0.2230649
ereri_intref	0.040633	0.0468895	0.87	0.386	-0.0512687
ereri_intmed	0.0497428	0.043925	1.13	0.257	-0.0363487
ereri_pie	0.0261161	0.0222969	1.17	0.241	-0.017585
terira	1.945976	0.3274355	5.94	0	1.304215
p_cde	0.8768554	0.0826256	10.61	0	0.7149121
p_intref	0.0429535	0.048857	0.88	0.379	-0.0528045
p_intmed	0.0525835	0.0434001	1.21	0.226	-0.0324791
p_pie	0.0276076	0.0242714	1.14	0.255	-0.0199636
op_m	0.0801911	0.0494976	1.62	0.105	-0.0168225
op_ati	0.095537	0.0843046	1.13	0.257	-0.0696969
op_e	0.1231446	0.0826256	1.49	0.136	-0.0387987
tereri	0.9375573	0.3191442	2.94	0.003	0.3120462
ereri_cde	0.9451581	0.3267035	2.89	0.004	0.304831
ereri_intref	-0.0266939	0.0403291	-0.66	0.508	-0.1057374
ereri_intmed	-0.004689	0.0209965	-0.22	0.823	-0.0458413
ereri_pie	0.0237821	0.026146	0.91	0.363	-0.0274631
terira	1.937557	0.3191442	6.07	0	1.312046
p_cde	1.008107	0.0580432	17.37	0	0.8943444
p_intref	-0.0284717	0.0425391	-0.67	0.503	-0.1118469
p_intmed	-0.0050013	0.0224223	-0.22	0.823	-0.0489481
p_pie	0.025366	0.0279106	0.91	0.363	-0.0293377
op_m	0.0203647	0.0277735	0.73	0.463	-0.0340703
op_ati	-0.033473	0.0625082	-0.54	0.592	-0.1559868
op_e	-0.008107	0.0580432	-0.14	0.889	-0.1218696
tereri	0.924907	0.3272635	2.83	0.005	0.2834823
ereri_cde	0.8052991	0.3091722	2.6	0.009	0.1993327

ereri_intref	0.0182789	0.0315215	0.58	0.562	-0.043502
ereri_intmed	0.0708414	0.0590159	1.2	0.23	-0.0448277
ereri_pie	0.0304876	0.0296316	1.03	0.304	-0.0275893
terira	1.924907	0.3272635	5.88	0	1.283482
p_cde	0.8706812	0.0839372	10.37	0	0.7061674
p_intref	0.019763	0.0338938	0.58	0.56	-0.0466677
p_intmed	0.076593	0.0600525	1.28	0.202	-0.0411078
p_pie	0.0329629	0.0329301	1	0.317	-0.031579
op_m	0.1095558	0.0595272	1.84	0.066	-0.0071153
op_ati	0.096356	0.0871947	1.11	0.269	-0.0745425
op_e	0.1293188	0.0839372	1.54	0.123	-0.035195
tereri	0.917728	0.317343	2.89	0.004	0.2957472
ereri_cde	0.8552202	0.3117479	2.74	0.006	0.2442056
ereri_intref	-0.0587201	0.0396594	-1.48	0.139	-0.1364511
ereri_intmed	-0.0402626	0.0766751	-0.53	0.6	-0.1905429
ereri_pie	0.1614905	0.0572754	2.82	0.005	0.0492329
terira	1.917728	0.317343	6.04	0	1.295747
p_cde	0.9318885	0.1051416	8.86	0	0.7258148
p_intref	-0.0639842	0.0466079	-1.37	0.17	-0.155334
p_intmed	-0.043872	0.0876717	-0.5	0.617	-0.2157054
p_pie	0.1759677	0.0789042	2.23	0.026	0.0213183
op_m	0.1320957	0.0816889	1.62	0.106	-0.0280116
op_ati	-0.1078562	0.1293326	-0.83	0.404	-0.3613434
op_e	0.0681115	0.1051416	0.65	0.517	-0.1379622

UCL	EPICLOCK
1.510169	HorvathAgeEAA
1.481567	HorvathAgeEAA
0.0985243	HorvathAgeEAA
0.0893977	HorvathAgeEAA
0.0143741	HorvathAgeEAA
2.510169	HorvathAgeEAA
1.086796	HorvathAgeEAA
0.1103869	HorvathAgeEAA
0.1001969	HorvathAgeEAA
0.0162388	HorvathAgeEAA
0.0793983	HorvathAgeEAA
0.1472337	HorvathAgeEAA
0.1394442	HorvathAgeEAA
1.587738	HannumAgeEAA
1.435904	HannumAgeEAA
0.1325347	HannumAgeEAA
0.1358342	HannumAgeEAA
0.0698172	HannumAgeEAA
2.587738	HannumAgeEAA
1.038799	HannumAgeEAA
0.1387116	HannumAgeEAA
0.1376461	HannumAgeEAA
0.0751787	HannumAgeEAA
0.1772046	HannumAgeEAA
0.260771	HannumAgeEAA
0.2850879	HannumAgeEAA
1.563068	DunedinPoAm
1.585485	DunedinPoAm
0.0523496	DunedinPoAm
0.0364634	DunedinPoAm
0.0750273	DunedinPoAm
2.563068	DunedinPoAm
1.12187	DunedinPoAm
0.0549034	DunedinPoAm
0.0389455	DunedinPoAm
0.0800697	DunedinPoAm
0.0747997	DunedinPoAm
0.0890408	DunedinPoAm
0.1056556	DunedinPoAm
1.566332	PhenoAgeEAA
1.411266	PhenoAgeEAA

0.0800599	PhenoAgeEAA
0.1865105	PhenoAgeEAA
0.0885644	PhenoAgeEAA
2.566332	PhenoAgeEAA
1.035195	PhenoAgeEAA
0.0861937	PhenoAgeEAA
0.1942937	PhenoAgeEAA
0.0975047	PhenoAgeEAA
0.2262269	PhenoAgeEAA
0.2672544	PhenoAgeEAA
0.2938326	PhenoAgeEAA
1.539709	GrimAgeMortEAA
1.466235	GrimAgeMortEAA
0.0190109	GrimAgeMortEAA
0.1100177	GrimAgeMortEAA
0.2737481	GrimAgeMortEAA
2.539709	GrimAgeMortEAA
1.137962	GrimAgeMortEAA
0.0273656	GrimAgeMortEAA
0.1279613	GrimAgeMortEAA
0.3306171	GrimAgeMortEAA
0.2922029	GrimAgeMortEAA
0.145631	GrimAgeMortEAA
0.2741852	GrimAgeMortEAA

Supplementary Datasheet 5. Four-way decomposition of the associations between frailty, epigenetic age acceleration, and m
NHANES and HRS: With adjustment for WBC composition

This datasheet presents cohort-specific four-way decomposition analyses partitioning the total effect of frailty on all-cause morta
direct effects, reference interaction, mediated interaction, and pure indirect effects through standardized epigenetic age accelera

Estimates include effect sizes with 95% confidence intervals and p-values, derived from counterfactual-based mediation models
demographic and relevant covariates. Results quantify the relative contributions of mediation and interaction pathways linking fra
through biological aging markers.

Parameter	Coefficient	Std. err.	z	P>z	LCL	UCL
tereri	0.0998235	0.0583467	1.71	0.087	-0.014534	0.214181
ereri_cde	0.0981619	0.0567634	1.73	0.084	-0.0130922	0.2094161
ereri_intref	-0.0085467	0.0360125	-0.24	0.812	-0.0791299	0.0620364
ereri_intmed	-0.0006359	0.002719	-0.23	0.815	-0.0059651	0.0046932
ereri_pie	0.0108442	0.0081755	1.33	0.185	-0.0051796	0.0268679
terira	1.099823	0.0583467	18.85	0	0.985466	1.214181
p_cde	0.9833555	0.3914149	2.51	0.012	0.2161964	1.750515
p_intref	-0.0856186	0.3817392	-0.22	0.823	-0.8338136	0.6625764
p_intmed	-0.0063706	0.0287005	-0.22	0.824	-0.0626225	0.0498814
p_pie	0.1086336	0.0977123	1.11	0.266	-0.082879	0.3001462
op_m	0.1022631	0.0897931	1.14	0.255	-0.0737281	0.2782543
op_ati	-0.0919891	0.4100883	-0.22	0.823	-0.8957473	0.7117691
op_e	0.0166445	0.3914148	0.04	0.966	-0.7505144	0.7838034
tereri	0.1877019	0.0640509	2.93	0.003	0.0621644	0.3132394
ereri_cde	0.1570305	0.0650611	2.41	0.016	0.029513	0.2845479
ereri_intref	0.0132531	0.0337203	0.39	0.694	-0.0528376	0.0793437
ereri_intmed	0.0015153	0.0039332	0.39	0.7	-0.0061936	0.0092242
ereri_pie	0.0159031	0.0088548	1.8	0.072	-0.0014519	0.0332581
terira	1.187702	0.0640509	18.54	0	1.062164	1.313239
p_cde	0.8365948	0.1988272	4.21	0	0.4469006	1.226289
p_intref	0.0706071	0.1750259	0.4	0.687	-0.2724373	0.4136515
p_intmed	0.0080729	0.0203574	0.4	0.692	-0.0318269	0.0479728
p_pie	0.0847252	0.0524396	1.62	0.106	-0.0180546	0.187505
op_m	0.0927981	0.0577317	1.61	0.108	-0.0203539	0.2059501
op_ati	0.07868	0.1949949	0.4	0.687	-0.3035029	0.4608629
op_e	0.1634052	0.1988272	0.82	0.411	-0.226289	0.5530994
tereri	0.3703079	0.0712733	5.2	0	0.2306148	0.5100011
ereri_cde	0.2709754	0.0690179	3.93	0	0.1357028	0.4062479
ereri_intref	0.066788	0.0389504	1.71	0.086	-0.0095533	0.1431293
ereri_intmed	0.0113585	0.0078964	1.44	0.15	-0.0041181	0.0268352
ereri_pie	0.021186	0.0095788	2.21	0.027	0.0024119	0.0399601
terira	1.370308	0.0712733	19.23	0	1.230615	1.510001
p_cde	0.7317568	0.118281	6.19	0	0.4999303	0.9635834
p_intref	0.1803581	0.0984299	1.83	0.067	-0.012561	0.3732772
p_intmed	0.0306731	0.0197791	1.55	0.121	-0.0080931	0.0694394
p_pie	0.0572119	0.0269526	2.12	0.034	0.0043858	0.110038
op_m	0.0878851	0.0390181	2.25	0.024	0.0114109	0.1643592
op_ati	0.2110313	0.1149524	1.84	0.066	-0.0142714	0.4363339
op_e	0.2682432	0.118281	2.27	0.023	0.0364166	0.5000697
tereri	0.2219949	0.067648	3.28	0.001	0.0894072	0.3545825
ereri_cde	0.2427589	0.0751273	3.23	0.001	0.095512	0.3900057

ereri_intref	-0.0373851	0.031715	-1.18	0.238	-0.0995453	0.0247751
ereri_intmed	-0.0059341	0.005509	-1.08	0.281	-0.0167315	0.0048634
ereri_pie	0.0225551	0.0098014	2.3	0.021	0.0033448	0.0417654
terira	1.221995	0.067648	18.06	0	1.089407	1.354583
p_cde	1.093534	0.1698929	6.44	0	0.7605499	1.426518
p_intref	-0.1684052	0.15455	-1.09	0.276	-0.4713176	0.1345073
p_intmed	-0.0267307	0.0262088	-1.02	0.308	-0.0780991	0.0246377
p_pie	0.101602	0.0533007	1.91	0.057	-0.0028653	0.2060694
op_m	0.0748714	0.0456316	1.64	0.101	-0.0145649	0.1643076
op_ati	-0.1951359	0.1789759	-1.09	0.276	-0.5459221	0.1556504
op_e	-0.0935338	0.1698929	-0.55	0.582	-0.4265177	0.2394501
tereri	0.6261133	0.0954787	6.56	0	0.4389785	0.8132481
ereri_cde	0.4672762	0.0831535	5.62	0	0.3042983	0.6302541
ereri_intref	0.0881226	0.050007	1.76	0.078	-0.0098894	0.1861345
ereri_intmed	0.0319296	0.0191463	1.67	0.095	-0.0055965	0.0694558
ereri_pie	0.0387848	0.0130474	2.97	0.003	0.0132123	0.0643574
terira	1.626113	0.0954787	17.03	0	1.438978	1.813248
p_cde	0.7463126	0.0989706	7.54	0	0.5523338	0.9402914
p_intref	0.1407454	0.0709039	1.99	0.047	0.0017762	0.2797146
p_intmed	0.0509966	0.0271083	1.88	0.06	-0.0021347	0.1041279
p_pie	0.0619454	0.0219748	2.82	0.005	0.0188756	0.1050152
op_m	0.112942	0.0371904	3.04	0.002	0.0400502	0.1858338
op_ati	0.191742	0.0964841	1.99	0.047	0.0026366	0.3808474
op_e	0.2536874	0.0989706	2.56	0.01	0.0597086	0.4476662

EPICLOCK
HorvathAgeEAA
HorvathAgeEAA
HorvathAgeEAA
HorvathAgeEAA
HorvathAgeEAA
HorvathAgeEAA
HorvathAgeEAA
HorvathAgeEAA
HorvathAgeEAA
HorvathAgeEAA
HorvathAgeEAA
HorvathAgeEAA
HorvathAgeEAA
HorvathAgeEAA
HannumAgeEAA
HannumAgeEAA
HannumAgeEAA
HannumAgeEAA
HannumAgeEAA
HannumAgeEAA
HannumAgeEAA
HannumAgeEAA
HannumAgeEAA
HannumAgeEAA
HannumAgeEAA
HannumAgeEAA
DunedinPoAm
DunedinPoAm
DunedinPoAm
DunedinPoAm
DunedinPoAm
DunedinPoAm
DunedinPoAm
DunedinPoAm
DunedinPoAm
DunedinPoAm
DunedinPoAm
DunedinPoAm
DunedinPoAm
PhenoAgeEAA
PhenoAgeEAA

PhenoAgeEAA
PhenoAgeEAA
PhenoAgeEAA
PhenoAgeEAA
PhenoAgeEAA
PhenoAgeEAA
PhenoAgeEAA
PhenoAgeEAA
PhenoAgeEAA
PhenoAgeEAA
PhenoAgeEAA
GrimAgeMortEAA
GrimAgeMortEAA
GrimAgeMortEAA
GrimAgeMortEAA
GrimAgeMortEAA
GrimAgeMortEAA
GrimAgeMortEAA
GrimAgeMortEAA
GrimAgeMortEAA
GrimAgeMortEAA
GrimAgeMortEAA
GrimAgeMortEAA
GrimAgeMortEAA

Parameter	Coefficient	Std. err.	z	P>z	LCL
tereri	0.0367358	0.0950408	0.39	0.699	-0.1495409
ereri_cde	-0.0779929	0.1045732	-0.75	0.456	-0.2829525
ereri_intref	0.1096104	0.0630521	1.74	0.082	-0.0139695
ereri_intmed	0.0019027	0.006325	0.3	0.764	-0.010494
ereri_pie	0.0032156	0.0105723	0.3	0.761	-0.0175057
terira	1.036736	0.0950408	10.91	0	0.8504591
p_cde	-2.123078	7.922102	-0.27	0.789	-17.65011
p_intref	2.98375	7.637792	0.39	0.696	-11.98605
p_intmed	0.0517937	0.1955436	0.26	0.791	-0.3314647
p_pie	0.087534	0.3330294	0.26	0.793	-0.5651916
op_m	0.1393277	0.5267912	0.26	0.791	-0.893164
op_ati	3.035544	7.741729	0.39	0.695	-12.13797
op_e	3.123078	7.922101	0.39	0.693	-12.40396
tereri	0.2689526	0.1032941	2.6	0.009	0.0664998
ereri_cde	0.157909	0.1152238	1.37	0.171	-0.0679254
ereri_intref	0.0806836	0.0591104	1.36	0.172	-0.0351706
ereri_intmed	0.0094722	0.0085925	1.1	0.27	-0.0073688
ereri_pie	0.0208878	0.0129436	1.61	0.107	-0.0044812
terira	1.268953	0.1032941	12.28	0	1.0665
p_cde	0.5871259	0.2794304	2.1	0.036	0.0394524
p_intref	0.2999919	0.2381423	1.26	0.208	-0.1667585
p_intmed	0.0352187	0.03251	1.08	0.279	-0.0284997
p_pie	0.0776634	0.050534	1.54	0.124	-0.0213815
op_m	0.1128822	0.0735862	1.53	0.125	-0.0313441
op_ati	0.3352106	0.2652151	1.26	0.206	-0.1846013
op_e	0.4128741	0.2794304	1.48	0.14	-0.1347994
tereri	0.2951472	0.1407961	2.1	0.036	0.0191919
ereri_cde	0.3031358	0.1617914	1.87	0.061	-0.0139696
ereri_intref	-0.0191557	0.0689096	-0.28	0.781	-0.1542161
ereri_intmed	-0.0011667	0.0043711	-0.27	0.79	-0.0097339
ereri_pie	0.0123338	0.0133962	0.92	0.357	-0.0139223
terira	1.295147	0.1407961	9.2	0	1.019192
p_cde	1.027066	0.2484554	4.13	0	0.5401028
p_intref	-0.0649021	0.2333582	-0.28	0.781	-0.5222757
p_intmed	-0.0039529	0.0147584	-0.27	0.789	-0.0328787
p_pie	0.0417885	0.0470504	0.89	0.374	-0.0504286
op_m	0.0378356	0.0447352	0.85	0.398	-0.0498439
op_ati	-0.0688549	0.247557	-0.28	0.781	-0.5540578
op_e	-0.0270665	0.2484553	-0.11	0.913	-0.5140299
tereri	0.2401726	0.104276	2.3	0.021	0.0357953
ereri_cde	0.1200534	0.1145276	1.05	0.295	-0.1044166

ereri_intref	0.0756379	0.0586964	1.29	0.198	-0.0394048
ereri_intmed	0.0135762	0.0116416	1.17	0.244	-0.0092409
ereri_pie	0.0309051	0.0150446	2.05	0.04	0.0014181
terira	1.240173	0.104276	11.89	0	1.035795
p_cde	0.4998631	0.3341743	1.5	0.135	-0.1551065
p_intref	0.3149315	0.2621548	1.2	0.23	-0.1988824
p_intmed	0.0565268	0.0498221	1.13	0.257	-0.0411227
p_pie	0.1286785	0.0740142	1.74	0.082	-0.0163866
op_m	0.1852053	0.1050964	1.76	0.078	-0.0207798
op_ati	0.3714583	0.3080838	1.21	0.228	-0.2323749
op_e	0.5001369	0.3341743	1.5	0.134	-0.1548328
tereri	0.5818702	0.1529941	3.8	0	0.2820072
ereri_cde	0.5819597	0.163325	3.56	0	0.2618485
ereri_intref	-0.0434185	0.0711411	-0.61	0.542	-0.1828526
ereri_intmed	-0.0129885	0.0215293	-0.6	0.546	-0.0551852
ereri_pie	0.0563176	0.0223427	2.52	0.012	0.0125267
terira	1.58187	0.1529941	10.34	0	1.282007
p_cde	1.000154	0.1595595	6.27	0	0.6874229
p_intref	-0.0746189	0.1268772	-0.59	0.556	-0.3232936
p_intmed	-0.0223221	0.0382893	-0.58	0.56	-0.0973677
p_pie	0.0967872	0.0430772	2.25	0.025	0.0123575
op_m	0.0744652	0.0479773	1.55	0.121	-0.0195686
op_ati	-0.0969409	0.1648197	-0.59	0.556	-0.4199816
op_e	-0.0001537	0.159564	0	0.999	-0.3128934

UCL	EPICLOCK
0.2230124	HorvathAgeEAA
0.1269667	HorvathAgeEAA
0.2331903	HorvathAgeEAA
0.0142994	HorvathAgeEAA
0.023937	HorvathAgeEAA
1.223012	HorvathAgeEAA
13.40396	HorvathAgeEAA
17.95355	HorvathAgeEAA
0.4350521	HorvathAgeEAA
0.7402596	HorvathAgeEAA
1.171819	HorvathAgeEAA
18.20905	HorvathAgeEAA
18.65011	HorvathAgeEAA
0.4714054	HannumAgeEAA
0.3837435	HannumAgeEAA
0.1965378	HannumAgeEAA
0.0263131	HannumAgeEAA
0.0462567	HannumAgeEAA
1.471405	HannumAgeEAA
1.134799	HannumAgeEAA
0.7667423	HannumAgeEAA
0.0989372	HannumAgeEAA
0.1767083	HannumAgeEAA
0.2571084	HannumAgeEAA
0.8550226	HannumAgeEAA
0.9605476	HannumAgeEAA
0.5711025	DunedinPoAm
0.6202411	DunedinPoAm
0.1159048	DunedinPoAm
0.0074005	DunedinPoAm
0.0385898	DunedinPoAm
1.571102	DunedinPoAm
1.51403	DunedinPoAm
0.3924716	DunedinPoAm
0.024973	DunedinPoAm
0.1340055	DunedinPoAm
0.1255151	DunedinPoAm
0.4163479	DunedinPoAm
0.459897	DunedinPoAm
0.4445498	PhenoAgeEAA
0.3445234	PhenoAgeEAA

0.1906807	PhenoAgeEAA
0.0363932	PhenoAgeEAA
0.060392	PhenoAgeEAA
1.44455	PhenoAgeEAA
1.154833	PhenoAgeEAA
0.8287455	PhenoAgeEAA
0.1541762	PhenoAgeEAA
0.2737437	PhenoAgeEAA
0.3911904	PhenoAgeEAA
0.9752916	PhenoAgeEAA
1.155107	PhenoAgeEAA
0.8817332	GrimAgeMortEAA
0.9020709	GrimAgeMortEAA
0.0960156	GrimAgeMortEAA
0.0292081	GrimAgeMortEAA
0.1001085	GrimAgeMortEAA
1.881733	GrimAgeMortEAA
1.312885	GrimAgeMortEAA
0.1740559	GrimAgeMortEAA
0.0527236	GrimAgeMortEAA
0.181217	GrimAgeMortEAA
0.168499	GrimAgeMortEAA
0.2260997	GrimAgeMortEAA
0.312586	GrimAgeMortEAA

Supplementary Datasheet 6. Four-way decomposition of the associations between epigenetic age acceleration, frailty and m NHANES and HRS: WBC composition adjustment
This datasheet presents cohort-specific four-way decomposition analyses partitioning the total effect of frailty on all-cause morta controlled direct effects, reference interaction, mediated interaction, and pure indirect effects through standardized epigenetic ag (EAA) measures.
Estimates include effect sizes with 95% confidence intervals and p-values, derived from counterfactual-based mediation models demographic and relevant covariates. Results quantify the relative contributions of mediation and interaction pathways linking bio markers to mortality through frailty.